doi : 10.17596/0003693

R/V Mirai Cruise Report MR01-K05 Leg-3/4

November 7 - December 19, 2001

Japan Marine Science and Technology Center (JAMSTEC)

Cruise Report for MR01-K05 Leg-3 and 4

[Contents]

< Appendix >

1. Introduction

Air-sea interaction is a key factor to understand the atmospheric and oceanic phenomena over the tropical western Pacific Ocean where the warmest sea surface temperatures exist and is called “warm water pool”. Since active convections developed over the warm water pool can release heat from the ocean to the atmosphere, this tropical western Pacific region is often called “heat engine of the globe”.

From the past studies, it is well known that atmospheric and oceanic features over the warm water pool are frequently modulated by the 30-60-day intraseasonal oscillation or MJO (Madden-Julian Oscillation, named after Madden and Julian, 1971, 1972, J. Atmos. Sci. papers). This MJO is very attractive phenomenon in terms of El Nino, too, because many authors have found the relation of occurrence/termination of El Nino with MJO(M.McPhaden, 1999, Science; Y. Takayabu et al. 1999, Nature). Furthermore, Nakazawa (1988, J. Meteor. Soc. Japan) found the hierarchy of convective systems within MJO. It stresses the importance of cloud clusters (several 100km horizontal scale, a couple of days life cycle) and super cloud clusters (several 1,000km scale with 7-10 days period) in this region.

Based on these past studies, in the current cruise, precipitation mechanism caused by the cloud clusters that are accompanied with MJO was the main target to be studied.

For the purpose above mentioned, stationary observation was conducted at (2N, 138E) for the period of one month from November 9 through December 9, 2001. During the intensive observation period (IOP), C-band weather Doppler radar, atmospheric sounding by radiosonde, surface meteorological measurement, CTD casting down to 500m, and ADCP current measurement were carried out as main missions. In addition, turbulent flux measurement, solar radiation measurement, 95-GHz cloud radar, Mie scattering LIDAR, greenhouse effect gases measurement, and other many observations were intensively conducted.

As found in the following sections, we could encounter the active phase of MJO in the end of observation period, so many precipitation systems were observed, while fine days lasted in early days of the period.

This cruise report summarizes the observation conducted during leg-3 and 4, and preliminary results are also included. In the first several sections, basic information such as cruise track, onboard personnel list are described. Details of each observation are stated in Section 6. We also attached useful information as Appendix.

2. Cruise Summary

2.1 Ship

Name	Research Vessel MIRAI
L x B x D	128.6m x 19.0m x 13.2m
Gross Tonnage	8,672 tons
Call Sign	JNSR
Mother Port	Mutsu, Aomori Prefecture

2.2 Cruise Code

MR01-K05 (Leg 3 and 4)

2.3 Project Name

The Study of the Air-Sea Interaction in the Tropics

2.4 Undertaking Institute

Japan Marine Science and Technology Center (JAMSTEC)
2-15, Natsushima, Yokosuka, Kanagawa 237-0061, JAPAN

2.5 Chief Scientist

Kunio YONEYAMA (Ocean Observation and Research Department, JAMSTEC)

2.6 Periods and Ports of Call

Nov. 7, 2001	departed Koror, Republic of Palau
Dec. 11 - 13, 2001	called at Koror, Republic of Palau
Dec. 19, 2001	arrived at Yokohama, Japan

2.7 Observation Summary

5GHz Doppler radar		continuously (10 min interval of 1 volume scan)
Radiosonde		241 times (every 3 hours from Nov.9 to Dec.9)
Ceilometer		continuously (every 1 min)
Total Sky Imager		continuously (every 5 min)
Surface Meteorology –	MIRAI SMET	continuously
	SOAR	continuously
CTD		180 times (500db depth, except 1000db at 1200Z)
Water sampling for greenhouse gases		8 times
ADCP		continuously (every 5 min)
Sea surface water monitoring		continuously (every 1 min)
Mie scattering LIDAR		continuously
95GHz vertical pointing cloud radar		continuously
Ocean colors / solar radiation		occasionally
Turbulent flux		continuously
Gravity / magnetic force / sea bottom depth		continuously within EEZ and open seas
PCO2/pCO2 measurement		continuously
Greenhouse gases measurement		continuously

2.8 Overview

In order to investigate precipitation mechanism caused by the cloud clusters that are accompanied with MJO(Madden-Julian Oscillation), stationary observation was conducted at (2N, 138E) for the period of one month from November 9 through December 9, 2001.

From the cloud images of Geostationary Meteorological Satellite of Japan Meteorological Agency shown below, it is evident that convectively active phase of MJO passed over the observational area in the last 10 days of IOP. During the whole observation period, westerly were dominant in the lower troposphere (see Fig.6.2-1). Accompanied with cloud activities there were two peaks of strong westerly in mid-November and early December, respectively. Furthermore, meridional wind components suggest that equatorial trapped waves were prevailed in this period.

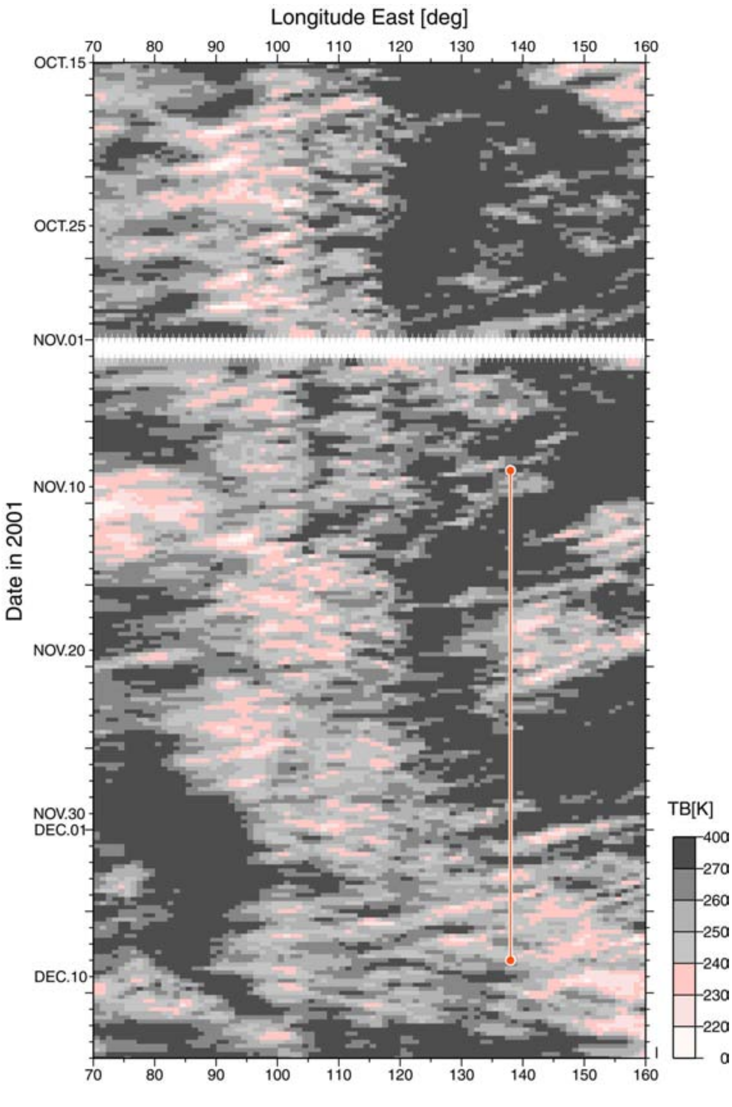

Time-Longitude cross section of GMS TBB.

2.9 Acknowledgment

We would like to express our sincere thanks to Captain M.Akamine and his crew for providing good conditions for observation with their skillful ship operation. Thanks are extended to technical staff of Global Ocean Development Inc. and Marine Works Japan, Co.Ltd. for their continuous support.

3. List of Instruments

3.1 Surface Meteorological Parameters

(a) JAMSTEC / Mirai Met System
- Anemometer: KE-500, Koshin Denki
- Thermometer: FT, Koshin Denki
- Dewpoint Meter DW-1, Koshin Denki
- Barometer: F-451, Yokogawa Co.
- Rain Gauge: 50202, R.M. Young
- Optical Rain Gauge: ORG-115DR, SCTI
- Shortwave Radiometer: MS-801, Eiko Seiki
- Longwave Radiometer: MS-200, Eiko Seiki
- Wave Height Meter: MW-2, Tsurumi-seiki

(b) JAMSTEC / SOAR system
- Anemometer: 05106, R. M. Young
- Thermometer / Hygrometer: HMP45A, Vaisala
- (with 43408 Gill aspirated radiation shield, R.M.Young)
- Barometer: 61201, R. M. Young
- Rain Gauge: 50202, R. M. Young
- Optical Rain Gauge: ORG-115DA, ScTi
- Sea Surface Skin Tempreature Sensor: SST-100, Brookhaven National Lab.
- Shortwave Radiometer: PSP, Eppley Labs.
- Longwave Radiometer: PIR, Eppley Labs.
- Fast Rotating Shadowband Radiometer: Yankee Engineering Systems
- Shortwave Radiometer (upwelling radiation): MS-801, Eiko Seiki
- Longwave Radiometer (upwelling radiation): MS-202, Eiko Seiki

(c) JAMSTEC / Total Sky Imager System
- Total Sky Imager: Yankee Engineering System

3.2 Radiosonde Observation

(a) JAMSTEC
- GPS radiosonde: RS-80-GH, Vaisala
- Receiver: DigiCORA MW11, Vaisala

3.3 Doppler Radar Observation

(a) JAMSTEC
- C-band Doppler Radar: RC-52B, Mitsubishi Electric Co.
- Signal Processor: RVP-7, Sigmet
- Antenna Controller: RCP-02, Sigmet
- Control and Processing Software: IRIS/Open, Sigmet
- Inertial Navigation Unit: DRUH, Honeywell

3.4 Ceilometer Observation

(b) JAMSTEC
- Ceilometer: CT-25K, Vaisala

3.5 Lidar Observation

(a) NIES and Tohoku Institute of Technology
Compact Mie Scattering Lidar

3.6 Cloud and Water Vapor Observation

(a) CRL
CRL W-band cloud profiling radar “SPIDER”
Microwave Radiometer: WVR26, Radiometrics Co.

3.7 Surface Turbulent Flux Measurement system

(a) FORSGC and Okayama Univ.
Supersonic Thermoanemometer: DA-600, Kaijo Co.
Infrared Hygrometer: AH-300, Kaijo Co.
Inclinometer: MD-900-T, Appied Geomechanics
Accelerometer: OA700-020, Applied Signal Inc.
Rate Gyros: QRS-0050-100, Sytron Donner
CO_2/H_2O turbulence sensor: LI-7500, LICOR
Data Logging System: Labview, National Intsruments Co.

3.8 Solar Radiation and Ocean Color Observation

(a) MUK, Okayama Univ, Toba-CMT and Kinki Univ.
Polarization Spectral Radiometer: PSR1000, Opto Research Co.
Spectroradiometer: GER1500, Geophysical & Environmental Research Co.
Thermalinfrared Radiometer: CE312, CIMEL Electronique

3.9 Ocean State Profiling

(a) JAMSTEC; CTD casts
CTD system: CTD 9plus, Sea-Bird
Temperature Sensor. SBE3-04F, Sea-Bird Electronics, Inc.
Conductivity Sensor. SBE4-04/0, Sea-Bird Electronics, Inc.
Dissolved Oxygen Sensor. SBE13-04-B, Sea-Bird Electronics, Inc.
Deck Unit:SBE 11plus, Sea-Bird Electronics, Inc.
Altimeter sensor: PSA-9000, Datasonics Inc.
Carousel water sampler: SBE32, Sea-Bird Electronics, Inc.
Guildline Autosal salinometer:model 8400B
Software: SEASOFT ver. 4.232, Sea-Bird Electronics, Inc.
Titrator: Metrohm Model 716 DMS Titrino / 10 ml of titration vessel
Metrohm Pt Electrode / 6.0403.100 (NC)
Software: “The Brinkmann Titrino Workcell”

(b) MUK
Shallow-water measurement unit: Chlorothec ACL-220-RS, Alec Electronics Co.

3.10 Current Profiling

(a) JAMSTEC
Broad-Band ADCP: VM-75, RD Instrument.

3.11 Sea Surface Water Monitoring

(a) JAMSTEC

Thermosalinograph: SBE-21, Sea-Bird Electronics, Inc.
Thermometer: SBE3S, Sea-Bird Electronics, Inc.
Dissolved Oxygen Sensor: 2127, Oubisufair Laboratories
Fluorometer: 10-AU-005, Turner Designs
Particle Size Sensor: P-05, Nippon Kaiyo Ltd.
Flowmeter: EMARG2W, Aichi Watch Electronics Ltd.

3.12 Greenhouse Effect Gasses Measurement

(a) MUK

N_2O analyzer: Model 46C, Thermo Environmental Instruments Inc.
CO_2 analyzer: Model VIA-510, HORIBA Ltd.
NOx analyzer: Model 42C-TL, Thermo Environmental Instruments Inc.
N_2O analyzer: Model 43C, Thermo Environmental Instruments Inc.

3.13 CO2/PCO2 Measurement

(a) OUS

CO_2 analyzer: Model LI-6252 LI-COR, INC.
Gas mixing unit: Model SO96NL-T, S-ONE, INC.
Equilibrumeter: Model SO96NL-T, S-ONE, INC.
Titration manager: TIM900, Radiometer
Auto-burette: ABU901, Radiometer
pH glass electrode: pHG201-7, Radiometer
Reference operating software: Tim Talk9, Lab Soft

(b) JAMSTEC

Carbon Dioxide Coulometer: Model 5012, UIC Inc.
Non-dispersive infrared gas analyzer: BINOS Model 4.1, Fisher-Rosemount

3.14 Underway geophysics

(a) JAMSTEC

Onboard Gravity Meter: S-116, LaCoste-Romberg
Three-Axes Fluxgate Magnetometer: Tierra Tecnica
Multi-Narrow beam echo sounding system: SeaBeam 2100, SeaBeam Inc.

3.15 Miscellaneous

(a) JAMSTEC

Navigation System: SAINS19, Sena Co.
GMS Receiving System: Nippon Hakuyo
HRPT Receiving System: Terascan
Observation Data Acquisition System: SCS (Scientific Computer System), NOAA

4. Cruise Track and Log

4.1 Cruise Track

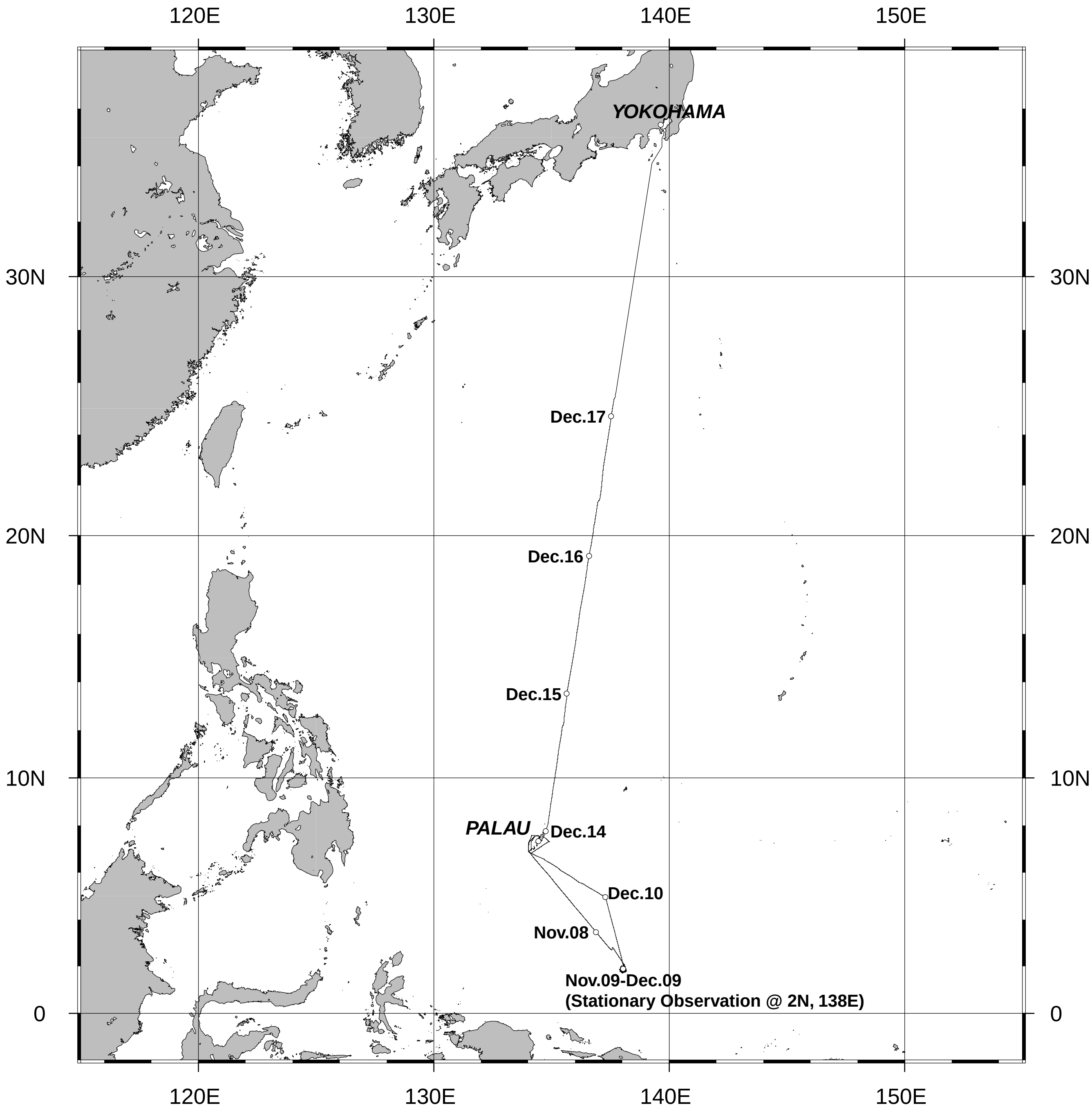

Ship Track (MR01K05) Leg3,4

Note: The position of each day is on 00UTC (09LST) of the day.

4.2 Cruise Log

Date	start (LST)	finish	Event	Lat.(deg.)	Lon. (deg.)
7-Nov	10:00		depart Koror		
	11:57		start surface water monitoring		
	13:00		start Doppler radar observation		
8-Nov	13:15	14:09	tethered radiosonde observation (around Mirai by powerboat)	2.71 N	137.53 E
	15:09	15:51	tethered radiosonde observation (around Mirai by powerboat)	2.81 N	137.59 E
	21:00		arrive stationary observation point	2.00 N	138.00 E
9-Nov	05:24		checking (2N,138E) TRITON buoy status	2.00 N	
	08:00		start stationary observation at (2N, 138E)	1.90 N	138.06 E
	08:39		RS (Radiosonde) -001 launch		
	08:40	09:10	CTD-001 (to 500m)		
	09:16	09:31	Shallow-water CTD casting (210m in wire length)		
	09:30	09:50	sea surface spectral radiance measurement		
	09:31		turbulent flux measurement		
	11:00	11:25	sea surface spectral radiance measurement		
	11:29		RS-002 launch		
	11:30	12:52	turbulent flux measurement		
	13:05	13:25	sea surface spectral radiance measurement		
	14:29		RS-003 launch		
	14:30	14:44	Shallow-water CTD casting		
	14:51	15:19	CTD-002 (500m)		
	15:27		turbulent flux measurement		
	17:29		RS-004 launch		
	17:30	18:55	turbulent flux measurement		
	20:39		RS-005 launch		
	20:43	21:22	CTD-003 (1000m)		
	21:30	21:43	Shallow-water CTD casting		
	21:44	22:45	turbulent flux measurement		
	23:29		RS-006 lanuch		
	23:40	01:10	turbulent flux measurement		
10-Nov	02:29		RS-007 launch		
	02:31	02:46	Shallow-water CTD casting		
	02:52	03:21	CTD-004 (500m)		
	03:22	04:32	turbulent flux measurement		
	05:29		RS-008 launch		
	05:30	06:50	turbulent flux measurement		
	08:20	08:47	CTD-005 (500m)		
	08:29		RS-009 launch		
	08:45	09:04	sea surface spectral radiance measurement		
	08:53	09:07	Shallow-water CTD casting		
	09:10	10:10	turbulent flux measurement		
	10:34	11:13	(2N, 138E) TRITON buoy operation: replace windvane		
	10:48	11:07	sea surface spectral radiance measurement		
	11:30		RS-010 launch		
	11:30	13:20	turbulent flux measurement		
	13:00	13:20	sea surface spectral radiance measurement		
	14:20	14:49	CTD-006 (500m)		
	14:30		RS-011 launch		
	14:45	15:03	sea surface spectral radiance measurement		
	14:55	15:08	Shallow-water CTD casting		
	15:10	16:30	turbulent flux measurement		
	17:29		RS-012 launch		
	17:29	18:52	turbulent flux measurement		
	20:20	21:14	CTD-007 (1000m)		
	20:29		RS-013 launch		
	21:19	21:32	Shallow-water CTD casting		
	21:35	22:36	turbulent flux measurement		
	23:29		RS-014 launch		
	23:30	01:05	turbulent flux measurement		
11-Nov	02:20	02:46	CTD-008 (500m)		
	02:29		RS-015 launch		
	02:51	03:04	Shallow-water CTD casting		
	03:05	04:20	turbulent flux measurement		
	05:39		RS-016 launch		

	05:40	06:55	turbulent flux measurement
	08:20	08:46	CTD-009 (500m)
	08:29		RS-017 launch
	08:51	09:03	Shallow-water CTD casting
	08:52	09:10	sea surface spectral radiance measurement
	09:10	10:15	turbulent flux measurement
	10:46	11:07	sea surface spectral radiance measurement
	11:29		RS-018 launch
	11:38	12:40	turbulent flux measurement
	13:02	13:20	sea surface spectral radiance measurement
	14:20	14:47	CTD-010 (500m)
	14:29		RS-019 launch
	14:52	15:05	Shallow-water CTD casting
	14:46	15:03	sea surface spectral radiance measurement
	15:06	16:20	turbulent flux measurement
	17:29		RS-020 launch
	17:30	17:44	satellite data receiving manuever
	17:44	19:15	turbulent flux measurement
	20:20	21:13	CTD-011 (1000m)
	20:29		RS-021 launch
	21:18	21:32	Shallow-water CTD casting
	21:34	22:40	turbulent flux measurement
	23:29		RS-022 launch
	23:34	00:58	turbulent flux measurement
12-Nov	02:20	02:45	CTD-012 (500m)
	02:29		RS-023 launch
	02:51	03:04	Shallow-water CTD casting
	03:10	04:15	turbulent flux measurement
	05:29		RS-024 launch
	05:30	07:03	turbulent flux measurement
	08:20	08:45	CTD-013 (500m)
	08:29		RS-025 launch
	08:49	09:02	Shallow-water CTD casting
	09:05	10:10	turbulent flux measurement
	10:45	11:09	sea surface spertor measurement
	11:29		RS-026 launch
	11:30	12:30	turbulent flux measurement
	12:33	14:18	CTD-014 (2000m)
	13:00	13:20	sea surface spertor measurement
	13:48	14:00	tethered radiosonde observation (on Mirai)
	14:23	14:49	CTD-015 (500m)
	14:30		RS-027 launch
	14:51	15:04	Shallow-water CTD casting
	14:45	15:05	sea surface spertor measurement
	15:05	16:05	turbulent flux measurement
	17:29		RS-028 launch
	17:33	19:00	turbulent flux measurement
	20:20	21:14	CTD-016 (1000m)
	20:29		RS-029 launch
	21:17	21:30	Shallow-water CTD casting
	21:30	22:35	turbulent flux measurement
	23:29		RS-030 launch
	23:35	01:05	turbulent flux measurement
13-Nov	02:20	02:46	CTD-017 (500m)
	02:29		RS-031 launch
	02:49	03:03	Shallow-water CTD casting
	03:05	04:25	turbulent flux measurement
	05:29		RS-032 launch
	05:33	07:00	turbulent flux measurement
	08:20	08:46	CTD-018 (500m)
	08:29		RS-033 launch
	08:45	09:01	sea surface spectral radiance measurement
	08:49	09:02	Shallow-water CTD casting
	09:04	10:10	turbulent flux measurement
	11:29		RS-034 launch
	11:30	13:07	turbulent flux measurement
	13:10	13:25	sea surface spectral radiance measurement
	14:20	14:45	CTD-019 (500m)
	14:29		RS-035 launch

	14:48	15:01	Shallow-water CTD casting
	15:05	16:15	turbulent flux measurement
	16:55	17:15	tethered radiosonde observation (on Mirai)
	17:39		RS-036 launch
	17:39	19:05	turbulent flux measurement
	20:20	21:09	CTD-020 (1000m)
	20:29		RS-037 launch
	21:13	21:26	Shallow-water CTD casting
	21:27	22:30	turbulent flux measurement
	23:29		RS-038 launch
	23:30	01:00	turbulent flux measurement
14-Nov	02:20	02:46	CTD-021 (500m)
	02:29		RS-039 launch
	02:50	03:04	Shallow-water CTD casting
	03:05	04:20	turbulent flux measurement
	05:29		RS-040 launch
	05:30	07:05	turbulent flux measurement
	08:20	08:45	CTD-022 (500m)
	08:29		RS-041 launch
	08:45	09:06	sea surface spectral radiance measurement
	08:48	09:01	Shallow-water CTD casting
	09:07	10:13	turbulent flux measurement
	10:45	11:15	sea surface spectral radiance measurement
	11:29		RS-042 launch
	11:35	12:55	turbulent flux measurement
	13:01	13:20	sea surface spectral radiance measurement
	13:53	14:12	tethered radiosonde observation (on Mirai)
	14:20	14:44	CTD-023 (500m)
	14:29		RS-043 launch
	14:47		sea surface spectral radiance measurement
	14:47	15:00	Shallow-water CTD casting
	15:05	16:10	turbulent flux measurement
	17:29		RS-044 launch
	17:34	19:05	turbulent flux measurement
	20:20	21:12	CTD-024 (1000m)
	20:29		RS-045 launch
	21:16	21:29	Shallow-water CTD casting
	21:35	22:35	turbulent flux measurement
	23:00	23:17	tethered radiosonde observation (on Mirai)
	23:39		RS-046 launch
	23:43	01:10	turbulent flux measurement
15-Nov	02:20	02:44	CTD-025 (500m)
	02:30		RS-047 launch
	02:48	03:00	Shallow-water CTD casting
	03:05	04:15	turbulent flux measurement
	05:29		RS-048 launch
	05:33	07:05	turbulent flux measurement
	08:20	08:44	CTD-026 (500m)
	08:29		RS-049 launch
	08:46	09:00	Shallow-water CTD casting
	08:48	09:01	sea surface spectral radiance measurement
	09:05	10:05	turbulent flux measurement
	10:58	11:11	sea surface spectral radiance measurement
	11:29		RS-050 launch
	11:30	12:31	turbulent flux measurement
	13:00	13:17	sea surface spectral radiance measurement
	14:20	14:46	CTD-027 (500m)
	14:30		RS-051 launch
	14:44	15:03	sea surface spectral radiance measurement
	14:49	15:03	Shallow-water CTD casting
	15:05	16:17	turbulent flux measurement
	17:29		RS-052 launch
	17:55		turbulent flux measurement
	20:20	21:11	CTD-028 (1000m)
			pause 6-hourly CTD obs.
	20:29		RS-053 launch
	21:15	21:27	Shallow-water CTD casting
	21:30	22:30	turbulent flux measurement
	23:29		RS-054 launch

	23:30	01:02	turbulent flux measurement
16-Nov	02:29		RS-055 launch
	02:35	04:05	turbulent flux measurement
	05:29		RS-056 launch
	05:33	07:08	turbulent flux measurement
			start 3-hourly CTD obs.
	08:20	08:45	CTD-029 (500m)
	08:30		RS-057 launch
	08:47	09:01	Shallow-water CTD casting
	09:08	10:15	turbulent flux measurement
	10:43		sea surface spectral radiance measurement
	11:18	11:43	CTD-030 (500m)
	11:29		RS-058 launch
	11:46	11:59	Shallow-water CTD casting
	12:00	13:00	turbulent flux measurement
	14:20	14:45	CTD-031 (500m)
	14:30		RS-059 launch
	14:47	15:00	sea surface spectral radiance measurement
	14:48	15:02	Shallow-water CTD casting
	15:05	16:10	turbulent flux measurement
	17:17	17:42	CTD-032 (500m)
	17:29		RS-060 launch
	17:46	18:00	Shallow-water CTD casting
	18:00	19:15	turbulent flux measurement
	20:20	21:15	CTD-033 (1000m)
	20:29		RS-061 launch
	21:18	21:31	Shallow-water CTD casting
	21:32	22:32	turbulent flux measurement
	23:20	23:45	CTD-034 launch
	23:39		RS-062 launch
	23:59	00:01	Shallow-water CTD casting
17-Nov	00:02	01:12	turbulent flux measurement
	02:20	02:44	CTD-035 (500m)
	02:29		RS-063 launch
	02:48	03:05	Shallow-water CTD casting
	03:05	04:12	turbulent flux measurement
	05:18	05:43	CTD-036 (500m)
	05:39		RS-064 launch
	05:47	06:00	Shallow-water CTD casting
	06:00	07:15	turbulent flux measurement
	08:19	08:45	CTD-037 (500m)
	08:29		RS-065 launch
	08:48	09:02	Shallow-water CTD casting
	09:04	10:05	turbulent flux measurement
	10:45	11:05	sea surface spectral radiance measurement
	11:19	11:46	CTD-038 (500m)
	11:29		RS-066 launch
	11:47	12:00	Shallow-water CTD casting
	12:00	13:18	turbulent flux measurement
	13:00	13:18	sea surface spectral radiance measurement
	14:20	14:47	CTD-039 (500m)
	14:40		RS-067 launch
	14:49	15:03	Shallow-water CTD casting
	15:05	16:13	turbulent flux measurement
	16:30	16:43	sea surface spectral radiance measurement
	17:18	17:42	CTD-040 (500m)
	17:30		RS-068 launch
	17:45	17:58	Shallow-water CTD casting
	18:00	19:15	turbulent flux measurement
	20:18	21:08	CTD-041 (1000m)
	20:29		RS-069 launch
	21:10	21:24	Shallow-water CTD casting
	21:25	22:25	turbulent flux measurement
	23:20	23:43	CTD-042 (500m)
	23:29		RS-070 launch
	23:47	23:59	Shallow-water CTD casting
18-Nov	00:00	01:13	turbulent flux measurement
	02:19	02:45	CTD-043 (500m)
	02:29		RS-071 launch

	02:49	03:03	Shallow-water CTD casting
	03:05	04:15	turbulent flux measurement
	05:18	05:44	CTD-044 (500m)
	05:30		RS-072 launch
	05:47	06:03	Shallow-water CTD casting
	06:05	07:18	turbulent flux measurement
	08:19	08:43	CTD-045 (500m)
	08:29		RS-073 launch
	08:46	08:59	Shallow-water CTD casting
	08:49	08:59	sea surface spectral radiance measurement
	09:00	10:10	turbulent flux measurement
	10:46	10:57	sea surface spectral radiance measurement
	11:18	11:43	CTD-046 (500m)
	11:46	11:59	Shallow-water CTD casting
	11:49		RS-074 launch
	12:00	13:12	turbulent flux measurement
	14:18	14:49	CTD-047 (500m)
	14:30		RS-075 launch
	14:52	15:06	Shallow-water CTD casting
	15:06	16:17	turbulent flux measurement
	17:16	17:41	CTD-048 (500m)
	17:30		RS-076 launch
	17:44	17:57	Shallow-water CTD casting
	18:00	19:12	turbulent flux measurement
	20:18	21:16	CTD-049 (1000m)
	20:29		RS-077 launch
	21:19	21:32	Shallow-water CTD casting
	21:35	22:35	turbulent flux measurement
	23:18	23:47	CTD-050 (500m)
	23:29		RS-078 launch
	23:50	00:04	Shallow-water CTD casting
19-Nov	00:05	01:18	turbulent flux measurement
	02:18	02:46	CTD-051 (500m)
	02:29		RS-079 launch
	02:49	03:01	Shallow-water CTD casting
	03:05	04:15	turbulent flux measurement
	05:18	05:43	CTD-052 (500m)
	05:29		RS-080 launch
	05:45	05:58	Shallow-water CTD casting
	06:00	07:20	turbulent flux measurement
	08:18	08:44	CTD-053 (500m)
	08:29		RS-081 launch
	08:47	09:00	Shallow-water CTD casting
	08:50	09:02	sea surface spectral radiance measurement
	09:05	10:05	turbulent flux measurement
	10:47	11:57	sea surface spectral radiance measurement
	11:18	11:43	CTD-054 (500m)
	11:29		RS-082 launch
	11:46	11:59	Shallow-water CTD casting
	12:00	13:07	turbulent flux measurement
	14:19	14:45	CTD-055 (500m)
	14:29		RS-083 launch
	14:47	15:00	Shallow-water CTD casting
	15:05	16:18	turbulent flux measurement
	16:30	16:45	sea surface spectral radiance measurement
	17:16	17:43	CTD-056 (500m)
	17:29		RS-084 launch
	17:46	17:58	Shallow-water CTD casting
	18:00	19:15	turbulent flux measurement
	20:19	21:09	CTD-057 (1000m)
	20:29		RS-085 launch
	21:12	21:25	Shallow-water CTD casting
	21:30	22:30	turbulent flux measurement
	23:18	23:44	CTD-058 (500m)
	23:29		RS-086 launch
	23:47	23:59	Shallow-water CTD casting
20-Nov	00:00	01:17	turbulent flux measurement
	02:19	02:47	CTD-059 (500m)
	02:29		RS-087 launch

	02:48	03:01	Shallow-water CTD casting
	03:03	04:15	turbulent flux measurement
	05:19	05:45	CTD-060 (500m)
	05:29		RS-088 launch
	05:48	06:01	Shallow-water CTD casting
	06:05	07:20	turbulent flux measurement
	08:18	08:45	CTD-061 (500m)
	08:29		RS-089 launch
	08:45		sea surface spectral radiance measurement
	08:49	09:03	Shallow-water CTD casting
	09:05	10:33	turbulent flux measurement
	10:45	10:58	sea surface spectral radiance measurement
	11:18	11:45	CTD-062 (500m)
	11:30		RS-090 launch
	11:47	12:00	Shallow-water CTD casting
	12:05	13:13	turbulent flux measurement
	14:18	14:46	CTD-063 (500m)
	14:30		RS-091 launch
	14:48	15:01	Shallow-water CTD casting
	15:02	16:23	turbulent flux measurement
	17:18	17:46	CTD-064 (500m)
	17:39		RS-092 launch
	17:49	18:02	Shallow-water CTD casting
	18:02	19:20	turbulent flux measurement
	20:19	21:09	CTD-065 (1000m)
	20:29		RS-093 launch
	21:12	21:25	Shallow-water CTD casting
	21:27	22:27	turbulent flux measurement
	23:18	23:44	CTD-066 (500m)
	23:19		RS-094 launch
	23:47	00:00	Shallow-water CTD casting
21-Nov	00:00	01:17	turbulent flux measurement
	02:19	02:45	CTD-067 (500m)
	02:29		RS-095 launch
	02:49	03:02	Shallow-water CTD casting
	03:03	04:20	turbulent flux measurement
	05:19	05:45	CTD-068 (500m)
	05:30		RS-096 launch
	05:48	06:01	Shallow-water CTD casting
	06:02	07:15	turbulent flux measurement
	08:17	08:43	CTD-069 (500m)
	08:29		RS-097 launch
	08:46	08:59	Shallow-water CTD casting
	08:49	09:04	sea surface spectral radiance measurement
	09:05	10:25	turbulent flux measurement
	10:45		sea surface spectral radiance measurement
	11:18	11:43	CTD-070 (500m)
	11:29		RS-098 launch
	11:46	11:59	Shallow-water CTD casting
	12:00	13:13	turbulent flux measurement
	13:30	13:47	sea surface spectral radiance measurement
	14:16	14:43	CTD-071 (500m)
	14:29		RS-099 launch
	14:45	14:58	Shallow-water CTD casting
	15:00	16:17	turbulent flux measurement
	17:17	17:41	CTD-072 (500m)
	17:30		RS-100 launch
	17:44	17:57	Shallow-water CTD casting
	18:00	19:20	turbulent flux measurement
	20:18	21:12	CTD-073 (1000m)
	20:29		RS-101 launch
	21:17	21:32	Shallow-water CTD casting
	21:33	22:33	turbulent flux measurement
	23:24	23:52	CTD-074 (500m)
	23:29		RS-102 launch
	23:56	00:09	Shallow-water CTD casting
22-Nov	00:11	01:15	turbulent flux measurement
	02:19	02:45	CTD-075 (500m)
	02:29		RS-103 launch

	02:48	03:01	Shallow-water CTD casting
	03:02	04:15	turbulent flux measurement
	05:17	05:43	CTD-076 (500m)
	05:29		RS-104 launch
	05:46	05:59	Shallow-water CTD casting
	06:00	07:10	turbulent flux measurement
	08:17	08:41	CTD-077 (500m)
	08:29		RS-105 launch
	08:44	08:57	Shallow-water CTD casting
	08:51	09:00	sea surface spectral radiance measurement
	09:00	10:20	turbulent flux measurement
	10:47	10:58	sea surface spectral radiance measurement
	11:16	11:41	CTD-078 (500m)
	11:29		RS-106 launch
	11:43	11:56	Shallow-water CTD casting
	12:00	13:14	turbulent flux measurement
	13:28	13:42	sea surface spectral radiance measurement
	14:17	14:45	CTD-079 (500m)
	14:29		RS-107 launch
	14:48	15:02	Shallow-water CTD casting
	15:05	16:14	turbulent flux measurement
	17:17	17:43	CTD-080 (500m)
	17:29		RS-108 launch
	17:45	17:59	Shallow-water CTD casting
	18:00	19:15	turbulent flux measurement
	20:18	21:12	CTD-081 (1000m)
	20:29		RS-109 launch
	21:15	21:28	Shallow-water CTD casting
	21:30	22:30	turbulent flux measurement
	23:21	23:48	CTD-082 (500m)
	23:29		RS-110 launch
	23:51	00:04	Shallow-water CTD casting
23-Nov	00:07	01:05	turbulent flux measurement
	02:18	02:43	CTD-083 (500m)
	02:29		RS-111 launch
	02:45	02:58	Shallow-water CTD casting
	03:00	04:13	turbulent flux measurement
	05:17	05:40	CTD-084 (500m)
	05:29		RS-112 launch
	05:43	05:58	Shallow-water CTD casting
	06:00	07:17	turbulent flux measurement
	08:17	09:01	CTD-085 (1000m)
	08:29		RS-113 launch
	09:05	09:18	Shallow-water CTD casting
	09:20	10:20	turbulent flux measurement
	10:46	10:58	sea surface spectral radiance measurement
	11:16	11:42	CTD-086 (500m)
	11:29		RS-114 launch
	11:49	12:02	Shallow-water CTD casting
	12:07	13:05	turbulent flux measurement
	13:30	13:45	sea surface spectral radiance measurement
	14:19	14:45	CTD-087 (500m)
	14:30		RS-115 launch
	14:48	15:01	Shallow-water CTD casting
	15:05	16:00	turbulent flux measurement
	16:40	16:42	sea surface spectral radiance measurement
	17:17	17:42	CTD-088 (500m)
	17:29		RS-116 launch
	17:44	17:57	Shallow-water CTD casting
	18:00	19:10	turbulent flux measurement
	20:27	21:18	CTD-089 (1000m)
	20:29		RS-117 launch
	21:20	21:34	Shallow-water CTD casting
	21:35	22:23	turbulent flux measurement
	23:18	23:42	CTD-090 (500m)
	23:29		RS-118 launch
	23:44	23:57	Shallow-water CTD casting
24-Nov	00:00	01:03	turbulent flux measurement
	02:18	02:44	CTD-091 (500m)

	02:29		RS-119 launch
	02:48	03:00	Shallow-water CTD casting
	03:03	04:05	turbulent flux measurement
	05:17	05:42	CTD-092 (500m)
	05:39		RS-120 launch
	05:45	05:58	Shallow-water CTD casting
	06:00	07:05	turbulent flux measurement
	08:17	08:43	CTD-093 (500m)
	08:29		RS-121 launch
	08:45	08:58	Shallow-water CTD casting
	09:00	10:05	turbulent flux measurement
	11:17	11:41	CTD-094 (500m)
	11:29		RS-122 launch
	11:44	11:56	Shallow-water CTD casting
	11:57	12:55	turbulent flux measurement
	12:57	13:16	sea surface spectral radiance measurement
	14:16	14:41	CTD-095 (500m)
	14:29		RS-123 launch
	14:43	14:55	Shallow-water CTD casting
	15:00	15:58	turbulent flux measurement
	16:05	16:10	sea surface spectral radiance measurement
	17:15	17:38	CTD-096 (500m)
	17:30		RS-124 launch
	17:40	17:52	Shallow-water CTD casting
	17:53	19:05	turbulent flux measurement
	20:18	21:12	CTD-097 (1000m)
	20:29		RS-125 launch
	21:15	21:28	Shallow-water CTD casting
	21:30	22:20	turbulent flux measurement
	23:17	23:43	CTD-098 (500m)
	23:29		RS-126 launch
	23:46	00:00	Shallow-water CTD casting
25-Nov	00:02	01:00	turbulent flux measurement
	02:19	02:45	CTD-099 (500m)
	02:29		RS-127 launch
	02:47	02:59	Shallow-water CTD casting
	03:00	04:10	turbulent flux measurement
	05:17	05:42	CTD-100 (500m)
	05:29		RS-128 launch
	05:44	05:57	Shallow-water CTD casting
	06:00	07:07	turbulent flux measurement
	08:16	08:40	CTD-101 (500m)
	08:31		RS-129 launch
	08:42	08:55	Shallow-water CTD casting
	08:48	08:58	sea surface spectral radiance measurement
	08:58	10:10	turbulent flux measurement
	10:47		sea surface spectral radiance measurement
	11:18	11:41	CTD-102 (500m)
	11:39		RS-130 launch
	11:43	11:56	Shallow-water CTD casting
	12:00	12:45	turbulent flux measurement
	13:01	13:20	sea surface spectral radiance measurement
	14:17	14:41	CTD-103 (500m)
	14:39		RS-131 launch
	14:45	14:58	Shallow-water CTD casting
	15:00	16:00	turbulent flux measurement
	16:30	16:45	sea surface spectral radiance measurement
	17:17	17:42	CTD-104 (500m)
	17:29		RS-132 launch
	17:45	17:58	Shallow-water CTD casting
	17:58	19:10	turbulent flux measurement
	20:17	21:10	CTD-105 (1000m)
	20:29		RS-133 launch
	21:12	21:25	Shallow-water CTD casting
	21:26	22:26	turbulent flux measurement
	23:18	23:43	CTD-106 (500m)
	23:29		RS-134 launch
	23:45	23:58	Shallow-water CTD casting
26-Nov	00:00	01:05	turbulent flux measurement

	02:19	02:42	CTD-107 (500m)
	02:29		RS-135 launch
	02:45	02:58	Shallow-water CTD casting
	03:00	04:05	turbulent flux measurement
	05:16	05:39	CTD-108 (500m)
	05:30		RS-136 launch
	05:41	05:54	Shallow-water CTD casting
	05:55	07:10	turbulent flux measurement
	08:16	08:40	CTD-109 (500m)
	08:29		RS-137 (500m)
	08:44	08:56	Shallow-water CTD casting
	08:50	08:57	sea surface spectral radiance measurement
	08:58	10:00	turbulent flux measurement
	10:50	10:59	sea surface spectral radiance measurement
	11:17	11:41	CTD-110 (500m)
	11:30		RS-138 launch
	11:44	11:57	Shallow-water CTD casting
	12:00	13:00	turbulent flux measurement
	13:04	13:24	sea surface spectral radiance measurement
	13:57	14:10	tethered radiosonde observation (on Mirai)
	14:16	14:41	CTD-111 (500m)
	14:29		RS-139 launch
	14:44	14:56	Shallow-water CTD casting
	15:00	16:03	turbulent flux measurement
	16:30	15:43	sea surface spectral radiance measurement
	17:16	17:39	CTD-112 (500m)
	17:29		RS-140 launch
	17:41	17:54	Shallow-water CTD casting
	17:55	19:00	turbulent flux measurement
	20:18	21:06	CTD-113 (1000m)
	20:29		RS-141 launch
	21:08	21:21	Shallow-water CTD casting
	21:23	21:25	turbulent flux measurement
	22:53	23:10	tethered radiosonde observation (on Mirai)
	23:17	23:41	CTD-114 (500m)
	23:29		RS-142 launch
	23:43	23:55	Shallow-water CTD casting
27-Nov	00:00	01:07	turbulent flux measurement
	02:17	02:42	CTD-115 (500m)
	02:29		RS-143 launch
	02:46	02:59	Shallow-water CTD casting
	03:00	04:07	turbulent flux measurement
	05:16	05:40	CTD-116 (500m)
	05:29		RS-144 launch
	05:43	05:56	Shallow-water CTD casting
	05:56	07:00	turbulent flux measurement
	08:16	08:40	CTD-117 (500m)
	08:29		RS-145 launch
	08:42	08:55	Shallow-water CTD casting
	08:55	10:18	turbulent flux measurement
	10:50	10:56	sea surface spectral radiance measurement
	11:17	11:40	CTD-118 (500m)
	11:29		RS-146 launch
	11:43	11:55	Shallow-water CTD casting
	11:55	12:48	turbulent flux measurement
	13:15		sea surface spectral radiance measurement
	14:19	14:40	CTD-119 (500m)
	14:29		RS-147 launch
	14:43	14:55	Shallow-water CTD casting
	15:00	16:00	turbulent flux measurement
	17:17	17:39	CTD-120 (500m)
	17:29		RS-148 launch
	17:42	17:54	Shallow-water CTD casting
	18:00	19:07	turbulent flux measurement
	20:17	21:08	CTD-121 (1000m)
	20:29		RS-149 launch
	21:11	21:23	Shallow-water CTD casting
	21:25	22:25	turbulent flux measurement
	23:22	23:46	CTD-122 (500m)

	23:29		RS-150 launch
	23:49	00:01	Shallow-water CTD casting
28-Nov	00:03	01:13	turbulent flux measurement
	02:18	02:43	CTD-123 (500m)
	02:29		RS-151 launch
	02:55	04:10	turbulent flux measurement
	05:18	05:42	CTD-124 (500m)
	05:29		RS-152 launch
	05:44	05:57	Shallow-water CTD casting
	06:00	07:05	turbulent flux measurement
	08:16	08:39	CTD-125 (500m)
	08:29		RS-153 launch
	08:41	08:54	Shallow-water CTD casting
	08:46	08:58	sea surface spectral radiance measurement
	09:00	10:20	turbulent flux measurement
	10:47		sea surface spectral radiance measurement
	11:17	11:38	CTD-126 (500m)
	11:29		RS-154 launch
	11:41	11:54	Shallow-water CTD casting
	12:07	13:15	turbulent flux measurement
	13:03	13:15	sea surface spectral radiance measurement
	14:17	14:40	CTD-127 (500m)
	14:29		RS-155 launch
	14:43	14:56	Shallow-water CTD casting
	15:00	16:08	turbulent flux measurement
	17:15	17:39	CTD-128 (500m)
	17:29		RS-156 launch
	17:41	17:54	Shallow-water CTD casting
	17:57	19:08	turbulent flux measurement
	20:17	21:08	CTD-129 (1000m)
	20:29		RS-157 launch
	21:11	21:24	Shallow-water CTD casting
	21:26	22:27	turbulent flux measurement
	23:17	23:40	CTD-130 (500m)
	23:29		RS-158 launch
	23:43	23:56	Shallow-water CTD casting
29-Nov	00:00	01:13	turbulent flux measurement
	02:17	02:41	CTD-131 (500m)
	02:29		RS-159 launch
	02:43	02:55	Shallow-water CTD casting
	02:57	04:05	turbulent flux measurement
	05:16	05:39	CTD-132 (500m)
	05:29		RS-160 launch
	05:41	05:54	Shallow-water CTD casting
	05:56	07:05	turbulent flux measurement
	08:16	08:40	CTD-133 (500m)
	08:29		RS-161 launch
	08:43	08:57	Shallow-water CTD casting
	08:47	08:57	sea surface spectral radiance measurement
	08:58	10:17	turbulent flux measurement
	10:48	10:58	sea surface spectral radiance measurement
	11:16	11:40	CTD-134 (500m)
	11:29		RS-162 launch
	11:42	11:55	Shallow-water CTD casting
	11:58	12:55	turbulent flux measurement
	13:00	13:24	sea surface spectral radiance measurement
	14:16	14:40	CTD-135 (500m)
	14:29		RS-163 launch
	14:42	14:54	Shallow-water CTD casting
	14:55	16:10	turbulent flux measurement
	16:30		sea surface spectral radiance measurement
	17:16	17:40	CTD-136 (500m)
	17:29		RS-164 launch
	17:42	17:55	Shallow-water CTD casting
	17:56	19:15	turbulent flux measurement
	20:17	21:04	CTD-137 (1000m)
	20:29		RS-165 launch
	21:06	21:19	Shallow-water CTD casting
	21:20	22:29	turbulent flux measurement

	23:17	23:39	CTD-138 (500m)
	23:29		RS-166 launch
	23:42	23:54	Shallow-water CTD casting
	23:56	01:15	turbulent flux measurement
30-Nov	02:16	02:41	CTD-139 (500m)
	02:29		RS-167 launch
	02:44	02:57	Shallow-water CTD casting
	03:00	04:10	turbulent flux measurement
	05:16	05:40	CTD-140 (500m)
	05:29		RS-168 launch
	05:42	05:56	Shallow-water CTD casting
	05:57	07:10	turbulent flux measurement
	08:15	08:39	CTD-141 (500m)
	08:29		RS-169 launch
	08:42	08:56	Shallow-water CTD casting
	08:50	09:01	sea surface spectral radiance measurement
	09:02	10:15	turbulent flux measurement
	10:45	10:56	sea surface spectral radiance measurement
	11:15	11:39	CTD-142 (500m)
	11:29		RS-170 launch
	11:41	11:54	Shallow-water CTD casting
	12:00	13:15	turbulent flux measurement
	13:00	13:15	sea surface spectral radiance measurement
	14:15	14:39	CTD-143 (500m)
	14:29		RS-171 launch
	14:50	16:09	turbulent flux measurement
	16:28	16:50	sea surface spectral radiance measurement
	17:17	17:39	CTD-144 (500m)
	17:29		RS-172 launch
	17:42	17:54	Shallow-water CTD casting
	18:56	19:10	turbulent flux measurement
	20:17	21:07	CTD-145 (1000m)
	20:29		RS-173 launch
	21:10	21:22	Shallow-water CTD casting
			finish 3-hourly CTD obs. : resume 6-hourly CTD obs.
	21:25	22:35	turbulent flux measurement
	23:29		RS-174 launch
	23:35	01:16	turbulent flux measurement
1-Dec	02:19	02:42	CTD-146 (500m)
	02:29		RS-175 launch
	02:45	03:47	turbulent flux measurement
	05:29		RS-176 launch
	05:34	06:36	turbulent flux measurement
	08:16	08:41	CTD-147 (500m)
	08:29		RS-177 launch
	08:45	09:45	turbulent flux measurement
	10:44	10:46	sea surface spectral radiance measurement
	11:29		RS-178 launch
	11:30	12:18	turbulent flux measurement
	13:36	13:43	tethered radiosonde observation (on Mirai)
	13:45	14:25	tethered rasiodonde observation (around Mirai, by powerboat)
	14:34	13:59	CTD-148 (500m)
	14:49		RS-179 launch
	15:00	16:12	turbulent flux measurement
	16:30	16:47	sea surface spectral radiance measurement
	16:57	17:06	tethered rasiodonde observation (on Mirai)
	17:29		RS-180 launch
	17:32	18:32	turbulent flux measurement
	20:16	21:04	CTD-149 (1000m)
	20:29		RS-181 launch
	21:05	22:35	turbulent flux measurement
	23:29		RS-182 launch
	23:30	01:05	turbulent flux measurement
2-Dec	02:16	02:40	CTD-150 (500m)
	02:29		RS-183 launch
	02:45	03:50	turbulent flux measurement
	05:29		RS-184 launch
	05:33	06:35	turbulent flux measurement
	08:16	08:43	CTD-151 (500m)

	08:29		RS-185 launch
	08:45	08:55	sea surface spectral radiance measurement
	08:45	09:45	turbulent flux measurement
	11:29		RS-186 launch
	11:40	13:00	turbulent flux measurement
	14:15	14:39	CTD-152 (500m)
	14:29		RS-187 launch
	14:30	15:50	turbulent flux measurement
	17:29		RS-188 launch
	17:32	18:33	turbulent flux measurement
	20:15	21:05	CTD-153 (1000m)
	20:29		RS-189 launch
	21:06	22:06	turbulent flux measurement
	23:30		RS-190 launch
	23:30	00:55	turbulent flux measurement
3-Dec	02:16	02:41	CTD-154 (500m)
	02:29		RS-191 launch
	02:45	03:48	turbulent flux measurement
	05:29		RS-192 launch
	05:35	06:35	turbulent flux measurement
	08:17	08:58	CTD-155 (500m)
	08:30		RS-193 launch
	08:44	08:58	sea surface spectral radiance measurement
	09:00	10:03	turbulent flux measurement
	10:49	11:00	sea surface spectral radiance measurement
	11:29		RS-194 launch
	11:30	12:30	turbulent flux measurement
	13:06	13:46	(2N, 138E) TRITON buoy operation for special sensors: change raingauge logger and recover GPS system
	14:15	14:39	CTD-156 (500m)
	14:29		RS-195 launch
	15:00	16:20	turbulent flux measurement
	17:29		RS-196 launch
	17:32	18:32	turbulent flux measurement
	20:17	21:09	CTD-157 (1000m)
	20:30		RS-197 launch
	21:10	22:10	turbulent flux measurement
	23:29		RS-198 launch
	23:30	00:57	turbulent flux measurement
4-Dec	02:17	02:42	CTD-158 (500m)
	02:30		RS-199 launch
	02:45	04:10	turbulent flux measurement
	05:29		RS-200 launch
	05:34	06:34	turbulent flux measurement
	08:17	09:06	CTD-159 (1000m)
	08:29		RS-201 launch
	08:49	08:59	sea surface spectral radiance measurement
	09:08	09:21	Shallow-water CTD casting
	09:24	10:15	turbulent flux measurement
	10:48	10:58	sea surface spectral radiance measurement
	11:29		RS-202 launch
	11:30	12:50	turbulent flux measurement
	13:50		sea surface spectral radiance measurement
	14:15	14:39	CTD-160 (500m)
	14:29		RS-203 launch
	14:42	14:55	Shallow-water CTD casting
	15:00	16:10	turbulent flux measurement
	16:29	16:42	sea surface spectral radiance measurement
	17:29		RS-204 launch
	17:34	18:38	turbulent flux measurement
	20:16	21:03	CTD-161 (1000m)
	20:29		RS-205 launch
	21:05	21:18	Shallow-water CTD casting
	21:20	22:15	turbulent flux measurement
	23:30		RS-206 launch
	23:30	00:55	turbulent flux measurement
5-Dec	02:16	02:40	CTD-162 (500m)
	02:29		RS-207 launch
	02:43	02:56	Shallow-water CTD casting

	03:00	04:15	turbulent flux measurement
	05:29		RS-208 launch
	05:35	06:36	turbulent flux measurement
	08:19	09:12	CTD-163 (1000m)
	08:29		RS-209 launch
	09:15	09:28	Shallow-water CTD casting
	08:43	08:57	sea surface spectral radiance measurement
	09:30	10:15	turbulent flux measurement
	10:44	10:55	sea surface spectral radiance measurement
	11:29		RS-210 launch
	11:30	12:40	turbulent flux measurement
	14:16	14:40	CTD-164 (500m)
	14:49		RS-211 launch
	14:55	15:08	Shallow-water CTD casting
	15:10	16:15	turbulent flux measurement
	17:29		RS-212 launch
	17:34	19:15	turbulent flux measurement
	20:19		RS-213 launch
	20:23	21:12	CTD-165 (1000m)
	21:14	21:27	Shallow-water CTD casting
	21:30	22:27	turbulent flux measurement
	23:29		RS-214 launch
	23:30	01:06	turbulent flux measurement
6-Dec	02:19		RS-215 launch
	02:25	02:51	CTD-166 (500m)
	02:53	03:06	Shallow-water CTD casting
	03:10	04:36	turbulent flux measurement
	05:29		RS-216 launch
	05:35	06:39	turbulent flux measurement
	08:19		RS-217 launch
	08:23	09:09	CTD-167 (1000m)
	08:45	08:55	sea surface spectral radiance measurement
	09:12	09:25	Shallow-water CTD casting
	09:27	10:27	turbulent flux measurement
	10:45	10:55	sea surface spectral radiance measurement
	11:29		RS-218 launch
	11:32	12:33	turbulent flux measurement
	14:15	14:39	CTD-168 (500m)
	14:29		RS-219 launch
	14:40	16:20	turbulent flux measurement
	17:29		RS-220 launch
	17:35	19:15	turbulent flux measurement
	20:17	21:07	CTD-169 (1000m)
	20:29		RS-221 launch
	21:10	22:40	turbulent flux measurement
	23:30		RS-222 launch
	23:40	00:58	turbulent flux measurement
7-Dec	02:17	02:41	CTD-170 (500m)
	02:30		RS-223 launch
	02:45	03:55	turbulent flux measurement
	05:29		RS-224 launch
	05:34	06:37	turbulent flux measurement
	08:15	08:40	CTD-171 (500m)
	08:29		RS-225 launch
	08:40	09:43	turbulent flux measurement
	10:45	10:57	sea surface spectral radiance measurement
	11:29		RS-226 launch
	11:30	12:45	turbulent flux measurement
	14:14	14:39	CTD-172 (500m)
	14:29		RS-227 launch
	14:40	16:15	turbulent flux measurement
	17:29		RS-228 launch
	17:36	19:08	turbulent flux measurement
	20:15	21:04	CTD-173 (1000m)
	20:29		RS-229 launch
	21:05	22:05	turbulent flux measurement
	23:29		RS-230 launch
	23:30	00:45	turbulent flux measurement
8-Dec	02:16	02:40	CTD-174 (500m)

	02:30		RS-231 launch				
	02:45	03:58	turbulent flux measurement				
	05:30		RS-232 launch				
	05:40	06:42	turbulent flux measurement				
	08:16	08:41	CTD-175 (500m)				
	08:29		RS-233 launch				
	08:42	09:45	turbulent flux measurement				
	08:47	08:57	sea surface spectral radiance measurement				
	11:30		RS-234 launch				
	11:35	12:55	turbulent flux measurement				
	14:14	14:38	CTD-176 (500m)				
	14:30		RS-235 launch				
	14:40	15:45	turbulent flux measurement				
	17:30		RS-236 launch				
	17:36	19:15	turbulent flux measurement				
	20:16	21:08	CTD-177 (1000m)				
	20:29		RS-237 launch				
	21:10	22:40	turbulent flux measurement				
	23:30		RS-238 launch				
	23:35	01:15	turbulent flux measurement				
9-Dec	02:16	02:40	CTD-178 (500m)				
	02:50		RS-239 launch				
	02:55	03:57	turbulent flux measurement				
	05:30		RS-240 launch				
	05:33	06:37	turbulent flux measurement				
	08:16	08:40	CTD-179 (500m)				
	08:30		RS-241 launch				
	09:00		finish stationary observation at (2N, 138E)				
	13:05		pause surface water monitoring				
10-Dec	08:54	09:27	(5N, 137E) TRITON buoy operation: replace windvane	4.94	N	137.29	E
11-Dec	06:00		pause Doppler radar observation				
	10:00		arrive Koror				
13-Dec	10:00		depart Koror				
	11:12		resume surface water monitoring				
	12:00		resume Doppler radar observation				
	14:03		XBT observation	7.10	N	134.13	E
	15:03	15:58	CTD-180 (to bottom: 1165m in depth)	6.95	N	134.13	E
	16:30	19:00	stationary observation off Peliliu Island	7.03	N	134.18	E
14-Dec	06:56	07:51	CTD-181 (to bottom: 1146m in depth)	7.50	N	134.67	E
17-Dec	01:22	03:00	"Sphere calibration" for Doppler radar	25.05	N	137.60	E
18-Dec	08:29		RS-242 launch	30.74	N	138.65	E
	11:29		RS-243 launch	31.48	N	138.79	E
	14:29		RS-244 launch	32.14	N	138.97	E
	17:00		Stop Doppler radar observatrion				
19-Dec	07:00		Stop sea surface water monitoring				
			Arrive Yokohama				

* LST of the ship is 9 hours ahead of UTC through the period.

5. Participants List

5.1 On Board Scientists / Engineer / Technical Staff / Observer

Name	Affiliation	On board
Yoneyama, Kunio	JAMSTEC	Koror(1) – Yokohama
Katsumata, Masaki	JAMSTEC	Koror(1) – Yokohama
Murata, Masahiko	JAMSTEC	Koror(2) – Yokohama
Chen, JingYang	FORSGC	Koror(1) – Koror(2)
Iwasaki, Suginori	FORSGC	Koror(1) – Koror(2)
Kouzai, Katsutoshi	MUK	Koror(1) – Koror(2)
Hayashi, Mitsuru	MUK	Koror(1) – Koror(2)
Egawa, Masakazu	MUK	Koror(1) – Koror(2)
Shimanoue, Masaya	MUK	Koror(1) – Koror(2)
Nakatani, Naoki	Osaka Pref. Univ.	Koror(1) – Koror(2)
Shiozaki, Takuhei	Osaka Pref. Univ.	Koror(1) – Koror(2)
Okada, Yasuhiko	Kinki Univ.	Koror(1) – Koror(2)
Ishida, Kunimitsu	Toba-CMT	Koror(1) – Koror(2)
Tsukamoto, Osamu	Okayama Univ.	Koror(1) – Koror(2)
Takahashi, Satoshi	Okayama Univ.	Koror(1) – Koror(2)
Okada, Ken’ichi	Okayama Univ.	Koror(1) – Koror(2)
Morito, Kaori	Okayama Univ.	Koror(1) – Koror(2)
Yamashita, Eiji	OUS	Koror(1) – Koror(2)
Idehara, Hirohisa	OUS	Koror(1) – Koror(2)
Hirayama, Osamu	Osaka Univ.	Koror(1) – Koror(2)
Nagasawa, Takeshi	Osaka Univ.	Koror(1) – Koror(2)
Kamei, Akihide	CRL	Koror(1) – Yokohama
Matsui, Ichiro	NIES	Koror(1) – Yokohama
Noda, Nobuo	Saga Univ.	Koror(2) – Yokohama
Urata, Kazuya	Saga Univ.	Koror(2) – Yokohama
Fukumiya, Kenji	Saga Univ.	Koror(2) – Yokohama
Hanyu, Masaki	GODI	Koror(1) – Yokohama
Sueyoshi, Soichiro	GODI	Koror(1) – Yokohama
Sakamoto, Kouhei	GODI	Koror(1) – Koror(2)
Komai, Nobuharu	MWJ	Koror(1) – Yokohama
Ozawa, Satoshi	MWJ	Koror(1) – Koror(2)
Takahashi, Naoko	MWJ	Koror(1) – Koror(2)
Sagishima, Katsunori	MWJ	Koror(1) – Yokohama
Kamata, Minoru	MWJ	Koror(1) – Yokohama
Shiraishi, Kentaro	MWJ	Koror(1) – Koror(2)
Yoshiike, Miki	MWJ	Koror(1) – Yokohama
Matsunaga, Fuma	MWJ	Sekinehama – Koror(2)
Ohkawa, Fumihide	MWJ	Koror(1) – Koror(2)

Japan Marine Science and Technology Center (JAMSTEC)
Frontier Observational Research System for Global Change (FORSGC)
Natsushima-cho 2-15, Yokosuka 237-0061 JAPAN
TEL: +81-468-66-3811
FAX: +81-468-67-9455

Maritime University of Kobe (MUK)
5-1-1, Fukae-minami, Higashi-Nada-ku, Kobe 658-0022 JAPAN

Osaka Prefecture University
1-1, Gakuen-cho, Sakai, Osaka 599-8531 JAPAN

Kinki University
3-4-1, Kowakae, Higashi-Osaka, Osaka 577-8502 JAPAN
TEL: +81-6-6721-2332

Toba National College of Marine Technology (Toba-CMT)
1-1, Ikagami, Toba, Mie 517-8501 JAPAN

Okayama University
3-1-1, Tsushimanaka, Okayama 700-8530 JAPAN

Okayama University of Science (OUS)
1-1, Ridai-cho, Okayama 700-0005 JAPAN

Osaka University
2-1, Yamadaoka, Suita, Osaka 565-0871 JAPAN

Communication Research Laboratory
Nukui Kita Machi 4-2-1, Koganei, Tokyo 184-8795 JAPAN

National Institute of Environmental Studies (NIES)
16-2, Onogawa, Tsukuba, Ibaraki 305-0053 JAPAN

Saga University
Honjocho 1, Saga, Saga JAPAN

Global Ocean Development Inc. (GODI)
3-65, Oppamahigashi-cho, Yokosuka 237-0063 JAPAN

Marine Works Japan Ltd. (MWJ)
1-1-7, Mutsuura, Kanazawa-ward, Yokohama 236-0031 JAPAN

5.2 Ship Crew

Master	Akamine, Masaharu
Chief Officer	Hashimoto, Takaaki
1st Officer	Shibata, Yuji
2nd Officer	Inoue, Haruhiko
3rd Officer	Isohi, Takeshi
Chief Engineer	Higashi, Koichi
1st Engineer	Araki, Nobuya
2nd Engineer	Masuno, Koji
3rd Engineer	Machino, Takahiro
Chief Radio Officer	Nakabayashi, Shuji
2nd Radio Officer	Shishido, Keiichiro
Boatswain	Kinoshita, Hirokazu
Able Seaman	Naruo, Hisashi
Able Seaman	Yamamoto, Yasuyuki
Able Seaman	Kawata, Seiichiro
Able Seaman	Omote, Kunihiko
Able Seaman	Horita, Kazunori
Able Seaman	Suzuki, Masaru
Able Seaman	Kudo, Kazuyoshi
Able Seaman	Sato, Tsuyoshi
Able Seaman	Aisaka, Takeharu
Able Seaman	Monzawa, Tsuyoshi
Able Seaman	Komata, Shuji
No.1 Oiler	Honda, Sadanori
Oiler	Sugimoto, Yoshihiro
Oiler	Miyazaki, Takashi
Oiler	Matsuo, Toshio
Oiler	Yamashita, Kazumi
Oiler	Taniguchi, Daisuke
Chief Steward	Koga, Yasuaki
Steward	Kurita, Yasutaka
Steward	Akita, Takayuki
Steward	Hiraishi, Hatsuji
Steward	Ota, Hitoshi
Steward	Yoshizawa, Hiroyuki

6. Summary of Observations

6.1. Surface meteorological parameters

(1) Personnel

Kunio Yoneyama (JAMSTEC): Principal Investigator
Masaki Katsumata (JAMSTEC)
Masaki Hanyu (GODI): Operation Leader
Souichiro Sueyoshi (GODI)
Kohei Sakamoto (GODI)

(2) Objective

The surface meteorological parameters are observed as a basic dataset of the meteorology. These parameters bring us the information about temporal variation of the meteorological condition surrounding the ship.

(3) Methods

The surface meteorological parameters were observed throughout MR01-K05 cruise from the departure of Koror on 7 November 2001 to the arrival of Yokohama on 19 December 2001.

This cruise, we used 3 systems for the surface meteorological observation.

1. Mirai meteorological observation system
2. Shipboard Oceanographic and Atmospheric Radiation (SOAR) system
3. Total Sky Imager (TSI)

(3-1) Mirai meteorological observation system

Instruments of Mirai met system are listed in Table 6.1-1 and measured parameters are listed in Table 6.1-2. Data was collected and processed by KOAC-7800 weather data processor made by Koshin Denki, Japan. The data set has 6-second averaged every 6-second record and 10-minute averaged every 10-minute record.

Table 6.1-1: Instruments and their installation locations of Mirai met system

Sensors	Type	manufacturer	location (altitude from surface)
Anemometer	KE-500	Koshin Denki, Japan	foremast (24m)
Thermometer	FT	Koshin Denki, Japan	compass deck (21m)
dewpoint meter	DW-1	Koshin Denki, Japan	compass deck (21m)
Barometer	F451	Yokogawa, Japan	weather observation room captain deck (13m)
rain gauge	50202	R. M. Young, USA	compass deck (19m)
optical rain gauge	ORG-115DR	SCTI, USA	compass deck (19m)
radiometer (short wave)	MS-801	Eiko Seiki, Japan	radar mast (28m)
radiometer (long wave)	MS-200	Eiko Seiki, Japan	radar mast (28m)
wave height meter	MW-2	Tsurumi-seiki, Japan	Bow

Table 6.1-2: Parameters of Mirai meteorological observation system

	Parameters	units	remarks
1	Latitude	degree	
2	Longitude	degree	
3	Ship's speed	knot	Mirai log
4	Ship's heading	degree	Mirai gyro
5	relative wind speed	m/s	6 sec. / 10 min. averaged
6	relative wind direction	degree	6 sec. / 10 min. averaged
7	True wind speed	m/s	6 sec. / 10 min. averaged
8	True wind direction	degree	6 sec. / 10 min. averaged
9	barometric pressure	hPa	adjusted to the sea surface level 6 sec. / 10 min. averaged
10	air temperature (starboard side)	degC	6 sec. / 10 min. averaged
11	air temperature (port side)	degC	6 sec. / 10 min. averaged
12	dewpoint temperature (stbd side)	degC	6 sec. / 10 min. averaged
13	dewpoint temperature (port side)	degC	6 sec. / 10 min. averaged
14	relative humidity (starboard side)	%	6 sec. / 10 min. averaged
15	relative humidity (port side)	%	6 sec. / 10 min. averaged
16	Rain rate (optical rain gauge)	mm/hr	6 sec. / 10 min. averaged
17	Rain rate (capacitive rain gauge)	mm/hr	6 sec. / 10 min. averaged
18	down welling shortwave radiometer	W/m^2	6 sec. / 10 min. averaged
19	down welling infra-red radiometer	W/m^2	6 sec. / 10 min. averaged
20	sea surface temperature	degC	-5m
21	significant wave height (fore)	m	3 hourly
22	significant wave height (aft)	m	3 hourly
23	significant wave period (fore)	second	3 hourly
24	significant wave period (aft)	second	3 hourly

(3-2) Shipboard Oceanographic and Atmospheric Radiation (SOAR) system

SOAR system, designed by BNL (Brookhaven National Laboratory, USA), is consisted of 3 parts.

1. Portable Radiation Package (PRP) designed by BNL – short and long wave down welling radiation
2. Zeno meteorological system designed by BNL – wind, Tair/RH, pressure and rainfall measurement
3. Scientific Computer System (SCS) designed by NOAA (National Oceanographic and Atmospheric Administration, USA) – centralized data acquisition and logging of all data sets

In adding to the original components, the short wave and long wave upwelling radiation were measured.

SCS recorded PRP data every 6.5 seconds, Zeno met data every 10 seconds and upwelling radiation data every 6 seconds.

Instruments and their locations are listed in Table 6.1-3 and measured parameters are listed in Table 6.1-4

Table 6.1-3: Instrument installation locations of SOAR system

Sensors	type	Manufacturer	location (altitude from surface)
Zeno/Met			
anemometer	05106	R. M. Young, USA	foremast (25m)
T/RH	HMP45A	Vaisala, USA	foremast (24m)
	with 43408 Gill aspirated radiation shield (R. M. Young)		
Barometer	61201	R. M. Young, USA	foremast (24m)
	with 61002 Gill pressure port (R. M. Young)		
rain gauge	50202	R. M. Young, USA	foremast (24m)
optical rain gauge	ORG-115DA	ScTi, USA	foremast (24m)
sea surface temperature	SST-100	BNL, USA	bow, 5m extension (-1cm)
PRP			
radiometer (short wave)	PSP	Eppley labs, USA	foremast (25m)
radiometer (long wave)	PIR	Eppley labs, USA	foremast (25m)
Upwelling radiation			
radiometer (short wave)	MS-801	Eiko Seiki, Japan	bow, 8m extension (6m)
radiometer (long wave)	MS-202	Eiko Seiki, Japan	bow, 8m extension (6m)

Table 6.1-4: Parameters of SOAR System

	parameters	Units	Remarks
1	latitude	Degree	
2	longitude	Degree	
3	Sog	Knot	
4	Cog	Degree	
5	relative wind speed	m/s	
6	relative wind direction	Degree	
7	barometric pressure	Hpa	
8	air temperature	DegC	
9	relative humidity	%	
10	sea surface temperature	DegC	-1cm, Seasnake
11	Rain rate (optical rain gauge)	mm/hr	
12	precipitation (capacitive rain gauge)	mm	reset at 50mm
13	down welling shortwave radiation	W/m^2	
14	down welling infra-red radiation	W/m^2	
16	up welling short wave radiation	W/m^2	
17	up welling infra-red radiation	W/m^2	

(3-3) Total Sky Imager (TSI)

The Total Sky Imager (TSI) was installed at the top deck midship, altitude of 17m from sea level. TSI was developed jointly by Penn State University, BNL and Yankee Environmental Systems, Inc. and manufactured by YES Inc. TSI recorded every 5 minutes from dawn to sunset. Measured parameters are listed in Table 6.1-5.

Table 6.1-5: Parameters of TSI system

	parameters	units
1	opaque cloud cover	%
2	Thin cloud cover	%

(4) Preliminary results

Wind (converted to U, V component), Tair/SSST, RH/precipitation, solar radiation and pressure observed from SOAR system during the Intensive Observation Period (IOP), from 9th November to 9th December is shown in Figure 6.1-1. The daytime cloud cover ratio obtained from TSI during IOP are shown in Figure 6.1-2. In the figures, accumulated precipitation data from SOAR capacitive rain gauge was converted to the precipitation amount in every hour and obvious noises were eliminated but not calibrated. Other figures are showing uncorrected data.

(5) Data archives

These raw data will be submitted to the Data Management Office (DMO) in JAMSTEC just after the cruise.

Remarks concerning about data quality are as follows;

1. SSST sensor of SOAR system was deployed from 0000UTC November 9th and recovered at 0005UTC December 9th.
2. Upwelling radiation measurement was conducted from 0000UTC November 9th to 0005UTC December 9th.

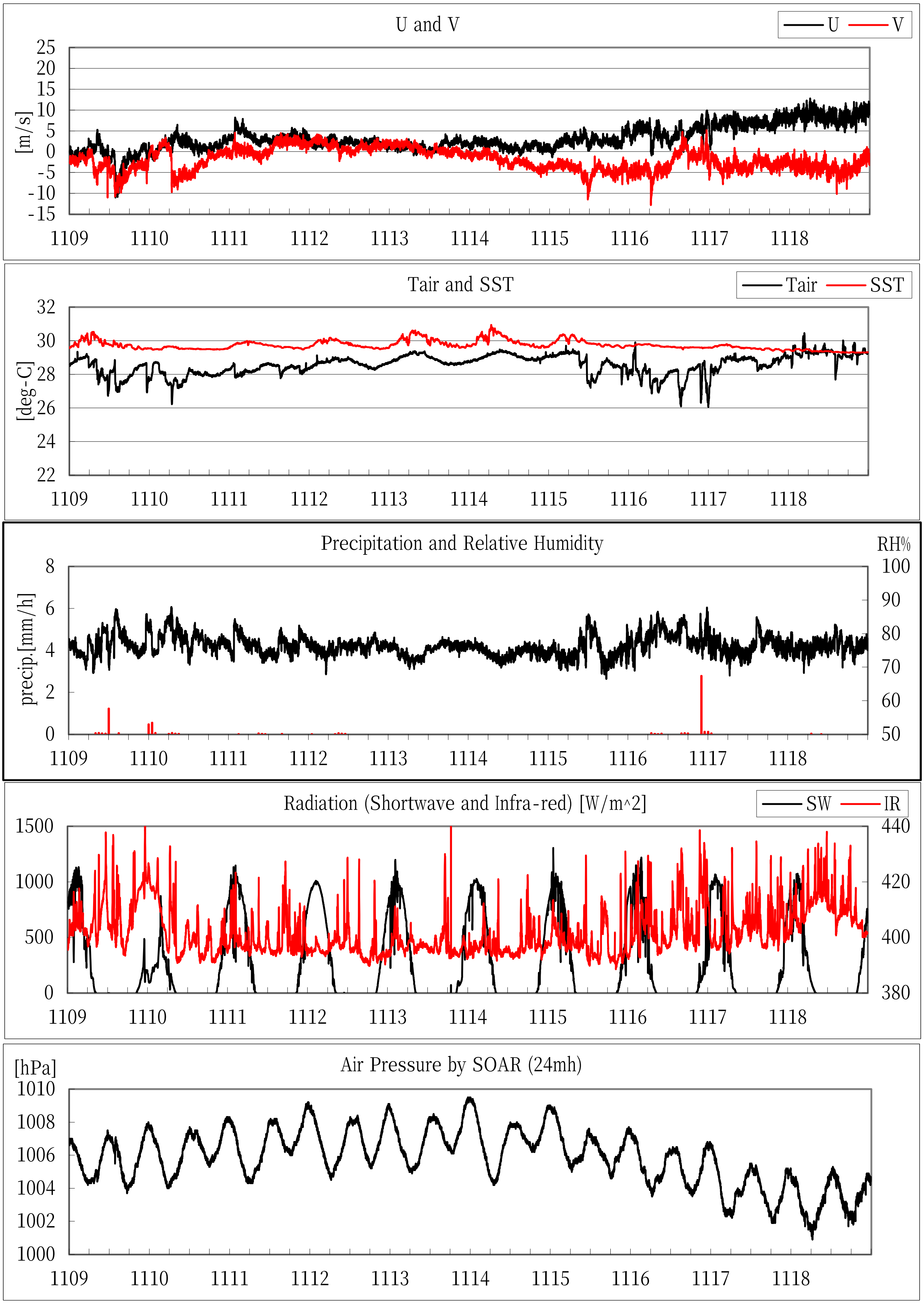

Fig.6.1-1: Temporal variations of observed surface meteorological parameters.

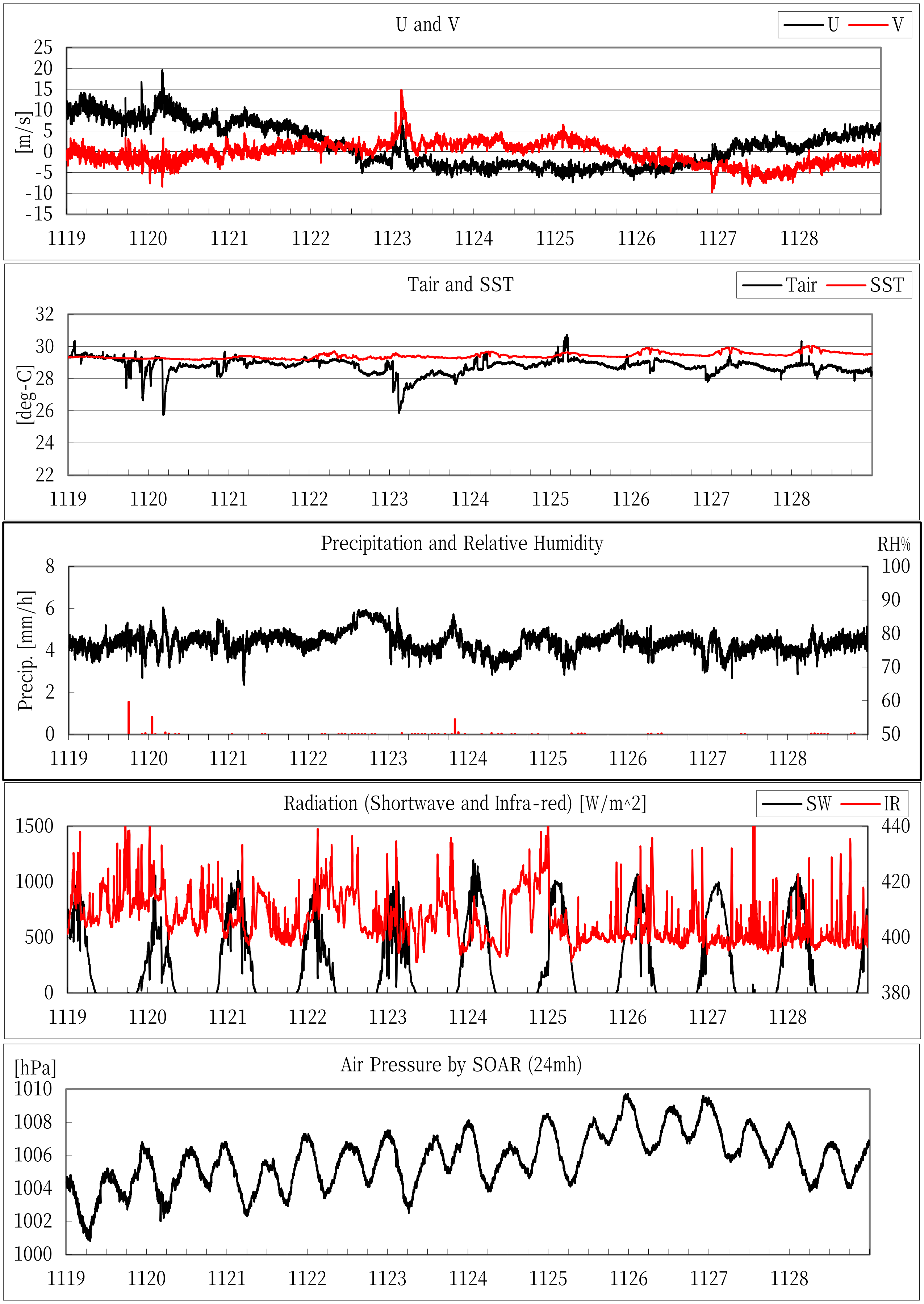

Fig.6.1-1 (continued)

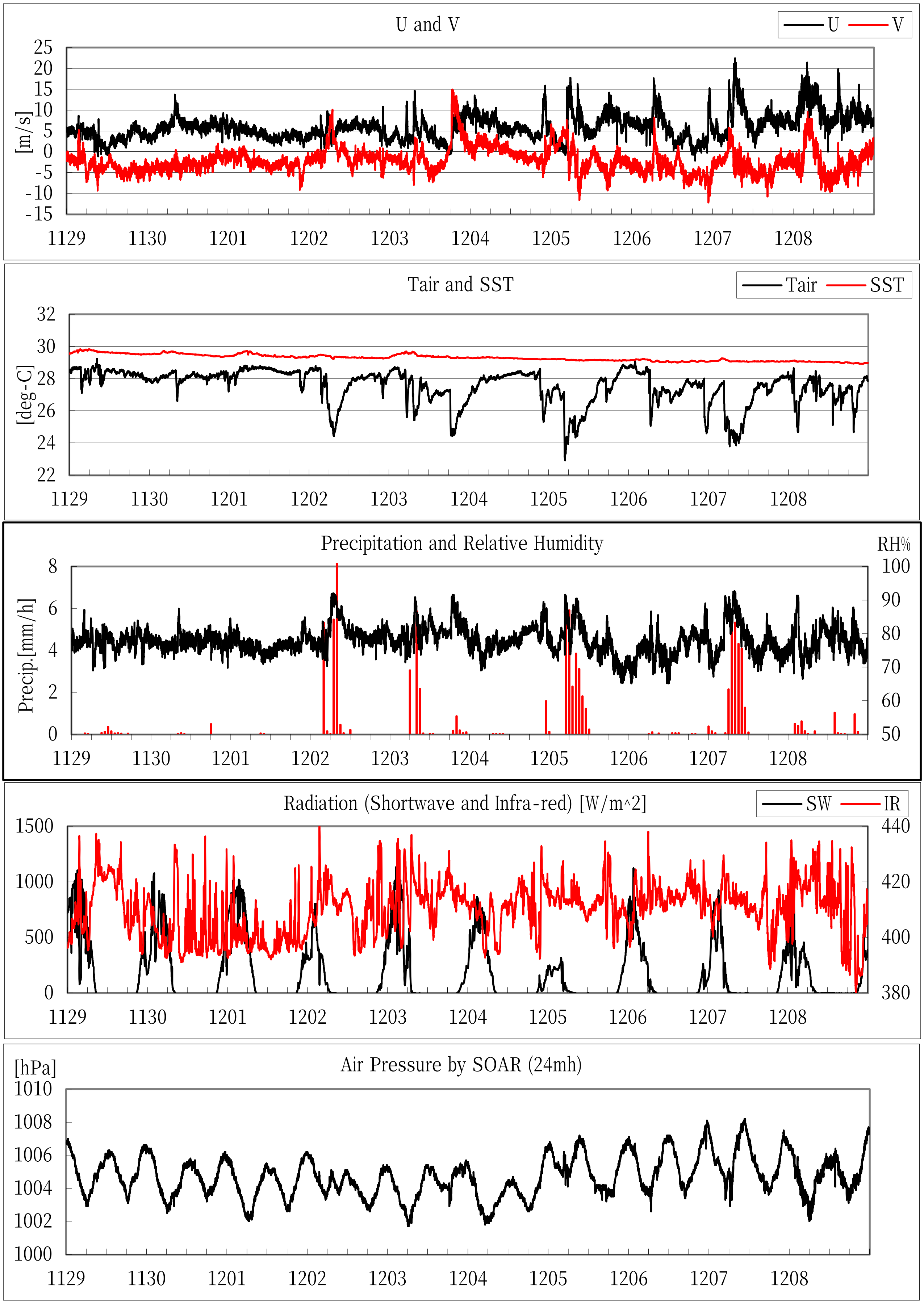

Fig.6.1-1 (continued)

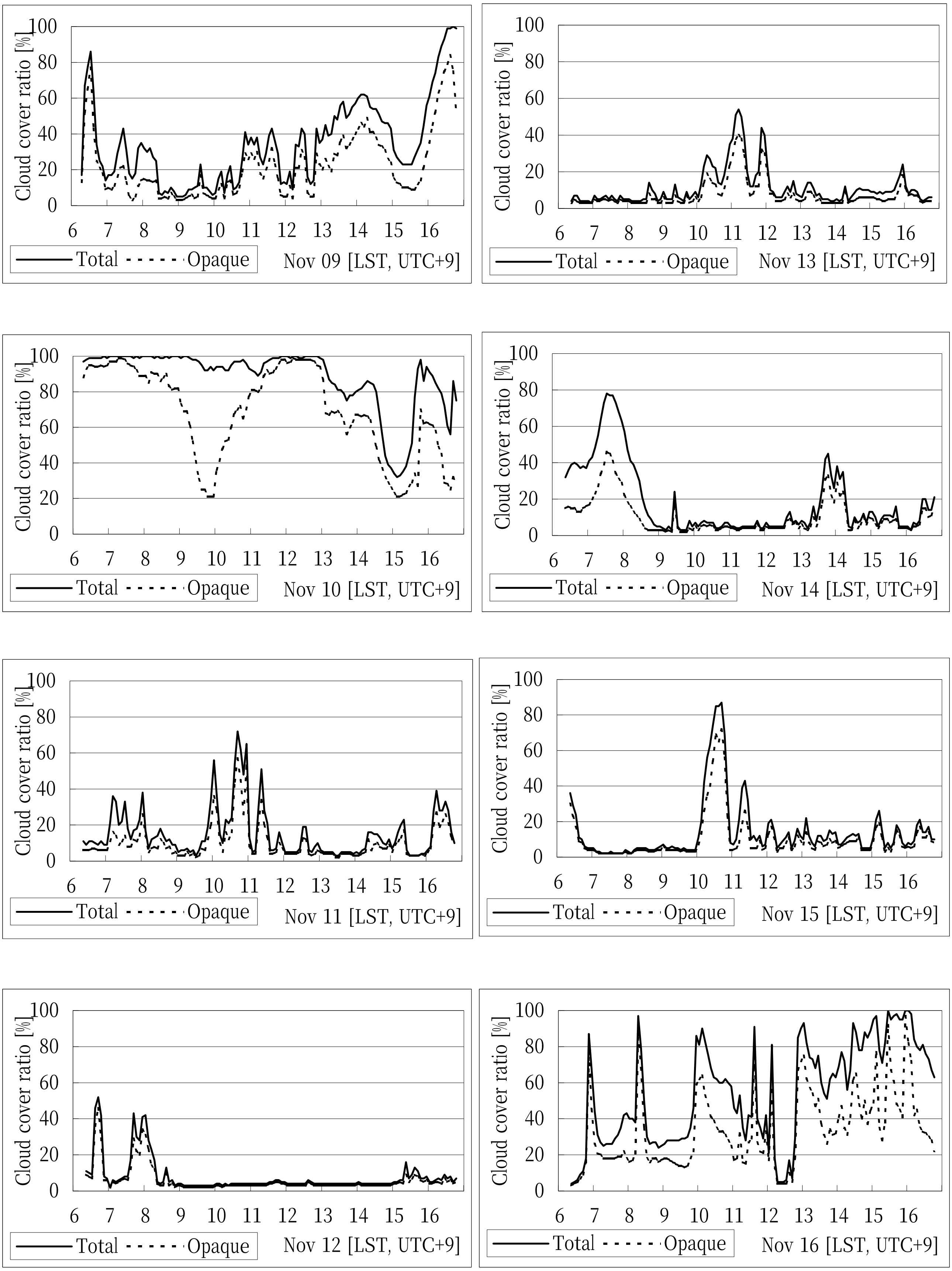

Fig 6.1-2: Daytime cloud cover ratio from TSI (1/4)

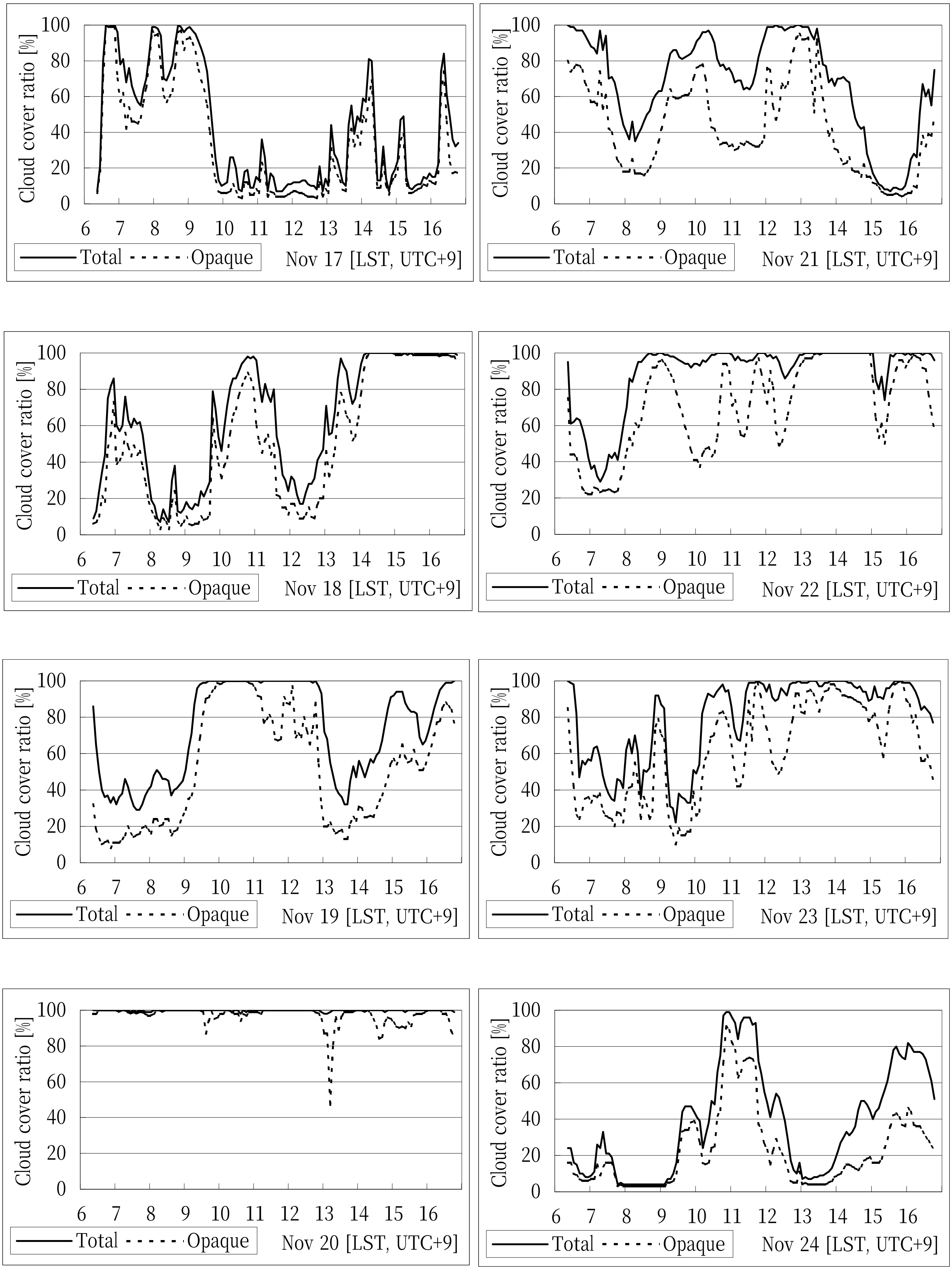

Fig 6.1-2: Daytime cloud cover ratio from TSI (2/4)

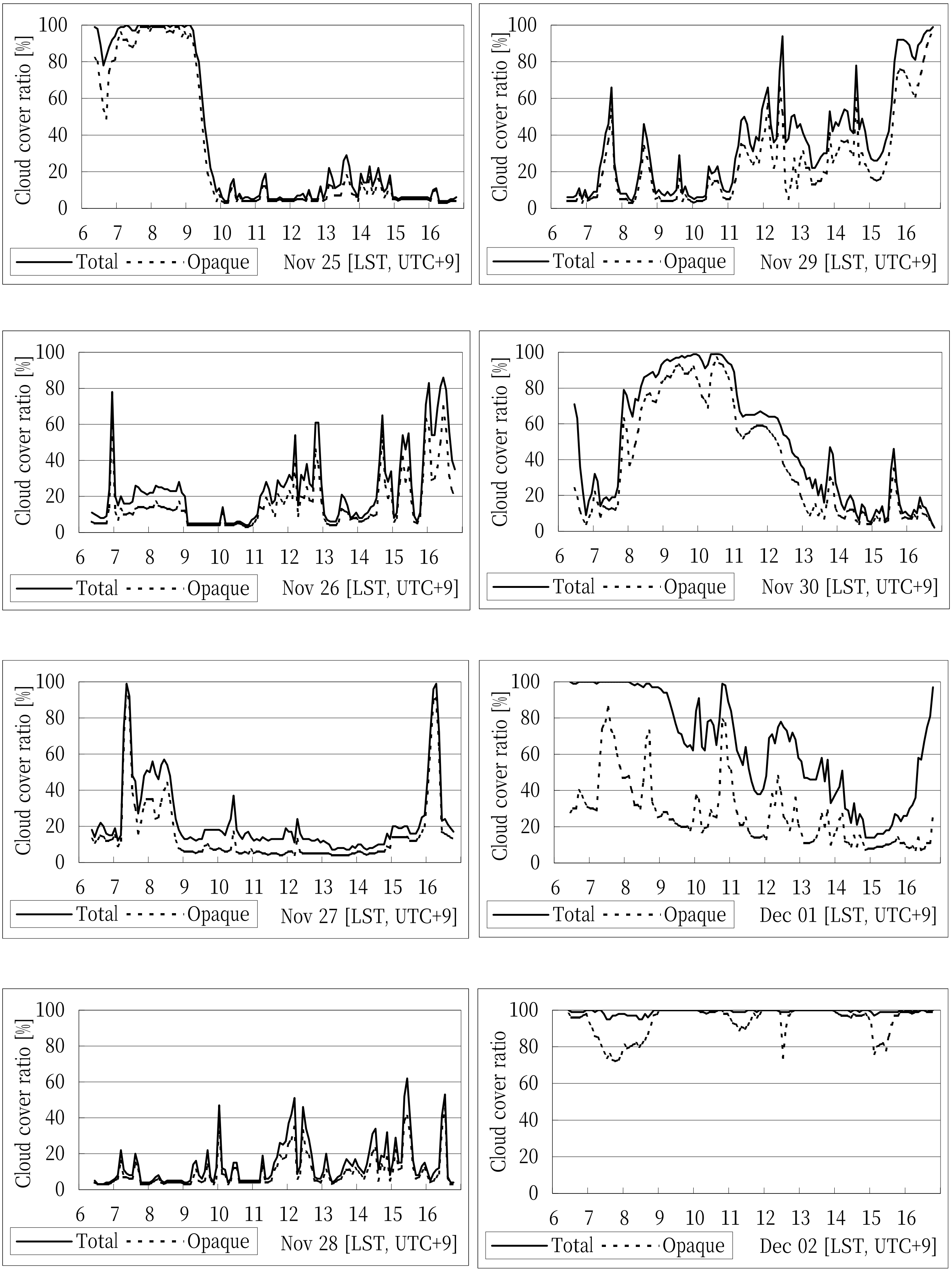

Fig 6.1-2: Daytime cloud cover ratio from TSI (3/4)

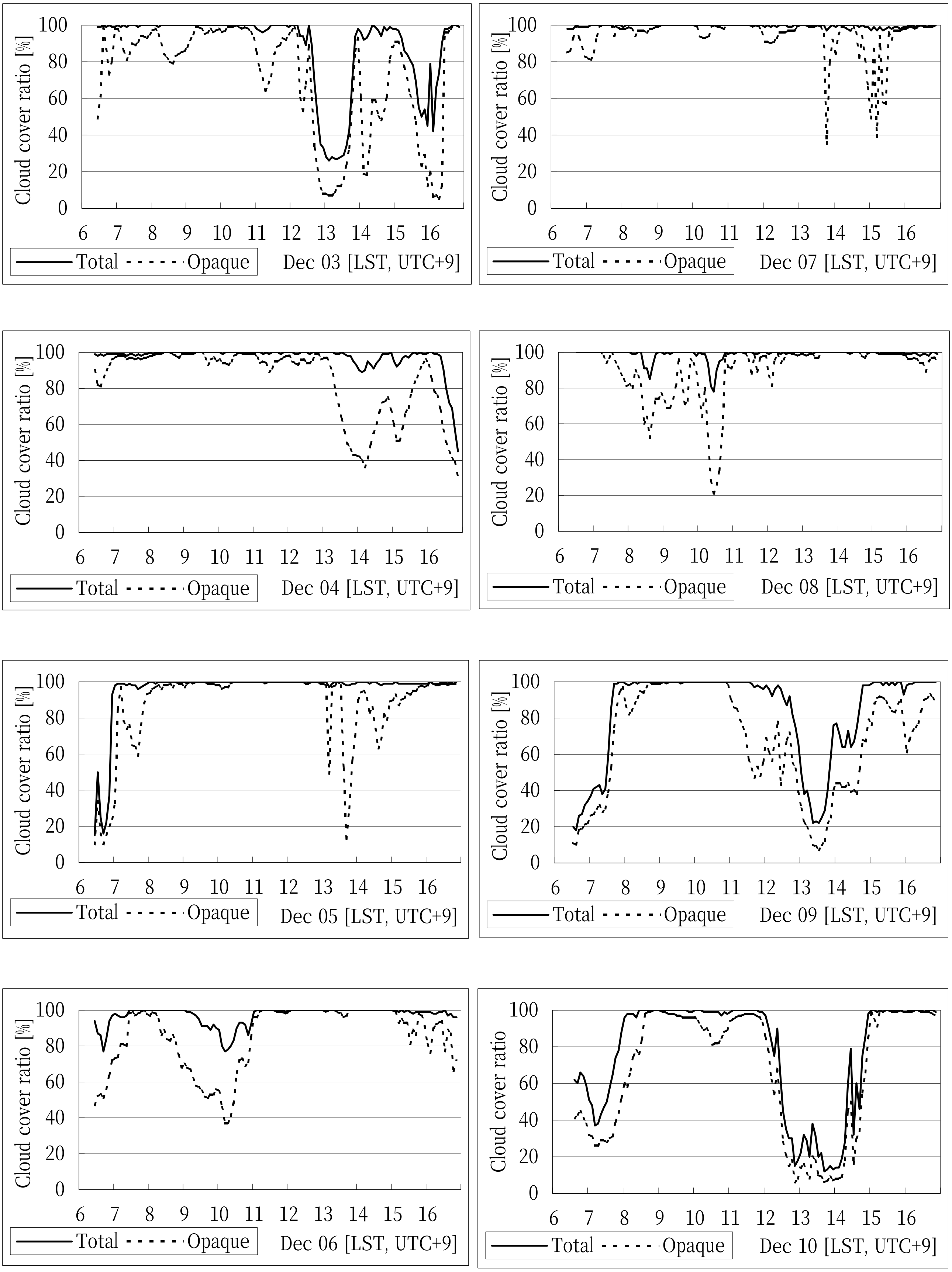

Fig 6.1-2: Daytime cloud cover ratio from TSI (4/4)

6.2 Radiosonde observation

(1) Personnel

Kunio Yoneyama	(JAMSTEC)	Principal Investigator
Masaki Katsumata	(JAMSTEC)	
Masaki Hanyu	(GODI)	
Souichoro Sueyoshi	(GODI)	
Kohei Sakamoto	(GODI)	

(2) Objective

Atmospheric soundings of temperature, humidity, and wind speed/direction.

(3) Method

Atmospheric sounding by radiosonde was carried out every 3 hours at (2N,138E) from November 9 through December 9, 2001. In total, 241 soundings were carried out (Table 6.2-1). The main system consists of processor (Vaisala, DigiCORA MW11), GPS antenna (GA20), UHF antenna (RB21), baloon launcher (ASAP), and GPS radiosonde sensor (RS80-15GH).

Prior to launch, humidity and temperature sensors were calibrated using humidity calibrator (Digilog Instruments, Vaporpak H-31) and pressure sensor was calibrated using Vaisala barometer (PTB220). Calibrator humidity was set at 70%.

In addition to normal soundings, we tried tethered radiosonde observation several times from MIRAI deck and small boat far from ship. The log is listed in Table 6.2-2. This was done to confirm the ship's structural influences onto near surface data. Details of this tethered radiosonde in addition to the launch procedure can be found in the recent paper Yoneyama et al.(2001) that are submitted to JAMSTECR (Vol.45).

(4) Preliminary results

Time-height cross sections of equivalent potential temperature, mixing ratio, zonal and meridional wind components are shown in Fig.6.2-1, respectively. Vertical profiles of temperature and dew point temperature are plotted on the thermodynamic chart with wind profiles. These figures can be found in Appendix-C.

During the whole observational period, westerly were prevaild in the lower troposphere. Especially, in mid-November and early December there were strong bursts could be caught. But they did not last long time. From GMS IR images shown in Appendix-B, the latter westerly wind peak seems to correspond the convectively active phase of Madden-Julian Oscillation.

Results of tethered radiosonde obtained on December 1 are shown in Fig.6.2-2. From this, we can confirm that near surface data from MIRAI deck are distorted but can be corrected using above layer's data (see Yoneyama et al., 2001).

(5) Data archive

Data were sent to the world meteorological community by Global Telecommunication System through the Japan Meteorological Agency, immediately after the each observation. Raw data is recorded as ASCII format every 2 seconds during ascent. These raw datasets will be submitted to JAMSTEC Data Management Office. Corrected and projected onto every 5hPa level datasets are available from K.Yoneyama of JAMSTEC.

Table 6.2-1 Radiosonde launch log.

Date YYYYMMDDHH	Lat. degN	Long. degE	Surface Conditions hPa	degC	%	deg	m/s	Maxi Altitude hPa	m	Cloud Amount	Type
2001110900	1.90	138.06	1007.1	28.7	77	333	2.9	35.8	22644	5	Cs,Cu,Ci
2001110903	1.94	138.06	1006.4	29.6	74	0	2.7	32.5	23260	6	Cu,Sc,Ci
2001110906	1.87	138.06	1004.6	29.4	71	295	0.8	34.6	22836	7	Cu,Cb,Ci
2001110909	1.87	138.04	1005.0	28.4	79	330	7.8	47.4	20904	10	Cb,Cu,Cs
2001110912	1.88	138.07	1007.0	26.5	81	356	2.5	46.1	21074	10	unknown
2001110915	1.93	138.05	1006.7	26.9	88	38	11.8	47.1	20952	5	As,Cb
2001110918	1.91	138.05	1004.3	27.5	80	357	6.8	46.1	21061	2	As,Cb
2001110921	1.94	138.02	1005.8	28.4	75	24	4.5	38.2	22233	8	As,Cu,Sc
2001111000	1.90	138.05	1008.1	27.1	85	37	3.9	61.1	19424	9	As,Sc
2001111003	2.06	138.05	1006.8	28.7	79	0	1.5	29.9	23828	8	As,Sc,Cu
2001111006	1.87	138.06	1004.3	27.6	84	222	1.6	30.1	23744	7	Cu,Cs,Ci
2001111009	1.84	138.03	1005.5	27.6	82	328	7.9	38.6	22189	3	Cu,Cb,St
2001111012	1.86	138.06	1007.6	27.7	79	334	7.3	39.3	22104	3	unknown
2001111015	1.88	138.04	1007.5	27.9	81	344	4.6	42.4	21617	2	Sc
2001111018	1.86	138.05	1005.9	28.0	77	348	1.2	44.8	21250	3	Sc,Cu
2001111021	1.86	138.07	1006.7	28.0	74	278	1.7	46.2	21118	7	Ci,Cu,Sc
2001111100	1.86	138.05	1008.4	28.3	78	266	1.7	28.8	24085	4	Sc,Cu
2001111103	1.82	138.03	1006.9	28.5	80	258	4.6	28.9	24039	3	Cu,Sc
2001111106	1.85	138.05	1004.6	28.3	76	243	5.2	37.9	22298	3	Cu,Sc
2001111109	1.86	138.04	1005.5	28.2	75	294	2.5	39.0	22112	2	Cu,Cb
2001111112	1.86	138.06	1007.8	28.5	73	271	2.9	39.0	22141	2	unknown
2001111115	1.85	138.02	1008.1	28.4	72	233	4.2	71.8	18444	1	Sc
2001111118	1.86	138.05	1006.6	28.2	77	229	5.4	42.0	21673	2	Cu,Sc
2001111121	1.86	138.05	1007.4	28.3	76	220	3.3	31.7	23413	3	Cu,Sc
2001111200	1.85	138.06	1009.3	28.3	77	246	4.6	31.7	23424	3	Cu,Sc
2001111203	1.85	138.05	1007.7	29.4	75	208	3.5	35.5	22704	1	Cu,Cs
2001111206	1.81	137.98	1005.3	29.3	69	241	2.8	36.5	22501	1	Cu,Cb
2001111209	1.85	138.03	1005.8	28.8	74	251	3.2	40.8	21800	3	Cu
2001111212	1.86	138.05	1008.3	28.7	76	256	2.9	46.2	21098	2	unknown
2001111215	1.85	138.04	1008.3	28.5	75	248	2.8	45.8	21128	1-	Cu
2001111218	1.86	138.05	1006.0	28.3	75	231	2.3	39.3	22038	0	-
2001111221	1.85	138.03	1006.8	28.1	78	212	3.8	38.9	22092	3	Cu,Sc
2001111300	1.86	138.05	1009.2	28.8	76	202	3.0	35.7	22631	2	Cu,Ci
2001111303	1.84	138.04	1007.5	29.5	74	217	2.4	31.2	23506	3	Cu
2001111306	1.86	138.05	1005.5	29.6	71	207	2.0	40.2	21918	4	Cu,Ci
2001111309	1.87	138.06	1005.8	29.1	71	213	0.7	71.4	18467	4	Cu,Ci
2001111312	1.86	138.06	1008.2	29.0	74	119	0.3	46.4	21047	2	unknown
2001111315	1.86	138.05	1008.3	28.8	75	257	1.0	46.0	21095	1	Sc
2001111318	1.86	138.05	1006.6	28.5	77	298	3.0	42.2	21598	1	Cu,Sc
2001111321	1.85	138.03	1007.5	28.5	76	274	3.4	33.4	23059	5	Cu,Ci
2001111400	1.86	138.05	1009.6	28.9	76	266	1.6	29.1	23960	4	Ci,Cu
2001111403	1.86	138.06	1008.1	29.1	75	279	2.7	27.1	24393	3	Cu,Sc,Cs
2001111406	1.86	138.05	1005.3	29.4	73	278	1.4	30.3	23713	2	Cu,Ci
2001111409	1.84	138.05	1005.0	29.3	72	291	3.9	54.1	20114	1	Cu,Ci
2001111412	1.86	138.05	1007.8	29.2	73	341	2.1	28.4	24142	2	unknown
2001111415	1.86	138.06	1008.1	28.9	74	352	1.9	39.4	22033	1-	Cu
2001111418	1.86	138.05	1007.0	28.8	75	355	3.5	42.3	21577	1	Cu
2001111421	1.87	138.06	1007.1	28.6	79	344	5.8	38.7	22136	1	Cb
2001111500	1.87	138.06	1009.1	29.2	73	347	4.6	25.5	24883	1-	Cb,Ci
2001111503	1.86	138.04	1008.4	29.7	72	327	4.8	33.2	23115	4	Cc,Cb
2001111506	1.87	138.04	1006.2	29.6	71	306	4.5	30.7	23620	1	Sc,Cu
2001111509	1.87	138.05	1006.3	29.2	73	317	4.3	50.8	20466	2	St,Cu,As

2001111512	1.86	138.05	1008.2	29.0	73	336	9.1	46.7	20994	2	unknown
2001111515	1.89	138.05	1006.9	27.6	81	325	4.6	37.0	22410	3	Cu,Sc
2001111518	1.86	138.04	1005.9	28.8	71	329	4.1	39.1	22046	5	Sc,Cu
2001111521	1.89	138.03	1006.4	28.5	72	327	5.0	33.6	23022	1	Cu,Cb,Ac
2001111600	1.87	138.06	1007.8	28.1	74	303	8.3	39.1	22051	4	Cu,Cb,Ac,Ci
2001111603	1.86	138.05	1006.6	28.3	78	303	9.4	25.0	24977	5	Cu
2001111606	1.86	138.05	1004.8	28.3	77	302	8.1	39.9	21952	6	St,Sc,Cu,Cb,As
2001111609	1.85	138.05	1005.2	27.4	80	314	7.5	50.6	20479	5	Ci,Sc,CU
2001111612	1.86	138.05	1006.7	27.8	81	314	4.9	47.5	20879	4	unknown
2001111615	1.86	138.06	1006.5	28.2	79	268	5.5	44.1	21332	5	Sc,St
2001111618	1.86	138.05	1004.7	27.4	83	250	3.6	48.4	20749	7	unknown
2001111621	1.85	138.05	1005.3	28.3	77	277	6.3	34.1	22973	2	Cu
2001111700	1.86	138.05	1007.2	27.1	82	270	9.6	33.9	22995	7	Cu,Cb
2001111703	1.86	138.05	1005.2	28.6	75	295	7.0	29.5	23890	5	Ac,Cb,Cu
2001111706	1.86	138.06	1003.3	29.0	75	292	9.3	46.1	21010	2	Ci,Cu,Cb
2001111709	1.87	138.04	1004.5	28.7	74	289	9.6	53.8	20111	4	Ci,Cu,As
2001111712	1.86	138.05	1005.5	29.1	74	303	8.9	60.4	19440	-	unknown
2001111715	1.86	138.06	1005.2	28.8	78	287	8.3	33.7	23042	7	Sc,St
2001111718	1.86	138.05	1003.3	28.3	77	294	7.4	37.9	22246	5	unknown
2001111721	1.86	138.05	1003.8	28.7	79	277	9.6	29.6	23900	6	Cb,Ac
2001111800	1.86	138.05	1005.6	28.9	77	276	10.2	31.2	23557	5	Cu,Cb,Ac
2001111803	1.86	138.06	1003.7	29.2	74	289	12.6	28.5	24127	5	Cb,Ac,Cu
2001111806	1.86	138.05	1002.4	29.3	75	282	9.7	28.9	23973	9+	As,Cu
2001111809	1.87	138.05	1003.3	29.0	79	292	11.6	41.1	21775	7	Ci,Cu,As
2001111812	1.86	138.05	1005.1	29.1	79	306	9.3	34.6	22870	-	unknown
2001111815	1.86	138.05	1004.8	28.2	80	308	8.0	41.2	21750	8	unknown
2001111818	1.86	138.05	1003.0	29.0	76	301	11.7	40.2	21899	6	Cu,Sc
2001111821	1.86	138.05	1004.1	29.2	76	283	12.6	27.7	24278	10	Sc,Cu
2001111900	1.86	138.05	1005.0	29.3	78	276	11.5	28.7	24098	6	Sc,Cu,Ci
2001111903	1.85	138.05	1004.3	29.5	75	264	10.4	29.8	23825	9	Cs,Cu
2001111906	1.85	138.06	1002.3	29.5	74	267	13.9	28.7	24054	4	Sc,Ci,As,Cu
2001111909	1.86	138.05	1003.1	29.2	74	274	13.3	49.0	20668	8	Ci,As,Sc
2001111912	1.86	138.05	1005.5	29.2	80	273	9.8	44.1	21357	10	unknown
2001111915	1.86	138.05	1005.1	29.0	79	283	9.6	42.0	21646	6	Sc
2001111918	1.86	138.05	1004.2	27.2	76	283	6.1	104.0	16353	9	unknown
2001111921	1.86	138.05	1005.4	29.1	82	275	8.3	37.1	22419	9	Cu,Cb,St
2001112000	1.87	138.05	1006.8	28.4	79	277	8.5	29.4	23937	9+	Sc,Cb
2001112003	1.86	138.05	1005.3	29.1	80	281	13.4	33.5	23105	9+	Sc,Cb
2001112006	1.85	138.06	1003.7	27.4	83	277	13.5	26.5	24557	6	Ci,As
2001112009	1.86	138.05	1004.7	28.4	81	280	11.4	114.9	15830	5	Ac,Ci,Sc
2001112012	1.86	138.06	1006.5	28.7	76	277	8.9	42.4	21612	10	unknown
2001112015	1.86	138.05	1006.6	28.4	80	270	7.9	29.1	23972	5	unknown
2001112018	1.86	138.05	1005.0	28.5	76	280	8.6	39.1	22090	5	Sc
2001112021	1.86	138.05	1005.0	28.9	76	299	5.8	32.7	23218	10	Cu,Ac,Sc
2001112100	1.86	138.06	1009.0	28.8	80	248	6.8	30.5	23717	7	Ci,Sc,Cs
2001112103	1.86	138.06	1005.2	29.2	74	260	9.5	27.0	24466	8	St,Sc,Cu
2001112106	1.86	138.05	1003.2	28.9	77	269	7.7	21.7	25928	4	Ci,Cs,Cu
2001112109	1.86	138.05	1004.1	28.8	77	273	8.0	27.4	24357	3	Cu,Cc,Ci
2001112112	1.86	138.05	1006.2	29.0	78	269	6.7	26.2	24664	3	Sc,As
2001112115	1.83	138.05	1005.3	28.7	81	241	6.0	35.4	22722	0	-
2001112118	1.86	138.05	1003.7	28.4	80	253	8.2	33.5	23059	1	unknown
2001112121	1.86	138.05	1005.2	28.7	77	241	5.4	23.8	25290	4	Cb,Cu,Cc
2001112200	1.86	138.05	1007.2	29.1	76	251	4.5	46.1	21100	9	Sc,Ac,Cb,Cu,St
2001112203	1.86	138.05	1006.2	29.3	76	248	4.7	27.5	24312	8	Cb,Cu,Cs
2001112206	1.86	138.06	1004.0	29.1	79	217	1.7	22.8	25583	10-	Sc,Cu
2001112209	1.86	138.05	1005.2	29.1	79	220	2.3	24.0	25229	6	Cu,Sc,Ac,As
2001112212	1.86	138.06	1007.1	28.7	82	141	0.6	29.6	23892	9-	Sc
2001112215	1.85	138.06	1006.7	28.6	83	183	0.8	28.1	24218	7	unknown

2001112218	1.86	138.06	1005.0	28.0	88	97	1.7	24.9	24983	7	unknown
2001112221	1.86	138.06	1005.2	28.0	87	103	2.1	27.6	24312	4	Cb,Cu,Ac
2001112300	1.86	138.05	1007.2	29.3	81	113	2.6	29.5	23912	4	Cu,Ci,Cc
2001112303	1.86	138.05	1006.2	28.6	75	184	6.7	23.1	25516	9	Cs,Cu
2001112306	1.86	138.05	1003.8	27.7	76	140	4.7	23.0	25531	8	Sc,Ac
2001112309	1.85	138.05	1004.7	27.9	75	146	2.7	25.1	24915	3	Sc
2001112312	1.86	138.06	1006.8	28.0	75	123	3.2	31.5	23475	8	Sc
2001112315	1.86	138.05	1007.6	28.4	74	112	3.8	25.0	24970	8	unknown
2001112318	1.86	138.05	1005.8	28.5	76	114	6.4	29.5	23885	8	unknown
2001112321	1.85	138.06	1005.0	28.0	80	90	3.6	29.3	23932	9	Ac,Cu,Sc
2001112400	1.86	138.06	1010.0	28.8	74	112	3.5	24.4	25161	1	Cs,Ci
2001112403	1.86	138.06	1006.2	28.9	73	117	5.4	22.8	25536	8	Ac,As,Cb,Ci
2001112406	1.86	138.06	1004.7	29.0	74	122	4.8	21.7	25885	5	Ac,Cu,Sc
2001112409	1.86	138.06	1005.5	28.9	70	132	3.1	23.0	25519	1	Sc,Ac
2001112412	1.86	138.05	1006.8	28.8	72	111	2.9	33.5	23102	2	Ac
2001112415	1.86	138.06	1006.8	28.7	73	106	2.8	23.6	25374	9	Cu,Ac
2001112418	1.86	138.06	1005.6	28.7	78	104	4.0	31.2	23512	9	Ac
2001112421	1.86	138.05	1005.2	28.7	77	104	5.8	25.3	24893	10	Cu,St
2001112500	1.86	138.05	1008.2	28.9	81	103	3.8	38.6	22180	9	Cu,Cb,As
2001112503	1.86	138.06	1007.8	29.4	76	118	7.2	42.8	21517	3	Cu,Cb,Ci
2001112506	1.86	138.05	1005.1	29.2	76	123	5.9	25.6	24824	1	Cu
2001112509	1.86	138.05	1005.5	29.1	73	93	5.3	25.6	24807	1-	Cu
2001112512	1.86	138.05	1007.7	28.8	77	112	4.6	26.9	24531	1-	Sc
2001112515	1.86	138.05	1008.2	28.8	77	89	4.2	29.5	23899	3	Cu
2001112518	1.86	138.06	1007.4	28.6	78	73	3.1	25.7	24800	1	Cu
2001112521	1.87	138.06	1008.2	28.4	82	87	4.3	24.7	25080	7	Cu,Ac,Sc
2001112600	1.86	138.06	1009.9	28.9	77	67	6.5	33.0	23190	1	Cu
2001112603	1.86	138.05	1008.4	29.1	80	55	4.3	23.8	25260	5	Cu,Cb
2001112606	1.86	138.05	1006.7	29.3	77	58	4.2	22.3	25684	5	Cb,Cu
2001112609	1.86	138.06	1007.0	29.0	76	49	5.3	26.3	24609	1	Cu,Ci
2001112612	1.86	138.05	1009.2	28.9	78	82	3.3	28.8	24067	2	Cu
2001112615	1.86	138.05	1009.1	28.7	79	46	3.9	27.9	24260	2	Cu
2001112618	1.86	138.06	1007.5	28.4	78	32	5.0	31.5	23446	1	Cu
2001112621	1.86	138.06	1008.5	28.6	78	31	4.8	24.2	25165	3	Ac,Sc,Cu
2001112700	1.86	138.05	1009.8	28.0	71	346	4.8	33.9	22986	2	Cb,As,Cu
2001112703	1.87	138.06	1008.7	28.6	80	14	3.4	39.0	22102	1-	Cb,Ci
2001112706	1.86	138.05	1006.3	29.0	73	324	4.3	19.3	26622	4	Cu,Cs
2001112709	1.87	138.05	1006.7	28.9	74	337	4.1	30.4	23665	4	Cu,Ci
2001112712	1.86	138.05	1008.6	28.9	74	332	6.1	24.2	25203	3	Cu
2001112715	1.86	138.05	1007.8	28.8	78	337	7.2	30.1	23747	3	Cu
2001112718	1.86	138.05	1006.4	28.4	77	319	6.0	28.5	24078	2	Cu
2001112721	1.86	138.05	1006.8	28.4	78	346	5.3	25.9	24699	4	Sc,Cu,Cb,Ci
2001112800	1.86	138.05	1008.2	28.9	75	8	2.6	22.5	25648	1-	Sc,Cu,Cb
2001112803	1.86	138.05	1006.8	29.0	74	325	3.7	23.2	25417	3	Cu
2001112806	1.86	138.05	1004.8	29.2	74	299	3.9	26.6	24504	4	Cu
2001112809	1.86	138.05	1004.9	28.4	75	322	5.1	25.6	24798	2	Cu,Ci
2001112812	1.86	138.05	1007.1	28.8	75	296	3.7	24.6	25077	2	Cu,Sc
2001112815	1.86	138.05	1006.8	28.5	78	291	4.6	30.1	23755	3	Cu
2001112818	1.86	138.05	1004.8	28.3	77	284	5.3	32.7	23182	2	Cu
2001112821	1.86	138.05	1005.8	28.3	78	287	5.3	30.7	23601	1	Cu,Cb,As,Sc
2001112900	1.86	138.05	1007.1	28.7	79	276	6.4	21.9	25792	3	Ci,Sc,Cb,Cu
2001112903	1.85	138.05	1006.4	28.7	77	285	5.2	19.9	26392	4	Cu,Cb,Sc,As
2001112906	1.86	138.05	1004.0	28.6	76	286	5.1	83.3	17578	7	Cu,Cb,Ac
2001112909	1.86	138.05	1005.2	28.7	77	320	5.2	27.1	24379	9	Cu,As,St
2001112912	1.86	138.05	1006.2	28.3	82	327	4.9	61.1	19386	10	As,Cu,Sc
2001112915	1.86	138.05	1006.4	28.2	77	318	4.0	23.5	25336	10	As,Cu
2001112918	1.86	138.05	1004.7	28.2	76	329	5.2	30.1	23708	10	Cu,Ac,As
2001112921	1.86	138.05	1005.3	28.2	82	299	8.1	33.7	22975	7	As,Ac,Cu,Sc,Cb

2001113000	1.86	138.05	1007.2	27.7	77	299	6.5	25.5	24813	7	Cu,Cb,Sc,As
2001113003	1.86	138.05	1006.2	27.8	77	302	5.8	30.0	23698	6	Ci,Cu,Cb,As
2001113006	1.86	138.05	1003.9	28.3	76	289	7.8	24.3	25073	5	Ci,Cu,Sc
2001113009	1.86	138.05	1004.5	26.7	84	265	11.0	52.0	20290	10	As,Sc,Cu
2001113012	1.86	138.05	1006.1	28.0	79	301	7.9	30.1	23743	6	Cu,Sc
2001113015	1.85	138.03	1006.0	28.3	77	297	7.2	31.3	23469	2	Cu
2001113018	1.86	138.05	1004.5	27.8	81	281	7.6	28.0	24172	3	Cu,Cb
2001113021	1.85	138.05	1005.0	28.0	81	267	4.8	20.6	26175	5	Cb,Cu,Ci
2001120100	1.86	138.05	1006.6	28.3	77	278	6.1	27.7	24269	8	Ci,As,Cb,Cu
2001120103	1.84	138.05	1005.1	28.6	77	296	7.7	35.8	22584	4	Ci,As,Cb,Cu
2001120106	1.84	138.07	1002.8	28.7	76	281	6.4	29.8	23747	6	Cu,Cs,Ci
2001120109	1.86	138.06	1003.9	28.6	76	298	5.9	26.7	24470	7	Cs,Cu,Cc
2001120112	1.86	138.06	1005.8	28.6	73	303	5.2	27.5	24315	7	Cu,As
2001120115	1.85	138.02	1005.6	28.4	75	307	4.7	35.3	22690	7	Cu,As
2001120118	1.86	138.05	1003.7	28.2	76	303	4.8	26.9	24424	9	As,Cu
2001120121	1.85	138.05	1004.6	28.3	76	305	5.7	29.7	23782	7	Ci,As,Ci,Cb
2001120200	1.86	138.05	1006.6	28.3	79	287	4.5	22.8	25549	7	Sc,Cu,As,Ac
2001120203	1.92	138.06	1005.4	28.8	75	266	5.7	24.4	25118	9	As,Ac,Ci,Cu,Cb
2001120206	1.86	138.05	1004.2	27.1	82	249	10.3	32.7	23176	10	As,St,Cu
2001120209	1.85	138.04	1004.8	25.1	89	275	5.6	53.9	20071	10	As,St
2001120212	1.86	138.05	1005.6	27.3	84	271	6.9	38.0	22219	10	As,St
2001120215	1.88	138.06	1004.8	28.0	81	286	8.1	30.3	23676	7	Cs,Cu
2001120218	1.86	138.05	1003.7	28.0	77	285	6.6	34.5	22833	9	Cu,Cs,Sc
2001120221	1.84	138.05	1004.3	28.0	80	281	7.7	23.4	25368	8	Cb,Cu
2001120300	1.86	138.05	1005.6	28.0	85	289	1.7	25.3	24867	8	Cs,Cu,Sc
2001120303	1.87	138.06	1004.4	28.9	77	300	5.4	24.9	24948	8	Cu,Ac,Cs
2001120306	2.03	138.09	1003.2	25.5	79	323	5.2	60.0	19447	9	Cu,As,Cb
2001120309	1.89	138.02	1003.9	25.3	86	281	5.8	574.9	4735	9+	Cu
2001120312	1.86	138.06	1006.0	27.4	84	312	6.1	32.3	23236	10	Nb,Cu
2001120315	1.84	138.03	1005.4	27.3	78	339	5.3	39.9	21921	8	Ci,As
2001120318	1.86	138.05	1004.8	27.3	79	266	1.0	32.0	23327	10	Ci,As
2001120321	1.85	138.04	1005.9	25.1	89	235	11.6	29.3	23893	10	Nb,As,Cu
2001120400	1.86	138.05	1005.8	26.3	82	263	8.7	25.8	24756	10-	Sc,Cu
2001120403	1.84	138.05	1004.7	27.9	80	251	11.5	32.3	23273	9	Ac
2001120406	1.86	138.06	1002.7	28.1	77	266	6.4	24.2	25083	7	Sc,Ac,Cu
2001120409	1.86	138.01	1003.7	27.9	76	248	6.6	35.8	22609	7	Ac,Cs,Sc
2001120412	1.86	138.05	1004.9	28.2	76	267	5.7	29.1	23932	9	Sc,Ac,Cs
2001120415	1.82	138.04	1004.8	28.2	78	273	6.4	29.7	23796	6	As,Ac
2001120418	1.86	138.05	1003.5	28.1	81	296	4.9	41.9	21592	10	Ac
2001120421	1.85	138.04	1004.4	28.0	81	305	6.7	28.0	24207	4	Cb,Cu,Ci
2001120500	1.86	138.05	1007.0	26.3	84	265	7.5	27.5	24356	10	Nb,Cu,Ci
2001120503	1.88	138.04	1006.0	27.6	76	197	3.8	24.0	25204	10	As,Sc
2001120506	1.86	138.05	1006.9	24.1	86	269	14.4	559.1	4925	10	As
2001120509	1.87	138.04	1007.1	24.7	88	303	12.1	593.6	4476	10	As
2001120512	1.89	138.02	1006.6	25.7	84	306	6.5	43.7	21312	10	unknown
2001120515	1.83	138.04	1004.9	27.1	78	288	7.5	55.4	19884	10	unknown
2001120518	1.87	138.02	1004.7	27.4	78	292	13.2	39.5	21928	10	unknown
2001120521	1.87	138.03	1005.7	28.2	70	270	9.5	22.9	25462	9+	Ac,Sc
2001120600	1.83	138.05	1007.3	28.8	71	286	8.7	23.4	25358	9	Ac,Cu
2001120603	1.83	138.04	1006.4	28.7	72	300	6.7	22.1	25709	9	Cu,Sc
2001120606	1.86	138.05	1004.4	28.4	75	307	5.7	29.0	23963	10	Ac,Cb
2001120609	1.87	138.04	1005.8	27.4	78	290	13.0	38.4	22149	10	Ac,Cu
2001120612	1.86	138.05	1007.7	27.0	70	315	7.7	126.4	15247	10	unknown
2001120615	1.88	138.03	1006.4	26.9	75	321	3.4	566.0	4872	10	unknown
2001120618	1.86	138.05	1004.8	27.8	76	333	7.9	48.7	20638	10	unknown
2001120621	1.86	138.04	1006.3	27.6	80	346	7.0	25.8	24706	10	Sc,Cu
2001120700	1.86	138.06	1008.7	24.7	79	312	9.8	52.9	20250	10	St
2001120703	1.84	138.04	1006.2	27.4	77	303	4.2	28.2	24164	10	Ac,Cu

2001120706	1.86	138.06	1005.0	24.9	86	243	10.8	105.2	16281	10	Ac,Cu,As
2001120709	1.85	138.03	1007.8	24.5	87	265	11.3	657.1	3630	10	As
2001120712	1.86	138.05	1008.1	26.0	84	303	8.2	618.2	4092	10	unknown
2001120715	1.85	138.04	1005.9	27.3	74	310	8.3	34.7	22800	10	St
2001120718	1.86	138.05	1005.0	27.6	78	300	10.7	26.3	24539	10	unknown
2001120721	1.85	138.05	1005.7	27.8	77	289	8.0	36.6	22467	8	Ac,Cu
2001120800	1.86	138.06	1007.4	28.1	75	288	7.0	22.1	25712	7	Cu,Ac
2001120803	1.83	138.04	1006.1	26.7	82	285	12.6	25.1	24868	10	St
2001120806	1.86	138.05	1003.9	27.6	76	248	14.8	25.8	24699	9	Ac
2001120809	1.87	138.03	1005.6	26.6	84	305	9.3	543.7	5126	10	As,Ac
2001120812	1.86	138.05	1006.4	27.3	84	314	10.9	63.0	19190	10	unknown
2001120815	1.88	138.03	1006.4	26.6	84	291	9.1	880.5	1123	10	unknown
2001120818	1.85	138.06	1004.5	27.4	80	276	9.6	35.3	22678	6	Sc,St,Ci,As
2001120821	1.85	138.05	1005.5	25.8	84	271	6.9	47.1	20887	8	As,Ci,Cc
2001120900	1.86	138.05	1008.0	28.1	74	270	6.8	26.9	24470	9	As,Ac,Cs

Table 6.2-2. Date and time of tethered radiosonde observation.

No.	Date(LST)		Sonde S/N	Relative Wind	Site	Repeat
1	Nov. 8	13:12-14:12	120304209	264deg 2.5m/s	boat	3 times
2	Nov. 8	15:07-16:02	120304209	330deg 3.9m/s	boat	2 times
					deck	1 time
3	Nov.11	13:46-13:56	120304209	344deg 3.5m/s	deck	1 time
4	Nov.13	16:50-17:03	120304207	9deg 4.0m/s	deck	1 time
5	Nov.14	13:51-14:05	050207612	330deg 3.7m/s	deck	2 times
6	Nov.14	22:54-23:08	050207612	349deg 2.5m/s	deck	1 time
7	Nov.26	13:52-14:07	120305207	308deg 2.3m/s	deck	2 times
8	Nov.26	22:50-23:04	120305207	323deg 3.3m/s	deck	2 times
9	Dec. 1	13:33-14:28	120305207	240deg 5.1m/s	deck	1 time
					boat	3 times
10	Dec. 1	16:51-17:11	050207612	96deg 1.9m/s	deck	1 time

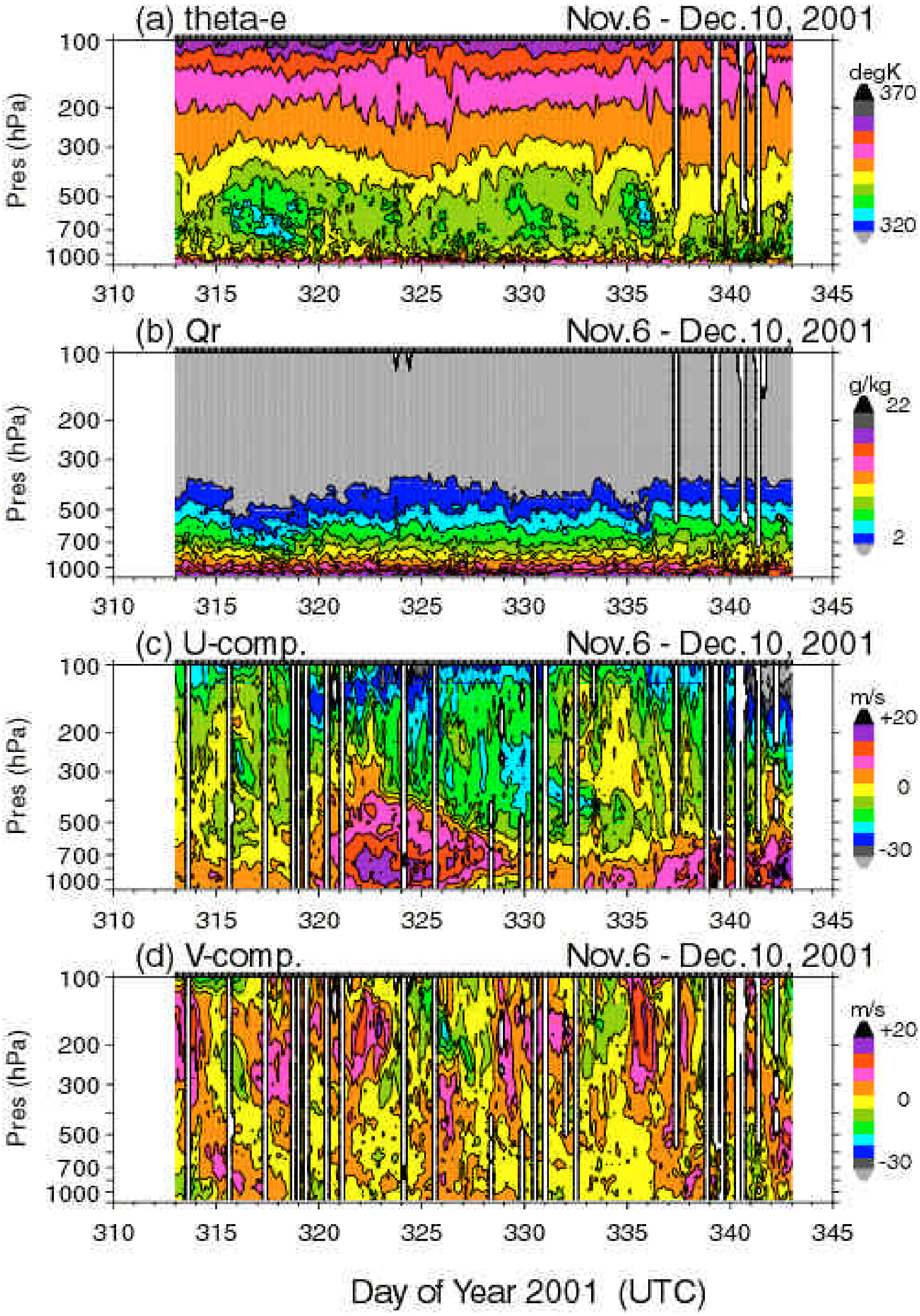

Fig.6.2-1 Time-height cross sections of (a) equivalent potential temperature (degK), (b) mixing ratio (g/kg), (c) zonal wind component (m/s), and (d) meridional wind component (m.s), respectively.

6.3 Doppler radar observation

(1) Personnel

Masaki Katsumata (JAMSTEC): Principal Investigator
Masaki Hanyu (GODI): Operation Leader
Kunio Yoneyama (JAMSTEC)
JingYang Chen (FORSGC)
Suginori Iwasaki (FORSGC)
Souichiro Sueyoshi (GODI)
Kohei Sakamoto (GODI)

(2) Objective

The Doppler radar is operated to obtain spatial and temporal distribution of rainfall amount, and structure of precipitating cloud systems. The objective of this observation is to investigate the life cycle of precipitating systems associated with the interseasonal oscillation.

(3) Methods

The hardware specification of this shipboard Doppler radar (RC-52B, manufactured by Mitsubishi Electric Co. Ltd., Japan) is:

Frequency:	5290 MHz
Beam Width:	better than 1.5 degrees
Output Power:	250 kW (Peak Power)
Signal Processor:	RVP-7 (Sigmet Inc., U.S.A.)
Inertial Navigation Unit:	DRUH (Honeywell Inc., U.S.A.)
Application Software:	IRIS/Open (Sigmet Inc., U.S.A.).

The hardware is calibrated by checking (1) frequency, (2) mean power output, (3) pulse repetition frequency (PRF) for once a day, and (4) transmitting pulse width and (5) receiver linearity at the beginning and the end of the intensive (stationary) observation period.

The observation is performed continuously from 07 November to 11 December 2001. During the observation, the programmed “tasks” are repeated every 10 minutes. One cycle consists of one “volume scan” (consists of PPIs for 21 elevations) with Doppler-mode (160-km range for reflectivity and Doppler velocity), one-elevation “Surveillance” PPI with Intensity-mode (420-km range for reflectivity). In the interval of the cycles, RHI (Range Height Indicator) scans were operated to obtain detailed vertical cross sections with Doppler-mode. The Doppler velocity is unfolded automatically by dualPRF unfolding algorithm, except for RHI after Nov.19. The parameters for the above three tasks are listed in Table 6.3-1.

Table 6.3-1: Parameters for each task.

	Surveillance PPI	Volume Scan	RHI
Pulse Width	2 [microsec]	0.5 [microsec]	
Scan Speed	18 [deg./sec.]		Automatically determined
PRF	260 [Hz]	900 / 720 [Hz]	
Sweep Integration	32 samples		
Ray Spacing	1.0 [deg.]		0.2 [deg.]
Bin Spacing	250 [m]	125 [m]	
Elevations	0.5	0.5, 1.2, 2.0, 3.0, 4.0, 5.0, 6.0, 7.0, 8.0, 9.0, 10.1, 11.3, 12.8, 14.6, 16.6, 18.9, 21.6, 25.0, 29.0, 34.0, 40.0	0.0 to 70.0
Azimuths	Full Circle		Optional
Range	420 [km]	160 [km]	

(4) Preliminary Results

The temporal variation of the radar-derived precipitating area is shown in Fig.6.3-1. On the radiosonde observation (see section 6.2), strong westerly was observed twice in the observation period (Nov.17-22 and Dec.2-9). The widespread and organized precipitating systems, however, appeared around the radar observation range only in the latter period.

The samples of the observed radar echo were shown in Figs.6.3-2 and 6.3-3. The first one (left panel of Fig.6.3-2) is in the first strong-westerly period: the scale of the individual echo mass is several tenth km and scattered. In contrast, right panel of Fig.6.3-2 is in the latter strong-westerly period and shows well-organized precipitating system. As shown in Fig.6.3-3, the system accompanied clear leading edge and trailing strong wind area. The shipboard instruments records gust of 18 m/s with temperature drop (to 23 deg.C.). The organized precipitating systems like this were observed so frequently in December. The detailed analyses for each systems are the future work.

(5) Data Archive

The inventory information of the Doppler radar data obtained during this cruise will be submitted to JAMSTEC DMO (Data Management Office). The original data will be archived at and available from Ocean Observation and Research Department of JAMSTEC (contact Masaki Katsumata).

(6) Remarks

(a) The new signal processing unit RVP-7 (Sigmet Inc.) was introduced from this cruise. This enables to remove second-trip echo by random-phase technique, while the data quality is different from the previous observation.

(b) The dual-PRF velocity unfolding is used for the Doppler velocity and velocity spectrum width, except the RHI scans after 1900UTC of Dec.3.

(c) Some surveillance PPIs include radial noisy echo and reflectivity is possibly not stable. For more detailed information, contact Masaki Katsumata of JAMSTEC.

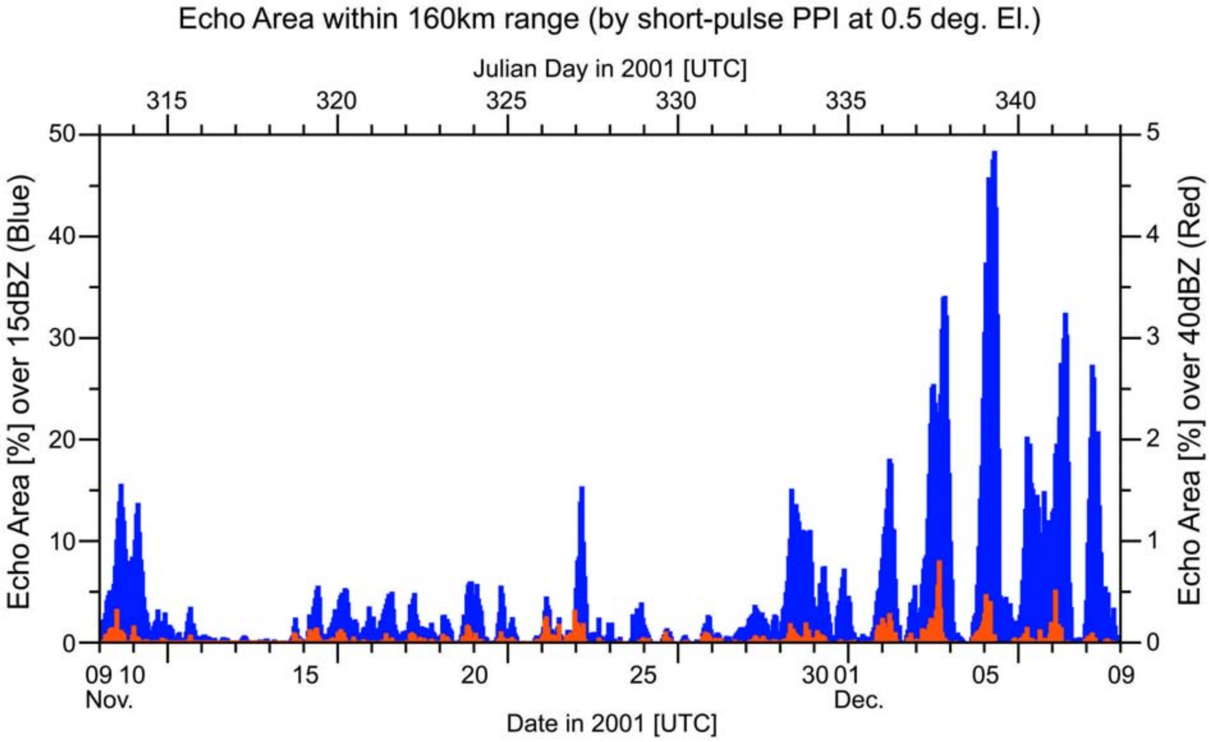

Fig. 6.3-1: Temporal variation of the echo area over 15dBZ (blue) and over 40dBZ (red), by the ratio to the radar observation area within 160-km range. The data is taken by PPI of lowest elevation (0.5) of the volume scan.

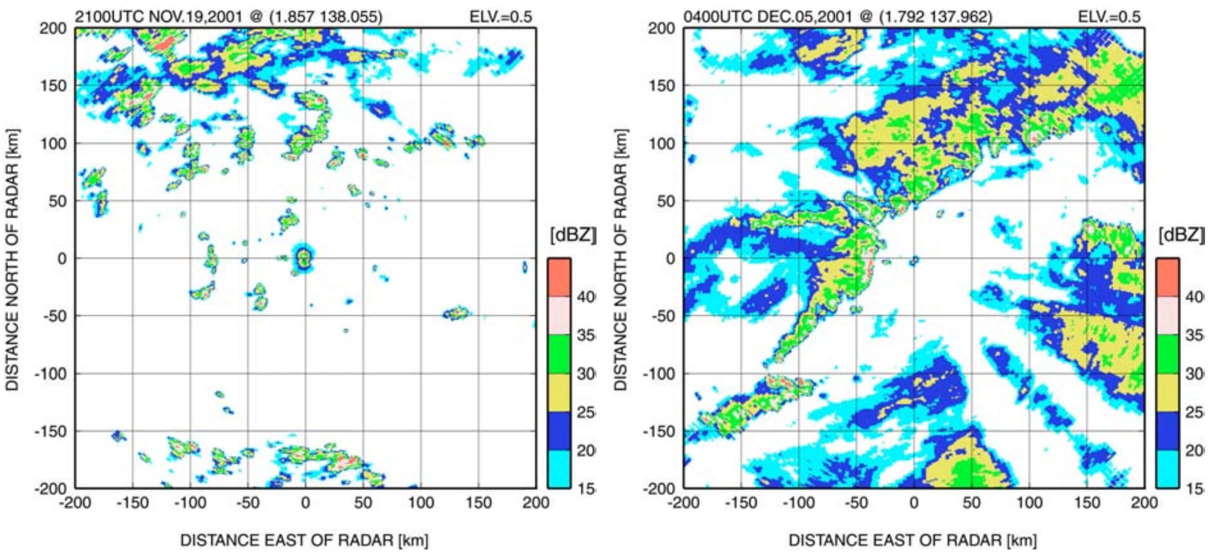

Fig. 6.3-2: Radar reflectivity fields by surveillance (intensity-mode) PPI at 21UTC on Nov.19, 2001 (left) and at 04UTC on Dec.05, 2001 (right), respectively.

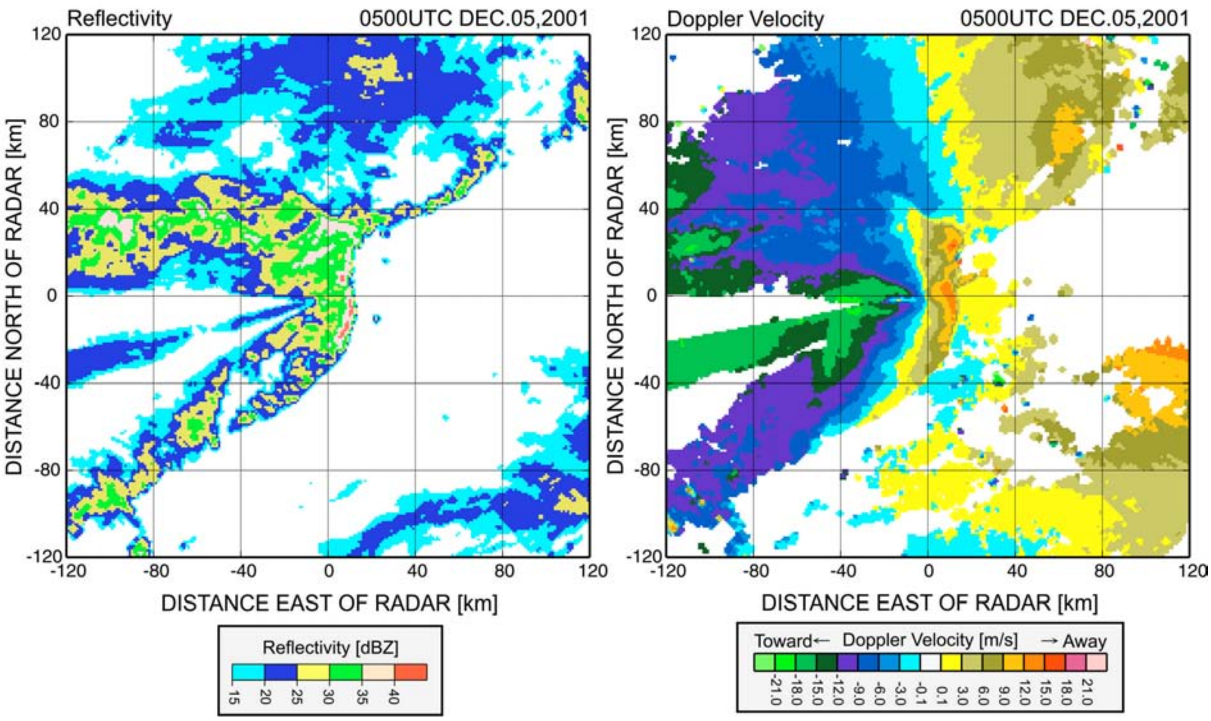

Fig. 6.3-3: Radar echo images by lowest elevation (0.5 deg.) PPI of the volume scan at 05UTC on Dec.5, 2001. The left and right panels are for reflectivity and Doppler velocity, respectively.

6.4 Ceilometer observation

(1) Personnel

Masaki Katsumata (JAMSTEC): Principal Investigator
Masaki Hanyu (GODI): Operation Leader
Kunio Yoneyama (JAMSTEC)
Souichiro Sueyoshi (GODI)
Kohei Sakamoto (GODI)

(2) Objectives

The information of the cloud base height and the liquid water amount around cloud base is important to understand the processes on the formation of the cloud. As few method to measure them, the ceilometer observation was carried out.

(3) Methods

We measured cloud base height and backscatter profiles using CT-25K ceilometer (Vaisala, Finland) from November 7 to the end of the cruise, December 19, except the territory of Palau Republic.

Principle specifications are as follows:

Laser source:	Indium Gallium Arsenide (InGaAs) Diode
Transmitting wave length:	905 +-5 nm at 25 deg-C
Transmitting average power:	8.9 mW
Repetition rate:	5.57 kHz
Detector:	Silicon avalanche photodiode (APD)
Responsibility at 905 nm:	65 A/W
Measurement range:	0 - 7.5 km
Resolution:	50 ft in full range
Sampling rate:	60 sec.

On the archived dataset, cloud base height and backscatter profile are recorded with the resolution of 30 m (100 ft.).

(4) Preliminary results

The time series of the detected cloud base height during IOP is shown in Fig.6.4-1. Most of the cloud base height is around 500 m. However, the high clouds are observed during Nov.22-25 and Dec.02-08. The former period is just after the period with the strong westerly but no active convection, while the latter is in the period with the strong westerly. In the latter case, the cloud base height change gradually from low cumulus to high (around 5000m), while the change is not continuous in the former period. This difference implies that the former high clouds came from the convective system far from the ship, while the latter high clouds are the continous system which passed over the ship. The more detailed analyses are in future work.

(5) Data archive

Ceilometer data obtained during this cruise will be submitted to and archived by the DMO (Data Management Office) of JAMSTEC.

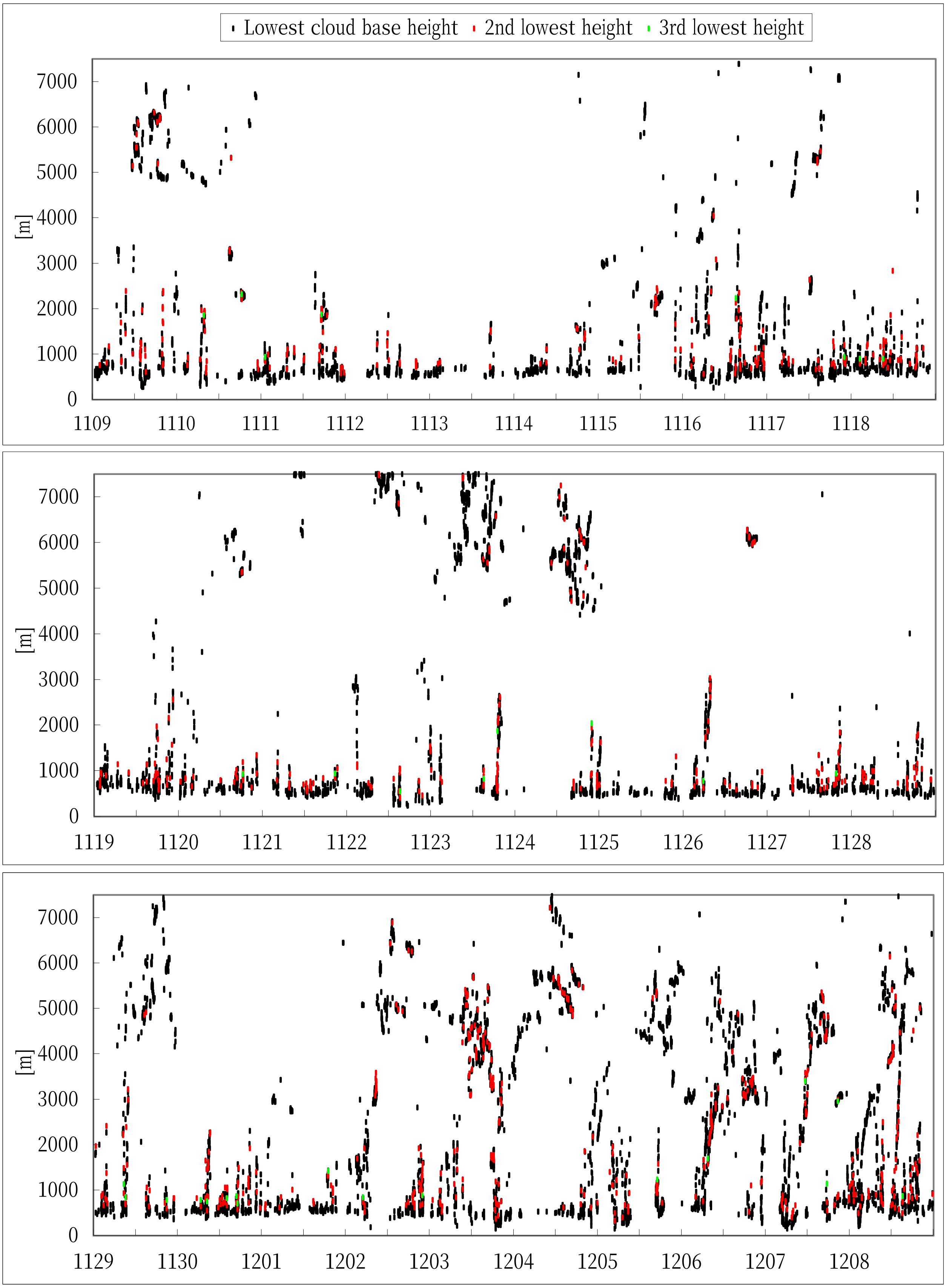

Fig.6.4-1: Observed cloud base height during IOP

6.5 Mie scattering Lidar observation

(1) Personnel

Ichiro Matsui (National Institute for Environmental Studies, on board)
Atsushi Shimizu (National Institute for Environmental Studies)
Nobuo Sugimoto (National Institute for Environmental Studies)
Kazuhiro Asai (Tohoku Institute of Technology)

(2) Objectives

Objectives of the observations and experiments in this cruise are

- to study distribution and optical characteristics of dust and other aerosols using a two-wavelength dual polarization lidar,
- to study microphysical parameters of ice clouds and thin water clouds with the combination of the lidar and the cloud profiling radar,
- to study a new polarization bistatic lidar method for measuring cloud particle size of lower water clouds.

(3) Method

Vertical profiles of aerosols and clouds were measured with a two-wavelength dual polarization lidar. The lidar employs a Nd:YAG laser as a light source which generates the fundamental output at 1064 nm and the second harmonic at 532 nm. Transmitted laser energy is typically 100 mJ per pulse at 1064 nm and 50 mJ per pulse at 532 nm. The pulse repetition rate is 10 Hz. The receiver telescope has a diameter of 25 cm. The receiver has three detection channels to receive the lidar signals at 1064 nm and the parallel and perpendicular polarization components at 532 nm. An analog-mode avalanche photo diode (APD) is used as a detector for 1064 nm, and photomultiplier tubes (PMTs) are used for 532 nm. The detected signals are recorded with a digital oscilloscope and stored on a hard disk with a computer. The lidar system was installed in a 20-ft container with the cloud profiling radar (CPR) of the Communications Research Laboratory (CRL). The container has a glass window on the roof, and the lidar was operated continuously regardless of weather.

The experiment on the bistatic lidar method was performed with additional receivers installed at distances of 13 m and 15 m from the lidar transmitter. The bistatic receivers detect backscatter from the lower clouds at a scattering angle of about 179 deg. Clouds particle size is derived from the ratio of signal intensity of two polarization components.

(4) Results

Figure 6.5-1 shows the quick-look time-height indication of the range-corrected signal during Leg.3 of the cruise.

The lower clouds at 600 m are continuously observed over western Pacific Ocean. Also higher cirrus around 15 km is detected in lower latitude where the tropopause is supposed to be located at 16-18 km. A close look into a middle cloud reveals fine structures of cloud system accompanied by precipitation. We can see a melting layer located at around 5 km, where the intensity and the depolarizaion ratio change greatly in vertical direction.

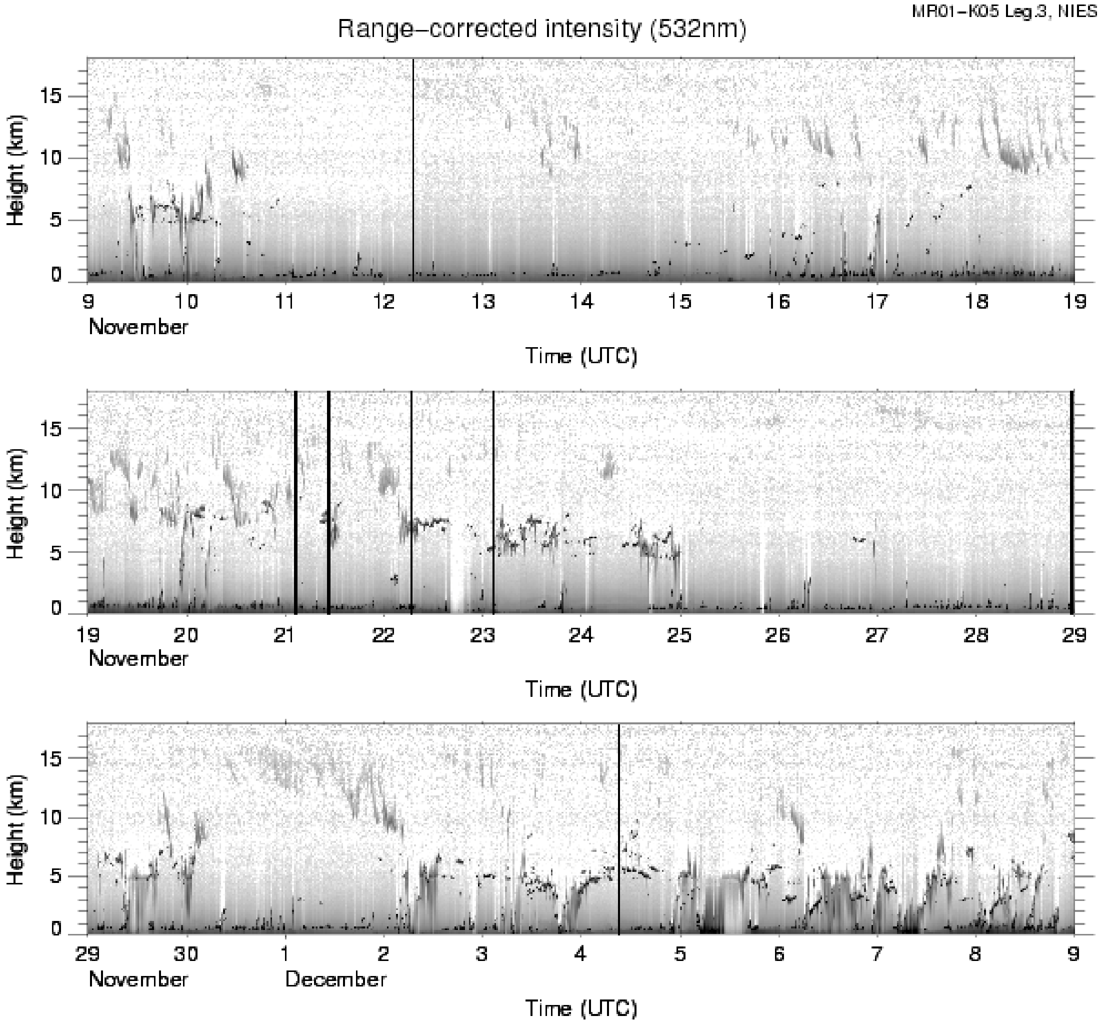

Fig. 6.5-1: Range-corrected signal at 532 nm.

(5) Data archive

- raw data
    - lidar signal at 532 nm (parallel polarization)
    - lidar signal at 532 nm (perpendicular polarization)
    - lidar signal at 1064 nm
    - temporal resolution 10 sec.
    - vertical resolution 6 m.
- processed data
    - cloud base height, apparent cloud top height, cloud phase
    - cloud fraction
    - boundary layer height (aerosol layer upper boundary height)
    - backscatter coefficient of aerosols
    - depolarization ratio

6.6 Cloud and water vapor observation

(1) Personnel

Akihide Kamei (Communications Research Laboratory): Operator
Hiroshi Kumagai (Communications Research Laboratory)
Hiroshi Kuroiwa (Communications Research Laboratory)
Hiroaki Horie (Communications Research Laboratory)
Hajime Okamoto (Tohoku University)

(2) Objectives

Clouds are known to affect primarily the energy and water cycle in the climate system. Their interactions with aerosols, with many chemical reactions in the atmosphere, and with the radiative energy transfer are still not understood. For this cruise, we work for studying vertical distribution and microphysics of clouds and aerosols by using cloud profiling radar (CPR) of Communications Research Laboratory (CRL) in collaboration with the lidar systems of National Institute for Environmental Studies (NIES). One of the great advantages in the active remote sensing is that these sensors provide cloud boundaries with high accuracy. The basic elements of observations are cloud boundaries, cloud microphysics such as effective radius and ice/liquid water content (IWC/LWC), fall velocity of the cloud particles, depolarizations (non-sphericity), and vertical distribution of aerosols. In addition, we expect to study longitudinal and latitudinal distribution of clouds and aerosols.

(3) Methods

CRL has developed an airborne W-band CPR named SPIDER operating at 95GHz. For the cruise of Mirai vessel, the CPR system was modified to be suitable for shipborne measurements. The CPR is operated in the vertical pointing mode and measures backscattering intensity of cloud particles by dual polarization. The radar measurements provide radar reflectivity factor, Doppler velocity, and linear depolarization ratio (LDR) in the vertical direction.

The CPR and the lidar system were co-located in the same container on the upper deck of Mirai. The lidar measurements provide backscattering coefficient in the vertical direction. Thus, it is possible to perform radar/lidar algorithm to retrieve vertical profiles of effective radius and ice/liquid water content of ice and thin water clouds.

The microwave radiometer with dual-frequencies (23.8GHz and 31.4GHz) was also installed. It provides water vapor amounts and liquid water paths of water clouds.

The CPR operation has continued almost all time. The basic operating parameters for CPR measurements are listed in Table 6.6.1.

(4) Results

Figure 6.6.1 shows an example for time-altitude profile of reflectivity factor (dBZ) and Doppler velocity (m/s) observed with the CPR on 6 December 2001. The vertical axis indicates altitude between 150 m and about 20 km with every 82.5 m range resolution. The horizontal axis indicates time (JST). The combination of the CPR and the microwave radiometer is used to retrieve cloud droplet effective radius and liquid water content of thick water clouds. Since the lidar instrument has a capability to detect aerosol signals, we might expect to study cloud-aerosol interactions. These studies will bring significant progress in our understandings of a role of clouds in relation to the cloud feedback processes and climate impact of anthropogenic aerosols through the cloud-aerosol interaction processes.

(5) Data Archive

All data obtained during this cruise will contribute to the APEX project directed by Prof. Teruyuki Nakajima (University of Tokyo) in a way that comparing these data sets with the modeling and satellite data should bring a breakthrough for the cloud-aerosol interaction studies. The CPR and the microwave radiometer data are archived at Communications Research Laboratory.

Table 6.6.1: Basic operating parameters for CPR measurements.

Pulse Width (nsec)	1100
Filter (MHz)	1.0
Polarized Wave	VVHV
Doppler	cc, cc, cc
Pulse Repetition Time (msec)	150, 150, 150, 6550
Number of Noise Samples	8
Number of Range Gates	242
Gate Spacing (m)	82.5
Range Gate Delay (m)	150
Maximum Range (m)	20115
Average Number	32
External Average	1
Acquisition Time (msec)	224

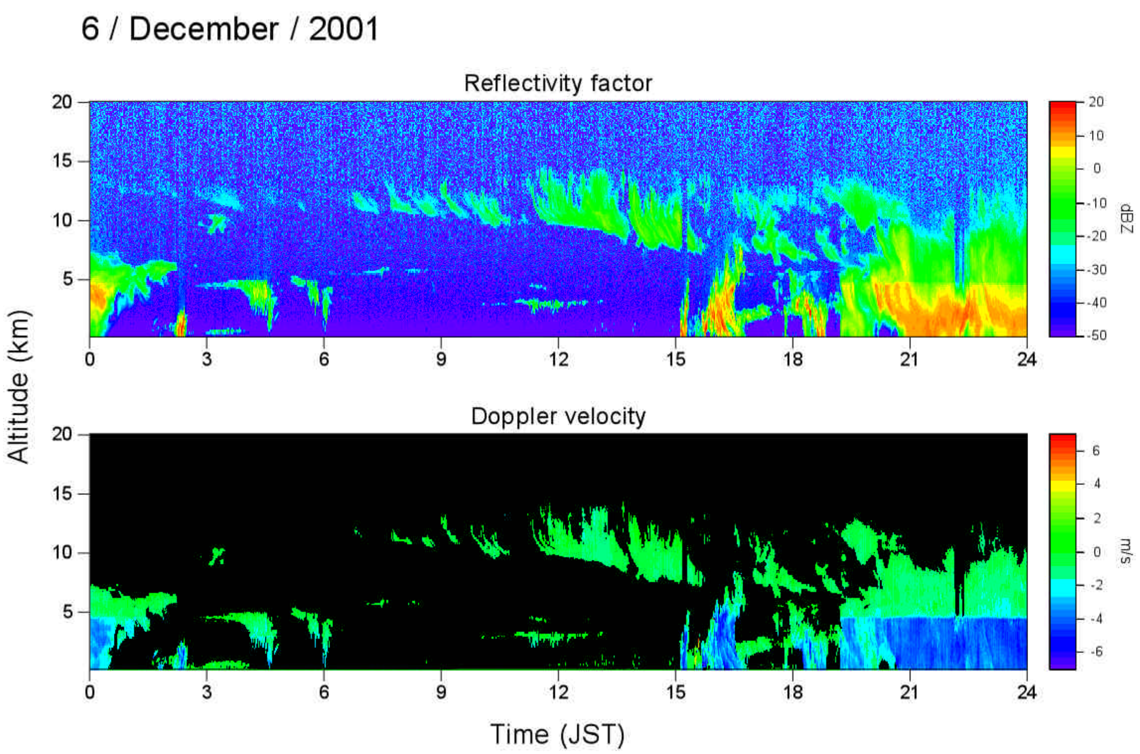

Fig. 6.6.1: Reflectivity factor and Doppler velocity for CPR observations on 6 December 2001.

6.7 Surface Turbulent Flux Measurement

(1) Personnel

Osamu Tsukamoto (Okayama University) : Principal Investigator
Satoshi Takahashi (Okayama University)
Ken'ichi Okada (Okayama University)
Takeshi Nagasawa (Osaka University)
Osamu Hirayama (Osaka University)
Hiroshi Ishida (Maritime University of Kobe / Frontier Observational Research System for Global Change)

(2) Objectives

For the understanding of air-sea interaction, accurate measurements of surface heat and fresh water budget are necessary as well as the momentum exchange through the sea surface. In addition to those exchanges, carbon dioxide surface flux is also indispensable for the global warming. Sea surface turbulent fluxes of momentum, sensible heat, latent heat(water vapor) and carbon dioxide were measured with the eddy correlation method, which is believed to be most accurate and free from assumptions. These surface heat flux data are combined with radiation fluxes, water temperature profiles to lead to the surface energy budget.

(3) Methods

The surface turbulent flux system consists of turbulence instruments (Kaijo Co.,Ltd) and ship motion sensors (Kanto Aircraft Instrument Co.,Ltd). A three-dimensional sonic anemometer- thermometer (Kaijo, DA-600) and an infrared hygrometer (Kaijo, AH-300) are installed at the top of the foremast since June 2000 (MR00-K04 cruise). The sonic anemometer measures wind components relative to the ship and including apparent wind velocity due to ship motion. The ship motions are independently measured by ship motion sensors, including a 2 axis inclinometer (Applied Geomechanics, MD-900-T), a 3-axis accelerometer (Applied Signal Inc., QA-700-020) and a 3-axis rate gyro (Systron Donner, QRS-0050-100).

In addition to those flux system, a new turbulence sensor were introduced in this cruise. The CO2/H2O turbulence sensor (LICOR, LI-7500) can measure turbulent signals of CO2 and water vapor simultaneously. Turbulent signals of water vapor is also available from the infrared hygrometer (AH-300), and it is found that the present LI-7500 sensor was found to be more useful with higher S/N ratio. Carbon dioxide flux was first obtained on R/V Mirai by introducing this CO2 sensor. The Fig.6.7-1 shows the installation at the top of the foremast.

These turbulence and ship motion signals were sampled at 10Hz with a PC based data logging system (Labview, National Instruments Co.,Ltd). During the present cruise, the data logging system was improved to real-time data processing system. In the previous version, the logged data file were processed off-line after the cruise. However, in the present new system, turbulent fluxes and statistics are calculated in on line real-time base and displayed on the PC. Furthermore, the data processing system get the ship speed and ship heading data through LAN system and absolute wind velocity components relative to the earth was evaluated. This is the first ship-board on line flux system in Japan.

During the cruise, 3hourly turbulent flux routines were carried out as ship operation sequence. R/V Mirai cruised against the wind direction about 6 knot to minimize ship body effects. Without the cruise, the ship effects can be appeared as dynamical or heat island effect.

(4) Results

The continuous measurements of turbulent fluctuations were carried out through the cruise (Leg3: Palau – 2N,138E – Palau, and Leg4, Palau – Yokohama). 3 hourly turbulent flux ship operation was carried out as listed in Table 6.7-1. Fig.6.7-2 shows the 3 hourly surface fluxes of sensible heat, latent heat and carbon dioxide.

(5) Data archives

The raw data of turbulent fluctuation time series were archived in MO disks in binary form and preliminary calculated fluxes and statistics were also archived in MO in ascii format. All of the data are submitted to JAMSTEC DMO. The processed data of turbulent fluxes will be archived in Okayama University and open to public after the careful quality check.

Fig.6.7-1
Installation of turbulence sensors
at the top of the foremast

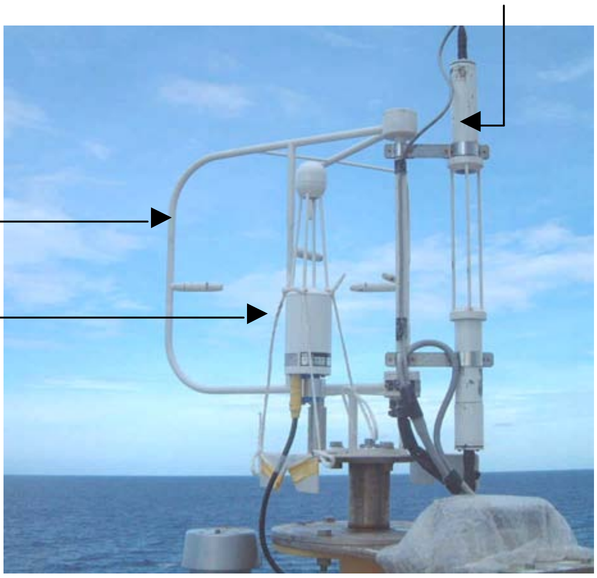

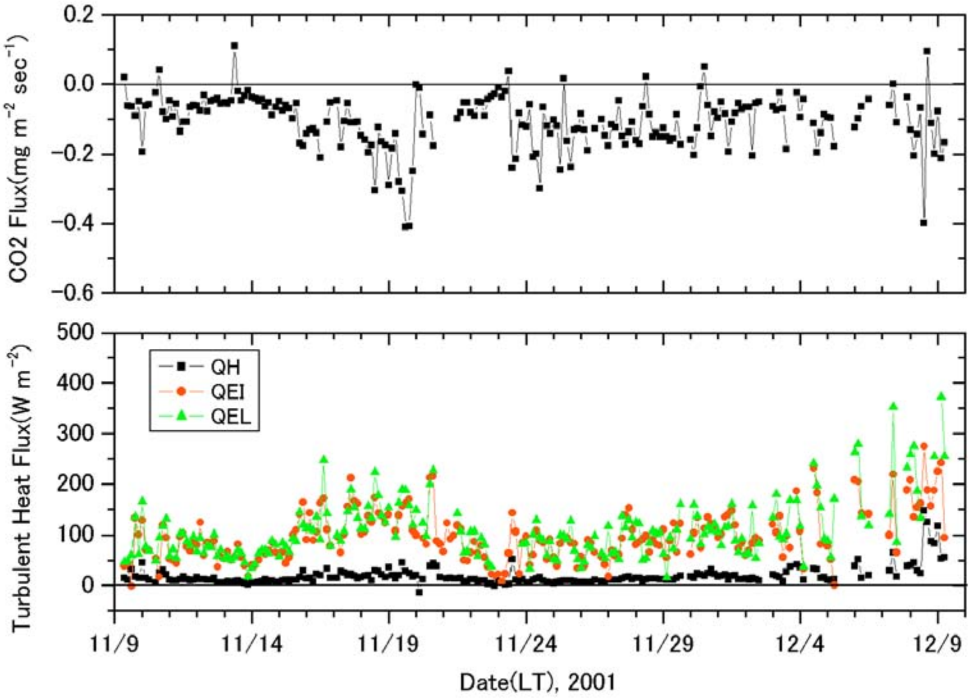

Fig.6.7-2 Time series of 3 hourly turbulent fluxes of sensible heat (QH), latent heat (QEI: from infrared hygrometer, AH-300, QEL: CO_2/H_2O sensor, LI-7500). Upper panel shows CO_2 Flux from LI-7500. It should be noted that all flux components increase clearly in high wind conditions, 16-22 Nov and 7-9 Dec. Latent heat flux is dominant and the average Bowen ratio is around 0.1. Two kinds of infrared hygrometer (AH-300, LI-7500) data shows almost consistent results after dynamic calibration. Carbon dioxide flux was downward for most of the period, this means that ocean is CO_2 sink in this situation.

Table 6.7-1 List of turbulent flux measurements

Date (JST)	Start Time (JST)	End Time (JST)	Duration (hr:min)	Remarks
9-Nov	9:30			fine
	11:30	12:52	1:22	fine
	15:27			fine
	17:30	18:55	1:25	fine
	21:45	22:45	1:00	fine
	23:40	1:10	1:30	cloudy
10-Nov	3:22	4:32	1:10	
	5:30	6:50	1:20	cloudy
	9:10	10:10	1:00	cloudy
	11:30	13:20	1:50	cloudy
	15:10	16:30	1:20	cloudy
	17:29	18:52	1:23	fine
	21:35	22:36	1:01	fine
	23:30	1:05	1:35	fine
11-Nov	3:05	4:20	1:15	
	5:40	6:55	1:15	fine
	9:10	10:15	1:05	fine
	11:38	12:40	1:02	fine
	15:06	16:20	1:14	fine
	17:44	19:15	1:31	fine
	21:34	22:40	1:06	fine
	23:34	0:58	1:24	fine
12-Nov	3:10	4:15	1:05	
	5:30	7:03	1:33	fine
	9:05	10:10	1:05	fine
	11:30	12:30	1:00	fine
	15:05	16:05	1:00	fine
	17:33	19:00	1:27	fine
	21:30	22:35	1:05	fine
	23:35	1:05	1:30	fine
13-Nov	3:05	4:25	1:20	
	5:33	7:00	1:27	fine
	9:04	10:10	1:06	fine
	11:30	13:07	1:37	fine
	15:05	16:05	1:00	fine
	17:39	19:05	1:26	fine
	21:27	22:30	1:03	fine
	23:30	1:00	1:30	fine
14-Nov	3:05	4:20	1:15	
	5:30	7:05	1:35	fine
	9:07	10:13	1:06	fine
	11:35	12:55	1:20	fine
	15:05	16:10	1:05	fine
	17:34	19:05	1:31	fine
	21:35	22:35	1:00	fine
	23:43	1:10	1:27	fine
15-Nov	3:05	4:15	1:10	
	5:30	7:05	1:35	fine
	9:05	10:50	1:45	fine
	11:30	12:31	1:01	fine
	15:05	16:17	1:12	fine
	17:55			fine
	21:30	22:30	1:00	fine
	23:30	1:02	1:32	fine
16-Nov	2:35	4:05	1:30	
	5:33	7:08	1:35	fine
	9:08	10:15	1:07	fine
	12:00	13:00	1:00	fine
	15:05	16:10	1:05	cloudy
	18:00	19:15	1:15	cloudy
	21:32	22:32	1:00	fine
	0:02	1:12	1:10	shower
17-Nov	3:05	4:12	1:07	
	6:00	7:15	1:15	fine,shower
	9:04	10:05	1:01	fine
	12:00	13:08	1:08	fine
	15:05	16:13	1:08	fine
	18:00	19:15	1:15	fine
	21:25	22:25	1:00	fine
	0:00	1:13	1:13	fine
18-Nov	3:05	4:15	1:10	
	6:05	7:18	1:13	fine
	9:00	10:10	1:10	fine
	12:00	13:12	1:12	fine
	15:06	16:17	1:11	cloudy
	18:00	19:12	1:12	cloudy
	21:35	22:35	1:00	cloudy
19-Nov	0:05	1:18	1:13	cloudy
	3:05	4:15	1:10	
	6:00	7:20	1:20	fine
	9:05	10:05	1:00	cloudy
	12:00	13:07	1:07	cloudy
	15:05	16:18	1:13	cloudy
	18:00	19:15	1:15	cloudy
	21:30	22:30	1:00	fine

Table 6.7-1 (continued)

Date (JST)	Start Time (JST)	End Time (JST)	Duration (hr:min)	Remarks
20-Nov	0:00	1:17	1:17	cloudy
	3:03	4:15	1:12	
	6:05	7:20	1:15	cloudy
	9:05	10:33	1:28	shower
	12:05	13:13	1:08	cloudy
	15:02	16:23	1:21	cloudy
	18:02	19:20	1:18	cloudy
	21:27	22:27	1:00	cloudy
21-Nov	0:00	1:17	1:17	fine
	3:03	4:20	1:17	
	6:02	7:15	1:13	fine
	9:05	10:25	1:20	fine
	12:00	13:13	1:13	fine
	15:00	16:17	1:17	fine
	18:00	19:20	1:20	cloudy
	21:33	22:33	1:00	fine
22-Nov	0:11	1:15	1:04	fine
	3:02	4:15	1:13	
	6:00	7:10	1:10	fine
	9:00	10:20	1:20	fine
	12:00	13:14	1:14	fine
	15:05	16:14	1:09	cloudy
	18:00	19:15	1:15	cloudy
	21:30	22:30	1:00	cloudy
23-Nov	0:07	1:05	0:58	cloudy
	3:00	4:13	1:13	
	6:00	6:55	0:55	fine
	9:20	10:20	1:00	fine
	12:07	13:05	0:58	fine
	15:05	16:00	0:55	cloudy
	18:00	19:10	1:10	cloudy
	21:35	22:23	0:48	cloudy
24-Nov	0:00	1:03	1:03	cloudy
	3:03	4:05	1:02	
	6:00	7:05	1:05	fine
	9:00	10:05	1:05	fine
	11:57	12:55	0:58	fine
	15:00	15:58	0:58	fine
	17:53	19:05	1:12	fine
	21:30	22:20	0:50	cloudy
25-Nov	0:02	1:00	0:58	cloudy
	3:00	4:10	1:10	
	6:00	7:07	1:07	cloudy
	8:58	10:10	1:12	fine
	12:00	12:45	0:45	fine
	15:00	16:00	1:00	fine
	17:58	19:10	1:12	fine
	21:26	22:26	1:00	fine

Date (JST)	Start Time (JST)	End Time (JST)	Duration (hr:min)	Remarks
26-Nov	0:00	1:05	1:05	fine
	3:00	4:05	1:05	
	5:55	7:10	1:15	fine
	8:58	10:00	1:02	fine
	12:00	13:00	1:00	fine
	15:00	16:03	1:03	fine
	17:55	19:00	1:05	fine
	21:33	22:25	0:52	fine
27-Nov	0:00	1:07	1:07	fine
	3:00	4:00	1:00	
	5:56	7:00	1:04	fine
	8:55	10:18	1:23	fine
	11:55	12:48	0:53	fine
	15:00	16:00	1:00	fine
	18:00	19:07	1:07	fine
	21:25	22:25	1:00	fine
28-Nov	0:03	1:13	1:10	fine
	2:55	4:10	1:15	
	6:00	7:05	1:05	fine
	9:00	10:47	1:47	fine
	12:07	13:15	1:08	fine
	15:00	16:08	1:08	fine
	17:57	19:08	1:11	fine
	21:26	22:27	1:01	fine
29-Nov	0:00	1:13	1:13	fine
	2:57	4:05	1:08	
	5:56	7:05	1:09	fine
	8:58	10:17	1:19	fine
	11:58	12:55	0:57	fine,cloudy
	14:55	16:10	1:15	cloudy
	17:56	19:15	1:19	shower
	21:20	22:29	1:09	shower
	23:56	1:15	1:19	cloudy
30-Nov	3:00	4:10	1:10	
	5:57	7:10	1:13	fine
	9:02	10:15	1:13	cloudy
	12:00	13:15	1:15	fine
	14:50	16:09	1:19	fine
	17:56	19:10	1:14	fine
	21:25	22:35	1:10	fine
	23:35	1:06	1:31	fine

Table 6.7-1 (continued)

Date (JST)	Start Time (JST)	End Time (JST)	Duration (hr:min)	Remarks
1-Dec	2:45	3:47	1:02	
	5:34	6:36	1:02	fine
	8:45	9:45	1:00	fine
	11:30	12:18	0:48	fine
	15:00	16:12	1:12	cloudy
	17:32	18:32	1:00	fine
	21:05	22:35	1:30	fine
	23:30	1:05	1:35	fine
2-Dec	2:45	4:25	1:40	
	5:33	6:35	1:02	cloudy
	8:45	9:45	1:00	fine
	11:30	13:00	1:30	cloudy
	14:30	15:50	1:20	shower
	17:32	18:33	1:01	cloudy
	21:06	22:06	1:00	loudy,showe
	23:30	0:55	1:25	fine
3-Dec	2:45	3:48	1:03	
	5:35	6:35	1:00	cloudy
	9:00	10:03	1:03	cloudy
	11:30	12:30	1:00	fine
	15:00	16:20	1:20	cloudy
	17:32	18:32	1:00	shower
	21:10	22:10	1:00	cloudy
	23:30	0:57	1:27	cloudy
4-Dec	2:45	4:10	1:25	
	5:34	6:34	1:00	shower
	9:24	10:15	0:51	cloudy
	11:30	12:50	1:20	cloudy
	15:00	16:10	1:10	cloudy
	17:34	18:38	1:04	cloudy
	21:20	22:15	0:55	cloudy
	23:30	0:55	1:25	cloudy
5-Dec	3:00	4:15	1:15	
	5:35	6:36	1:01	fine
	9:30	10:15	0:45	shower
	11:30	12:40	1:10	shower
	15:10	16:15	1:05	shower
	17:34	19:15	1:41	shower
	21:30	22:27	0:57	shower
	23:30	1:06	1:36	cloudy
6-Dec	3:10	4:36	1:26	
	5:35	6:39	1:04	cloudy
	9:27	10:27	1:00	fine
	11:32	12:33	1:01	fine
	14:40	16:20	1:40	shower
	17:35	19:15	1:40	loudy,showe
	21:10	22:40	1:30	shower
	23:40	0:58	1:18	shower

Date (JST)	Start Time (JST)	End Time (JST)	Duration (hr:min)	Remarks
7-Dec	2:45	3:55	1:10	
	5:34	6:37	1:03	cloudy
	8:40	9:43	1:03	shower
	11:30	12:45	1:15	cloudy
	14:40	16:15	1:35	shower
	17:36	19:08	1:32	shower
	21:05	22:05	1:00	cloudy
	23:30	0:45	1:15	cloudy
8-Dec	2:45	3:58	1:13	
	5:40	6:42	1:02	cloudy
	8:42	9:45	1:03	cloudy
	11:35	12:55	1:20	shower
	14:40	15:45	1:05	cloudy
	17:36	19:15	1:39	cloudy
	21:10	22:40	1:30	cloudy
	23:35	1:15	1:40	cloudy
9-Dec	2:55	3:57	1:02	
	5:33	6:37	1:04	fine

6.8 Solar radiation and ocean color measurement

(1) Personnel

Katsutoshi Kozai (Kobe University of Mercantile Marine) : Principal Investigator
Osamu Tsukamoto (Okayama University)
Kunimitsu Ishida (Toba National College of Maritime Technology)
Takuhei Shiozaki (Osaka Prefecture University)
Yasuhiko Okada (Kinki University)

(2) Objectives

Aerosol optical properties and their effects on ocean color at the western equatorial Pacific Ocean are important parameters for the coupled atmosphere-ocean system. The purpose of the observation is to investigate the aerosol effects on the satellite-derived ocean color using in situ observations of aerosol optical thickness and water-leaving radiance synchronized with SeaWiFS satellite overpass.

(3) Methods

SeaWiFS is an abbreviation of Sea-viewing Wide Field-of-view Sensor onboard the SeaStar launched in 1998. The sensor has eight bands in the visible and near infrared wavelengths and the tilt mechanism to avoid sun glitter as shown in Table 6.8-1. During the research cruise SeaWiFS LAC (Local Area Coverage) scenes are received by the station onboard R/V Mirai once (or twice) a day under the authorization of NASA SeaWiFS project as the temporary real-time agreement. Polarization spectral radiometer (Opto Research Corp., PSR1000) measures the atmospheric absorption of the solar radiation and the polarization degree at 5 different angles (45, 60, 75, 90 and 105 degrees) from the sun direction at six wavelengths (e.g. 443, 490, 565, 670, 765 and 865nm). Spectroradiometer (Geophysical & Environmental Research Corp., GER1500) covers the ultraviolet, visible and near infrared wavelengths from 350 to 1050nm with 512 spectral bands. This radiometer is used to measure the calibrated whiteboard spectral radiance and the upward spectral radiance from ocean surface, which produce the spectral reflectance of ocean surface twice a day (1045, 1300 LST). Furthermore the sea surface spectral radiation temperature (spectral skin temperature) is observed by the thermal-infrared radiometer (CIMEL Electronique, CE312) four times a day (0845, 1045, 1300, 1445(1630) LST). The specification of CE312 is shown in Table 6.8-2. The atmospheric depositions and rain were also sampled onboard to analyze chemical components. These data will be analyzed after the cruise. Table 6.8-3 shows the list of observation parameter and schedule.

Table 6.8-1 Specification of SeaWiFS.

Band No.	wavelength (nm)
1	402-422
2	433-453
3	480-500
4	500-520
5	545-565
6	660-680
7	745-785
8	845-885
Equator Crossing	Local Noon(±20min), descending
Orbit type	Sun Synchronous at 705km
Spatial resolution	1.13km(LAC), 4.5km(GAC)
Swath width	2801km(LAC), 1502km(GAC)
Scan Plane Tilt	+20°,0°,-20°

Table 6.8-2 Specification of thermal-infrared radiometer CE312.

Sensed temperature range	-80 to 50 degrees C
Resolution	broad band 8mK at 20 degrees C Other band 50mK at 20 degrees C
Response time	1s
Field of View	10 degrees
Spectral bandpasses	4 bands (8-13, 11.5-12.5, 10.5-11.5, 8.2-9.2 micrometer)
Detector	Thermopile
Operating environment	-20 to 50 degrees C, Resistant to various severe weather Conditions (rain, dust, frost, heat, humidity and corrosion)

Table 6.8-3 List of observation parameter and schedule.

	GER1500	PSR-1000		CIMEL	SeaWiFS	Remarks
day	direct	direct	scat			
9-Nov				○		
10-Nov				○		
11-Nov	○	○	○	○		
12-Nov	○	○	○	○	○	Clear all day
13-Nov	○	○	○	○		
14-Nov	○	○	○	○	○	
15-Nov	○	○	○	○	○	
16-Nov	○			○	○	
17-Nov	○			○	○	
18-Nov	○			○	○	
19-Nov				○	○	
20-Nov				○	○	
21-Nov				○	○	
22-Nov				○	○	
23-Nov				○	○	
24-Nov	○	○	○	○	○	
25-Nov	○	○	○	○	○	
26-Nov	○	○	○	○	○	
27-Nov	○	○	○	○	○	
28-Nov	○	○	○	○	○	Clear all day
29-Nov	○			○	○	
30-Nov				○	○	
1-Dec				○	○	
2-Dec				○	○	
3-Dec				○	○	
4-Dec				○	○	
5-Dec				○	○	
6-Dec				○	○	
7-Dec				○	○	
8-Dec				○	○	
9-Dec				○		
10-Dec				○		

Note: “Direct” and “scat” mean the observation of solar radiation in a direct and polarized scattering mode, respectively.

(4) Preliminary Results

The measurements of solar radiation and ocean color were made on the fine and calm weather conditions during the whole cruise. The spectral radiation temperature measurement was carried out everyday except rainy and windy conditions. And the atmospheric deposition was sampled once a day. The results of each observation are shown in the following tables and figures.

Aerosol optical properties

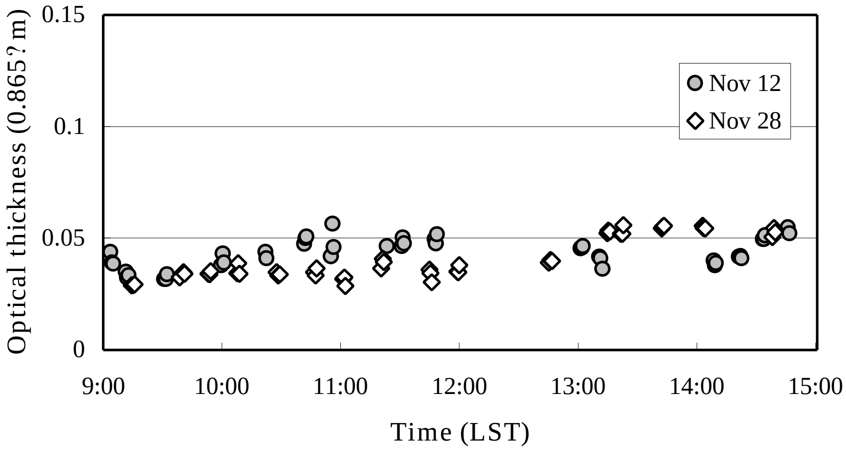

Fig. 6.8-1 Time variation of aerosol optical thickness at 0.865?m

Fig 6.8-1 shows the temporal variation of optical thickness of aerosols at 0.865?m. Two clear days data out of all the measured data are plotted as preliminary results. At Nov. 12th the aerosol optical thickness has small variations around 0.05. On the other hand, at Nov. 28th the aerosol optical thickness increases with time.

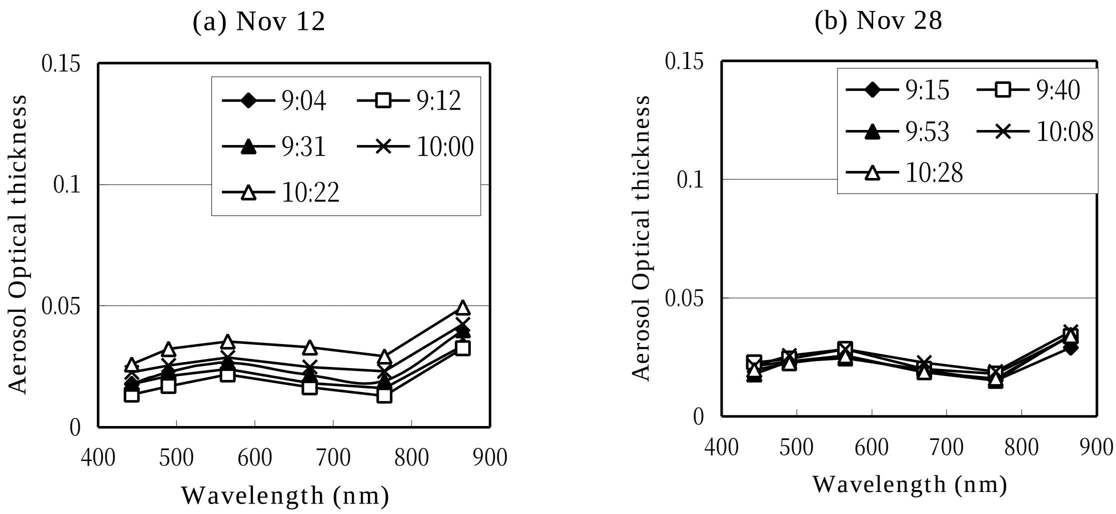

Fig. 6.8-2 Spectral aerosol optical thickness. (a) Nov 12th, (b) Nov 28th

Fig 6.8-2 (a) and (b) show the wavelength dependence of the aerosol optical thickness at the same days of Figure 6.8-1. There is a small variation of the optical thickness with wavelength. Wavelength dependence has a relation with the size distribution of aerosols (e.g. small variations for large natural originated aerosols while large variations for small anthropogenic aerosols). From the preliminary results which is shown in Fig 6.8.6, the distribution of large natural originated aerosols (like oceanic aerosols) can be seen.

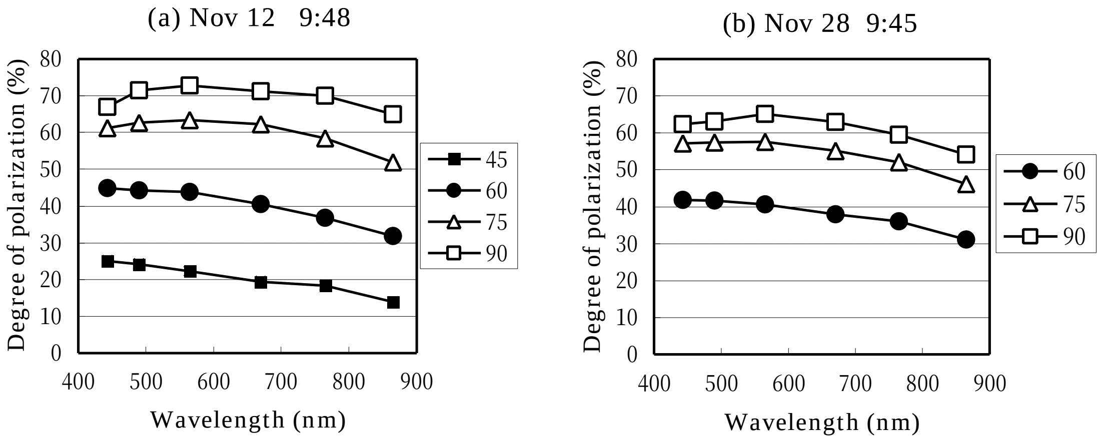

Fig. 6.8-3 Degree of polarization with different observed angles. (a) Nov 12th, (b) Nov 28th (Legends show the degree of observation from sun direction.)

Fig 6.8-3 (a) and (b) show the measured values of degree of polarization with wavelengths. These measured values can be utilized for the retrieval of aerosol parameters which cannot be retrieved only with radiance data (direct sunlight measurement).

Ocean color characteristics

In situ observation by GER1500

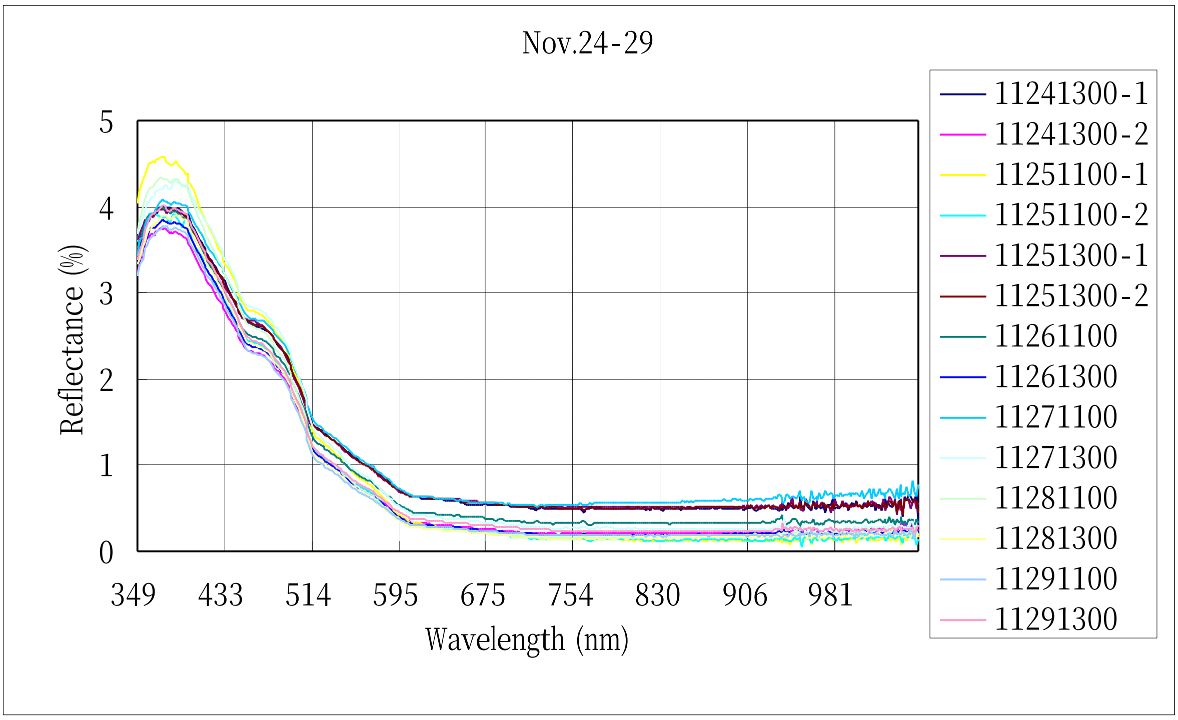

Fig.6.8-4 Variation of sea surface spectral reflectance from Nov.24 to 29. (Legend shows the month,

day, time(LST) and the number of repeated observation.)

Fig.6.8-4 shows the variation of sea surface spectral reflectance during the period from Nov.24 to 29. The maximum reflectances of about 4% are frequently observed around 370nm and the minimums are seen longer than 700nm of the near-infrared wavelength. Since the electromagnetic energy in this wavelength region is known to be absorbed at the sea surface, small reflectance in the near-infrared may indicate various sea surface conditions such as glittering, form and breaking wave.

SeaWiFS data

SeaWiFS data are received onboard the R/V MIRAI receiving station during the period of temporal license agreement from NASA during the period from Nov.14 to Dec.10. All SeaWiFS raw data are decrypted by using the OGP software provided by NASA GSFC. Higher level products such as chlorophyll-a concentration, aerosol optical thickness and spectral reflectance are generated by using SeaDAS software.

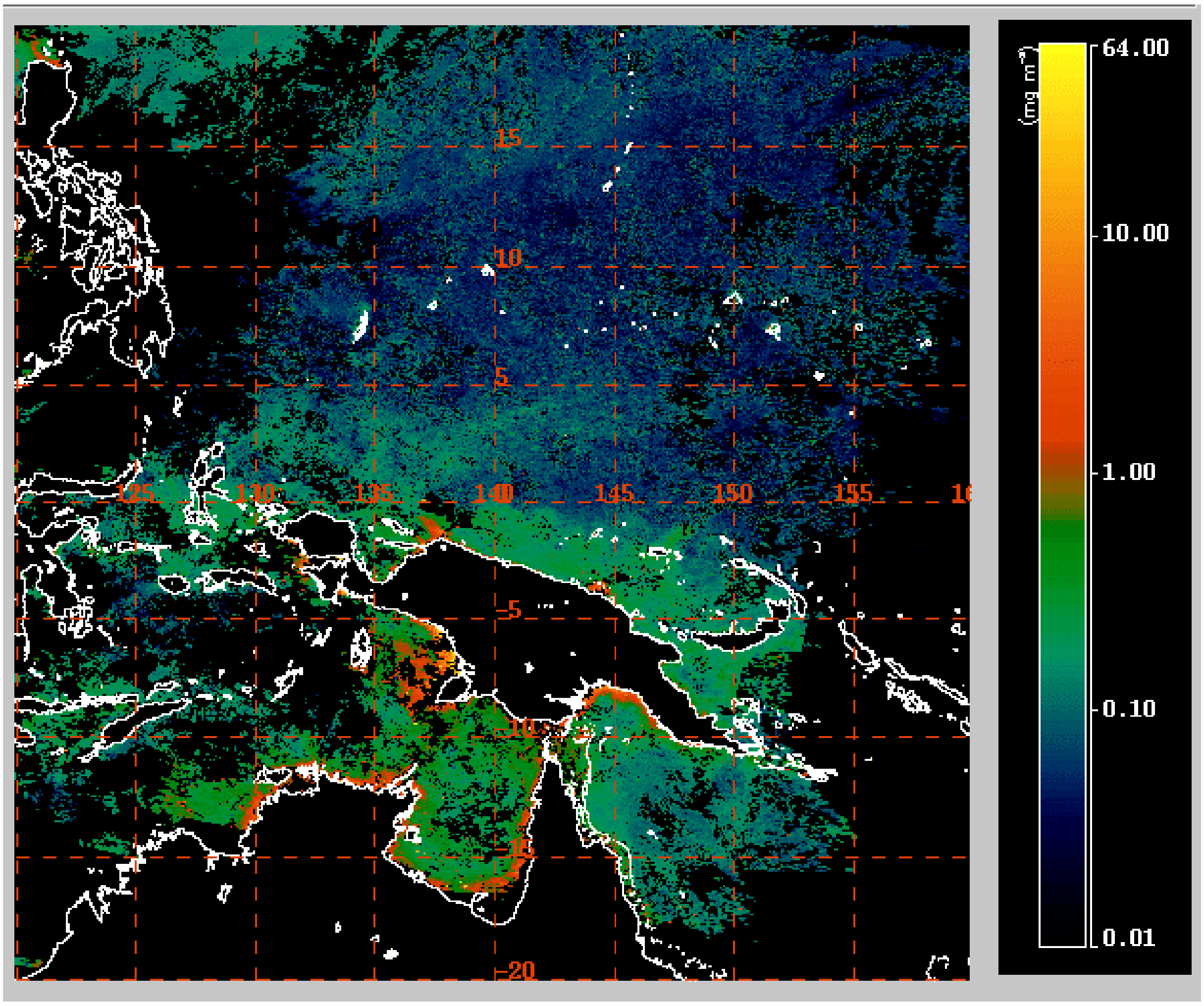

Fig.6.8-5 Chlorophyl-a concentration composite from Nov.25 to 30 derived from SeaWiFS data.

Fig.6.8-5 shows the distribution of chlorophyl-a concentration derived from SeaWiFS. At the location of R/V MIRAI (2N, 138E) the concentration is higher than 0.1mg/m^3, while the region east of 140 degrees longitude indicates the area of low concentration less than 0.1mg/m^3.

Spectral radiation temperature measurement

Normally, the measurements were carried out 4 times a day (9:00, 11:00, 13:00, 16:30 LT). The radiometer was deployed on the deck for about 10minutes to be averaged.

On 24, 27 in Nov and 1 in Dec, continuous measurements were carried out throughout the day as shown in Table 6.8-4.

Table 6.8-4 List of continuous measurement

Date	Start Time(LT)	Stop Time(LT)
24 Nov	8:09	16:05
27 Nov	6:14	19:47
1 Dec	6:06	23:42

Fig.6.8-6 shows the time series of SSST(Sea Surface Skin Temperature) measured by CH-1(8-13mm) of the radiometer including continuous measurements. It is clearly represented that SSST increase in midday is more than 1 degC in 13, 14 Nov. The minimum temperature in the early morning increases gradually in 9 – 14 Nov. Those are considered to be related with calm and sunny condition during the period. After 16 Nov, rather high wind or cloudy condition was dominant and SSST increase during the daytime was within 0.5 degC. Especially in Dec, heavy cloud and rain continued accompanying high wind and lead to unidentified diurnal variations.

Fig.6.8-7 shows the continuous diurnal time series for 3 days as listed in Table 6.8-4. It is common for the days that SSST maximum was observed 14-15 LT. Another common feature is that SSST dips were observed around 11:30 and 14:30. When compared with other sea water temperature measurements, “sea snake”(representing several cm near the surface) and intake(at 5m depth) data also show the same dips. Those can be considered as the effect of water mixing by ship thruster operation during CTD measurements.

As the contrast to those dips, some prominent peaks were identified in 27 Nov and 1 Dec. These increases of SSST are consistent with downwelling longwave radiation as measured by SOAR system. So the apparent SSST peaks are affected by cloudiness(sky temperature). Sky temperature correction should be applied with longwave radiation data. The differences of SSST between 4 spectral bands are also interesting and should be discussed later.

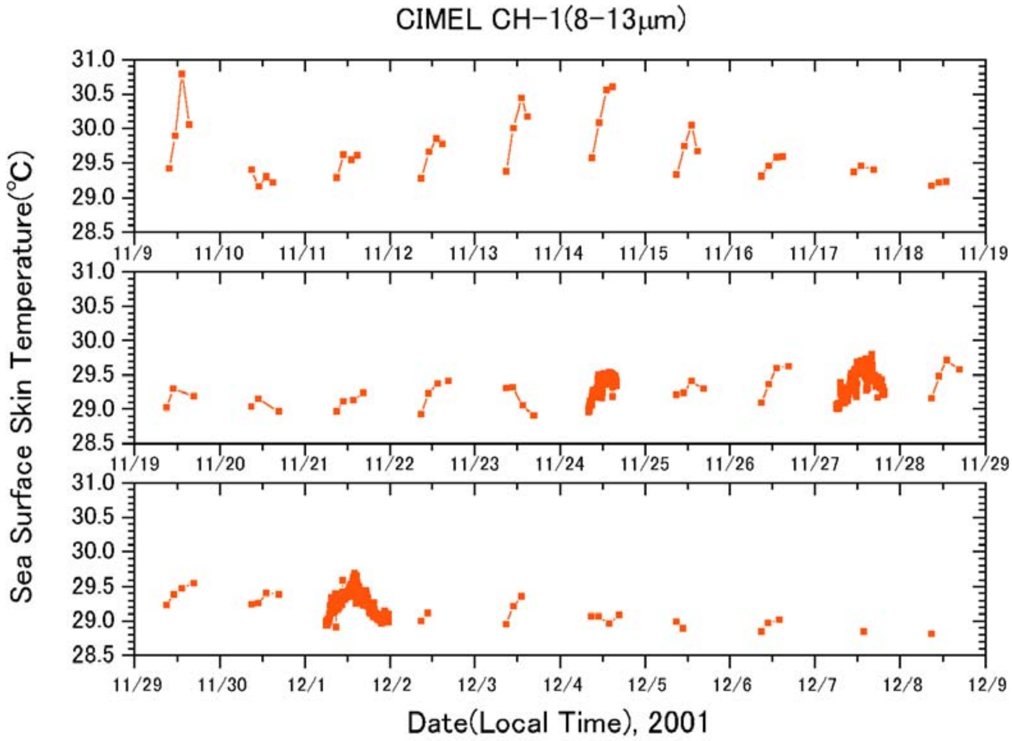

Fig.6.8-6 Time series of SSST during 9 Nov – 8 Dec based on 4 times measurement and . continuous measurement.

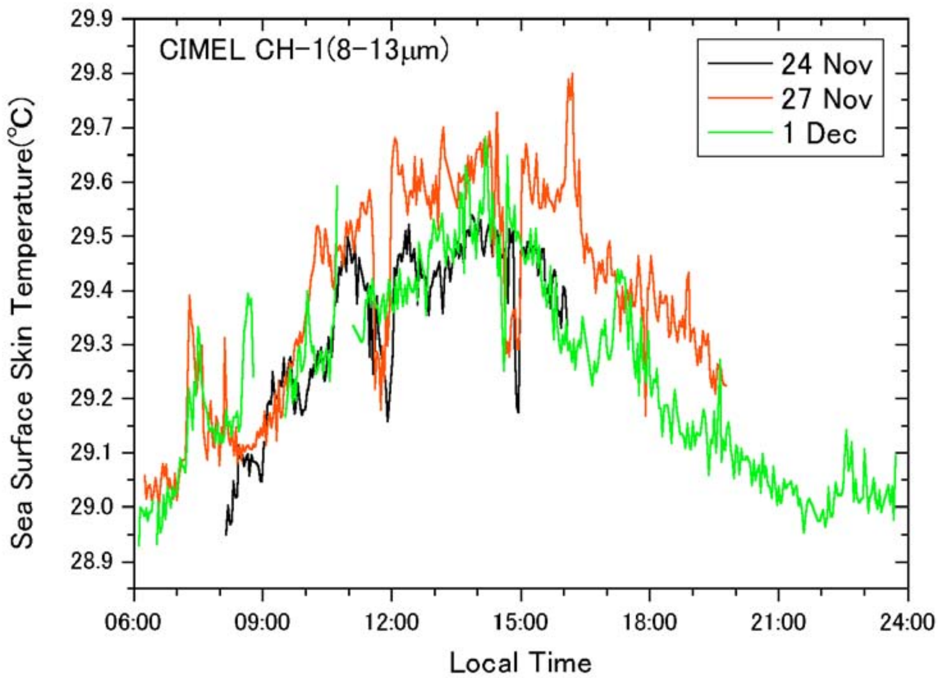

Fig.6.8-7 Continuous time series of SSST on 24 Nov, 27 Nov and 1 Dec.

(5) Data archives

The SeaWiFS raw data received by the station onboard R/V Mirai will be submitted to NASA. The other products such as spectral radiance and aerosol optical thickness derived from SeaWiFS are archived in CD-Rs. The raw data of the solar radiation are archived in a floppy disk. Samples of atmospheric deposition are analyzed on their chemical components etc., and the results are archived in a floppy disk. After the quality check of those data, they will be published open to public. All data will be archived at Kobe University of Mercantile Marine. The data and sample inventory information are submitted to JAMSTEC DMO.

6.9 Observation of the oceanic profile

6.9.1 CTD observation

(1) Personnel

Kunio Yoneyama (JAMSTEC): Principal Investigator
Satoshi Ozawa (MWJ): Operation leader
Kentaro Shiraishi (MWJ)
Miki Yoshiike (MWJ)
Naoko Takahashi (MWJ)
Fuma Matsunaga (MWJ)
Fumihide Okawa (MWJ)

(2) Objectives

Investigation of the oceanic structure and its time variation by measuring vertical profiles of temperature and salinity.

(3) Methods

We observed vertical profile of temperature and salinity by CTD / Carousel (Conductivity Temperature Depth profiler / Carousel Multi Water Sampler). The temperature sensor, conductivity sensor, pressure sensor, oxygen sensor, and altimeter were attached to CTD unit. Salinity was calculated from observed pressure, conductivity and temperature. The CTD / Carousel was deployed from starboard on working deck. Descending rate and ascending were kept about 1.2 m/s respectively. In Leg3, sea surface temperature (SST) was also observed on the every cast.

The CTD raw data was acquired in real time by using the SEASAVE utility from SEASOFT software (ver.4.232) provided by SBE and stored on the hard disk of an IBM personal computer. Water samplings were made during up-cast by sending a fire command from the computer.

In Leg3, we have three phases of CTD measurements at stationary observation point (2N, 138E). In first (Nov.09-Nov.15) and third (Dec.1-Dec.9) phase, CTD casting was conducted every 6 hours (05:20, 14:20, 17:20, 23:20, in UTC). In second phase (Nov.15-Nov.31), it was conducted every 3hours (02:20, 05:20, 08:20, 11:20, 14:20, 17:20, 20:20, 23:20, in UTC). The casts were to 1,000 m at 11:20, while the other casts were to 500 m. In total, 178 casting were carried out (see Table 6.9.1-1). Every day we sampled water on 11:20 (UTC) at 1000m to calibrate salinity data.

In Leg4, the casts were to 30 m above the bottom. Two cast were carried out (see Table 6.9.1-1). We sampled water at the depth 30 m above the bottom to calibrate salinity data.

The CTD raw data was processed using SEASOFT (ver.4.232). Data processing procedures and used utilities of SEASOFT were as follows:

DATCNV: Converts the binary raw data to output on physical unit.
This utility selects the CTD data when bottles closed to output on another file.
SECTION: Remove the unnecessary data.
WILDEDIT: Obtain an accurate estimate of the true standard deviation of the data.
Std deviations for Pass 1:2
Std deviations for Pass 2:10
Points per block: 48
ALIGNCTD: ALIGNCTD aligns oxygen measurements in time relative to pressure.

Primary Oxygen sensor relative to pressure = 3.0 seconds

CELLTM: Remove to conductivity cell thermal mass effects from the measured conductivity.
Primary alpha = 0.03, 1/beta = 7.0

FILTER: Run a low-pass filter on one or more columns of data.
Filter A = 0.15sec
Variable to Filter: Pressure: Low Pass Filter A

LOOPEDIT: Marks scans bad by setting the flag value associated with the scan to badflag in input .cnv files that have pressure slowdowns or reversals.
Minimum Velocity Selection = Fixed Minimum Velocity.
Minimum CTD Velocity [m/sec] = 0.0
Exclude Scan Marked Bad in LOOPEDIT = Yes

DERIVE: Calculates oceanographic parameters from the input.cnv file.

BINAVG: Calculation the averaged data in every 1db (in Leg3).
Calculation the averaged data in every 1m (in Leg4).

SPLIT: Splits the data made in CNVfiles into upcast and downcast files.

ROSSUM: Edits the data of water sampled to output a summary file.

Specifications of sensors are listed below.

Under water unit: CTD 9plus (S/N 51190 Sea-bird Electronics, Inc.)
Calibration date: 27-Oct-1999

Primary Temperature Sensor: SBE3-04/F (S/N 032453 Sea-bird Electronics, Inc.)
Calibration date: 03-Aug-2001

Primary Conductivity Sensor: SBE4-04/0 (S/N 042240 Sea-bird Electronics, Inc.)
Calibration date: 03-Aug-2001

D.O. sensor: SBE13-04 (S/N 130575 Sea-bird Electronics, Inc.)
Calibration date: 09-Oct-2001

D.O. sensor: SBE13-04 (S/N 130540 Sea-bird Electronics, Inc.)
Calibration date: 18-Jun-2001

The D.O. sensors are used as:

From Cast001 to Cast109 in Leg3:
Primary: SBE13-04 (S/N 130540)

From cast110 to Cast117 and from Cast125 to cast178 in Leg3, and Leg4:
Primary: SBE13-04 (S/N 130575)
Secondary: SBE13-04 (S/N 130540)

From Cast118 to Cast124 in Leg3:
Primary: SBE13-04 (S/N 130540)
Secondary: SBE13-04 (S/N 130575)

Altimeter sensor: Benthos 2110-2 (S/N 228 Benthos, Inc.)

Deck unit: SBE11 (S/N 11P7030-0272, Sea-bird Electronics, Inc.)

Carousel water sampler: SBE32 (S/N3222295-0171 Sea-bird Electronics, Inc.)

(4) Preliminary Results

Time series sections of temperature and salinity, and sigma-theata are shown in Fig6.9.1-1. The site of a change in time of the SST is shown in Figs. 6.9.1-2 and 6.9.1-3. Individual vertical profiles on each cast are attached in the following Appendix. Note that in these figures, the correction of salinity and oxygen data by sampled water is not applied.

(5) Remarks

The discontinuous shift of the observed D.O. profiles was found between cast052 and cast053. Though the secondary D.O. sensor (S/N130540) was added to check the sensor reliability, it is difficult to identify causes because the difference of the observed values from two sensors varied so large. The reported values are from the primary sensor.

(6) Data archive

All raw and processed CTD data file were copied into magnetic optional disk (MO) and submitted to JAMSTEC Data Management Office (DMO) and will be under their control.

Table 6.9-1 CTD Cast Table

Line	Cast No.	File Name	Lat. [N]	Long. [E]	Date [UTC]	Start Time	End Time	Max. Press. [db]	Max. Wire Out [m]	SST [deg-C]	Depth [m]	Water Samplin g	Note
Leg3	001	K5S001	01-54.09N	138-03.54E	08.Nov.2001	23:41	00:06	505.256	503.3	29.4	4661		
Leg3	002	K5S002	01-53.61N	138-03.62E	09.Nov.2001	05:56	06:16	504.033	499.8	29.7	4672		
Leg3	003	K5S003	01-52.73N	138-04.36E	09.Nov.2001	11:30	12:19	1008.640	1007.5	29.7	4661	○	
Leg3	004	K5S004	01-53.45N	138-03.09E	09.Nov.2001	17:56	18:17	504.961	504.4	29.5	4671		
Leg3	005	K5S005	01-53.58N	138-03.50E	09.Nov.2001	23:25	23:44	504.575	501.6	29.4	4668		
Leg3	006	K5S006	01-51.79N	138-03.49E	10.Nov.2001	05:25	05:50	504.638	506.4	29.5	4670		D.O.:ERROR
Leg3	007	K5S007	01-51.36N	138-03.72E	10.Nov.2001	11:25	12:11	1010.050	1007.5	29.4	4684	○	
Leg3	008	K5S008	01-51.87N	138-03.22E	10.Nov.2001	17:24	17:43	504.531	501.1	29.4	4678		
Leg3	009	K5S009	01-51.43N	138-02.90E	10.Nov.2001	23:25	23:43	505.210	505.6	29.4	4681		
Leg3	010	K5S010	01-51.38N	138-03.23E	11.Nov.2001	05:25	05:44	504.421	500.0	29.7	4687		
Leg3	011	K5S011	01-51.60N	138-03.49E	11.Nov.2001	11:24	12:10	1007.469	1013.4	29.6	4673	○	
Leg3	012	K5S012	01-51.52N	138-03.07E	11.Nov.2001	17:25	17:43	504.087	503.4	29.5	4696		
Leg3	013	K5S013	01-51.01N	138-03.51E	11.Nov.2001	23:25	23:43	504.848	500.5	29.4	4698		
Leg3	014	K5S014	01-48.34N	137-58.64E	12.Nov.2001	05:27	05:45	503.355	501.2	29.6	4563		
Leg3	015	K5S015	01-51.43N	138-03.17E	12.Nov.2001	11:24	12:11	1009.348	1007.3	29.8	4687	○	
Leg3	016	K5S016	01-51.60N	138-03.26E	12.Nov.2001	17:24	17:43	504.985	500.7	29.4	4677		
Leg3	017	K5S017	01-51.43N	138.03.27E	12.Nov.2001	23:25	23:43	504.015	501.1	29.4	4680		
Leg3	018	K5S018	01-51.40N	138-03.25E	13.Nov.2001	05:24	05:42	505.184	500.9	30.1	4682		
Leg3	019	K5S019	01-51.58N	138-03.20E	13.Nov.2001	11:24	12:07	1008.328	1004.7	29.5	4685	○	
Leg3	020	K5S020	01-51.50N	138.03.27E	13.Nov.2001	17:24	17:44	504.161	500.3	29.7	4687		
Leg3	021	K5S021	01-51.60N	138-03.33E	13.Nov.2001	23.:25	23:42	503.454	499.6	29.5	4680		
Leg3	022	K5S022	01-51.47N	138-03.09E	14.Nov.2001	05:24	05:42	505.5	501.2	30.6	4683		
Leg3	023	K5S023	01-51.98N	138-03.24E	14.Nov.2001	11:24	12:10	1007.779	1004.9	30.5	4515	○	
Leg3	024	K5S024	01-51.60N	138-03.12E	14.Nov.2001	17:24	17:41	505.136	501.6	29.6	-		
Leg3	025	K5S025	01-51.72N	138-03.38E	14.Nov.2001	23:24	23:42	505.311	501.1	29.5	-		
Leg3	026	K5S026	01-51.49N	138-03.14E	15.Nov.2001	05:24	05:44	503.304	500.3	29.9	4515		
Leg3	027	K5S027	01-51.54N	138-03.34E	15.Nov.2001	11:24	12:08	1009.266	1011.0	29.7	4681	○	
Leg3	028	K5S028	01-51.32N	138-03.40E	15.Nov.2001	23:24	23:42	505.371	502.2	29.6	4691		
Leg3	029	K5S029	01-51.54N	138-03.29E	16.Nov.2001	02:22	02:41	505.386	500.7	29.5	4686.0		
Leg3	030	K5S030	01-51.63N	138-03.17E	16.Nov.2001	05:24	05:47	503.872	500.7	29.7	4695		
Leg3	031	K5S031	01-51.00N	138-03.12E	16.Nov.2001	08:20	08:40	508.600	508.4	29.5	4697.0		
Leg3	032	K5S032	01-51.48N	138-03.28E	16.Nov.2001	11:23	12:13	1010.127	1005.7	29.5	4690.0	○	
Leg3	033	K5S033	01-51.42N	138-03.31E	16.Nov.2001	14:24	14:42	505.397	507.9	29.5	4686.0		
Leg3	034	K5S034	01-51.23N	138-03.23E	16.Nov.2001	17:24	17:42	503.850	503.1	29.4	4698		
Leg3	035	K5S035	01-51.35N	138-03.19E	16.Nov.2001	20:22	20:40	504.609	507.1	29.4	4694		
Leg3	036	K5S036	01-51.26N	138-03.61E	16.Nov.2001	23:22	23:42	503.247	509.0	29.4	4696		
Leg3	037	K5S037	01-51.45N	138-03.42E	17.Nov.2001	02:22	02:42	504.253	503.8	29.5	4685		
Leg3	038	K5S038	01-51.30N	138-03.54E	17.Nov.2001	05:24	05:44	503.382	554.2	29.6	4684		
Leg3	039	K5S039	01-51.40N	138-03.36E	17.Nov.2001	08:22	08:39	504.640	504.2	29.4	4685		
Leg3	040	K5S040	01-51.43N	138-03.29E	17.Nov.2001	11:22	12:06	1008.383	1011.5	29.5	4694	○	
Leg3	041	K5S041	01-51.41N	138-03.43E	17.Nov.2001	14:23	14:41	504.197	504.0	29.4	4681		
Leg3	042	K5S042	01-51.29N	138-03.52E	17.Nov.2001	17:24	17:43	504.122	509.1	29.4	4690		
Leg3	043	K5S043	01-51.43N	138-03.23E	17.Nov.2001	20:22	20:41	503.992	504.7	29.3	4686		
Leg3	044	K5S044	01-51.34N	138-03.37E	17.Nov.2001	23:23	23:40	504.770	506.9	29.3	4683		
Leg3	045	K5S045	01-51.39N	138-03.53E	18.Nov.2001	02:22	02:40	504.939	502.2	29.4	4682		
Leg3	046	K5S046	01-51.31N	138-03.64E	18.Nov.2001	05:28	05:46	505.107	506.9	29.4	4683		
Leg3	047	K5S047	01-51.78N	138-03.28E	18.Nov.2001	08:20	08:38	505.600	502.5	29.2	4679		

Table 6.9-1 CTD Cast Table (continue)

Line	Cast No.	File Name	Lat. [N]	Long. [E]	Date [UTC]	Start Time	End Time	Max. Press. [db]	Max. Wire Out [m]	SST [deg-C]	Depth [m]	Water Sampling	Note
Leg3	048	K5S048	01-51.42N	138-03.31E	18.Nov.2001	11:24	12:13	1008.940	1004.5	29.2	4682	○	
Leg3	049	K5S049	01-51.45N	138-03.29E	18.Nov.2001	14:22	14:45	503.665	502.2	29.2	4682		
Leg3	050	K5S050	01-51.46N	138-03.42E	18.Nov.2001	17:23	17:43	504.482	509.1	29.2	4682		
Leg3	051	K5S051	01-51.50N	138-03.34E	18.Nov.2001	20:21	20:40	505.426	507.9	29.1	4683		
Leg3	052	K5S052	01-51.38N	138-03.31E	18.Nov.2001	23:22	23:41	503.797	504.4	29.1	4689		
Leg3	053	K5S053	01-51.23N	138-03.66E	19.Nov.2001	02:22	02:41	505.451	504.5	29.2	4684		
Leg3	054	K5S054	01-50.09N	138-04.00E	19.Nov.2001	05:22	05:41	504.704	503.6	29.2	4679		
Leg3	055	K5S055	01-51.34N	138-02.01E	19.Nov.2001	08:20	08:29	505.684	507.9	29.2	4695		
Leg3	056	K5S056	01-51.60N	138-03.37E	19.Nov.2001	11:22	12:07	1008.512	1029.7	29.2	4676	○	
Leg3	057	K5S057	01-51.45N	138-03.36E	19.Nov.2001	14:22	14:41	505.223	503.3	29.2	4681		
Leg3	058	K5S058	01-51.40N	138-03.42E	19.Nov.2001	17:23	17:43	504.743	504.2	29.1	4686		
Leg3	059	K5S059	01-51.74N	138-03.25E	19.Nov.2001	20:23	20:43	504.419	501.8	29.1	4674		
Leg3	060	K5S060	01-51.55N	138-03.30E	19.Nov.2001	23:23	23:43	502.284	506.0	29.1	4682		
Leg3	061	K5S061	01-51.58N	138-03.36E	20.Nov.2001	02:21	02:41	507.006	514.7	29.1	4676		
Leg3	062	K5S062	01-51.13N	138-03.38E	20.Nov.2001	05:22	05:42	507.781	509.0	29.0	4701		
Leg3	063	K5S063	01-51.68N	138-03.32E	20.Nov.2001	08:22	08:43	508.942	548.1	29.0	4677		
Leg3	064	K5S064	01-51.41N	138-03.43E	20.Nov.2001	11:22	12:06	1008.214	1034.7	29.1	4684	○	
Leg3	065	K5S065	01-51.41N	138-03.36E	20.Nov.2001	14:22	14:42	503.158	503.3	29.1	4695		
Leg3	066	K5S066	01-51.45N	138-03.34E	20.Nov.2001	17:23	17:43	503.521	504.9	29.1	4684		
Leg3	067	K5S067	01-51.50N	138-03.31E	20.Nov.2001	20:23	20:43	504.077	501.6	29.1	4684		
Leg3	068	K5S068	01-51.41N	138-03.37E	20.Nov.2001	23:21	23:40	504.505	523.1	29.1	4694		
Leg3	069	K5S069	01-51.53N	138-03.31E	21.Nov.2001	02:21	02:40	504.402	508.6	29.2	4682		
Leg3	070	K5S070	01-51.61N	138-03.27E	21.Nov.2001	05:20	05:40	506.977	507.3	29.2	4680		
Leg3	071	K5S071	01-51.47N	138-03.25E	21.Nov.2001	08:20	08:39	504.040	509.4	29.2	4694		
Leg3	072	K5S072	01-51.42N	138-03.20E	21.Nov.2001	11:23	12:09	1008.386	1014.1	29.1	4697	○	
Leg3	073	K5S073	01-50.72N	138-03.05E	21.Nov.2001	14:30	14:49	502.322	520.5	29.1	4694		
Leg3	074	K5S074	01-51.45N	138-03.24E	21.Nov.2001	17:23	17:42	504.334	505.5	29.1	4684		
Leg3	075	K5S075	01-51.58N	138-03.10E	21.Nov.2001	20:21	20:40	504.280	509.9	29.0	4692		
Leg3	076	K5S076	01-51.36N	138-03.05E	21.Nov.2001	23:21	23:39	504.674	514.5	29.1	4699		
Leg3	077	K5S077	01-51.56N	138-03.05E	22.Nov.2001	02:20	02:39	504.435	513.6	29.3	4685		
Leg3	078	K5S078	01-51.28N	138-03.34E	22.Nov.2001	05:21	05:41	504.274	528.6	29.4	4686		
Leg3	079	K5S079	01-51.37N	138-02.92E	22.Nov.2001	08:20	08:40	504.194	518.0	29.4	4691		
Leg3	080	K5S080	01-51.27N	138-03.48E	22.Nov.2001	11:22	12:09	1009.832	1015.9	29.1	4682	○	
Leg3	081	K5S081	01-51.07N	138-03.71E	22.Nov.2001	14:25	14:45	504.899	519.2	29.2	4681		
Leg3	082	K5S082	01-51.49N	138-03.47E	22.Nov.2001	17:22	17:40	504.114	507.9	29.2	4681		
Leg3	083	K5S083	01-51.38N	138-03.57E	22.Nov.2001	20:20	20:38	505.185	506.4	29.2	4673		
Leg3	084	K5S084	01-51.57N	138-03.16	22.Nov.2001	23:21	23:59	1008.325	1024.8	29.3	4696		
Leg3	085	K5S085	01-51.50N	138-03.11E	23.Nov.2001	02:20	02:40	504.970	509.3	29.4	4685		
Leg3	086	K5S086	01-51.38N	138-03.23E	23.Nov.2001	05:23	05:42	505.128	510.4	29.3	4688		
Leg3	087	K5S087	01-51.19N	138-03.13E	23.Nov.2001	08:20	08:38	504.497	504.9	29.3	4694		
Leg3	088	K5S088	01-51.57N	138-03.61E	23.Nov.2001	11:31	12:16	1008.182	1042.2	29.2	4669	○	
Leg3	089	K5S089	01-51.48N	138-03.47E	23.Nov.2001	14::22	14:39	503.921	505.5	29.2	4678		
Leg3	090	K5S090	01-51.18N	138-03.10E	23.Nov.2001	17:22	17:41	503.875	500.3	29.1	4699		
Leg3	091	K5S091	01-51.17N	138-03.38E	23.Nov.2001	20:20	20:39	503.842	503.4	29.1	4700		
Leg3	092	K5S092	01-51.59N	138-03.67E	23.Nov.2001	23:21	23:40	504.301	504.5	29.2	4659		
Leg3	093	K5S093	01-51.51N	138-03.44E	24.Nov.2001	02:20	02:38	504.923	507.5	29.4	4677		
Leg3	094	K5S094	01-51.66N	138-03.63E	24.Nov.2001	05:19	05:38	504.740	504.4	29.6	4657		

Table 6.9-1 CTD Cast Table (continue)

Line	Cast No.	File Name	Lat. [N]	Long. [E]	Date [UTC]	Start Time	End Time	Max. Press. [db]	Max. Wire Out [m]	SST [deg-C]	Depth [m]	Water Sampling	Note
Leg3	095	K5S095	01-51.40N	138-03.38E	24.Nov.2001	08:18	08:35	504.367	500.1	29.3	4682		
Leg3	096	K5S096	01-51.47N	138-03.41E	24.Nov.2001	11:23	12:09	1008.291	1001.1	29.3	4678	○	
Leg3	097	K5S097	01-51.39N	138-03.54E	24.Nov.2001	14:21	14:40	503.566	500.0	29.25	4688		
Leg3	098	K5S098	01-51.60N	138-03.31E	24.Nov.2001	17:23	17:41	503.881	499.8	29.2	4677		
Leg3	099	K5S099	01-51.61N	138-03.38E	24.Nov.2001	20:21	20:39	504.440	501.8	29.2	4675		
Leg3	100	K5S100	01-51.55N	138-03.41E	24.Nov.2001	23:20	23:37	505.259	502.9	29.2	4672		
Leg3	101	K5S101	01-51.60N	138-03.56E	25.Nov.2001	02:21	02:38	504.746	506.0	29.4	4680		
Leg3	102	K5S102	01-51.62N	138-03.29E	25.Nov.2001	05:20	05:39	504.633	502.3	29.5	4681		
Leg3	103	K5S103	01-51.72N	138-03.29E	25.Nov.2001	08:20	08:39	504.703	501.8	29.3	4684		
Leg3	104	K5S104	01-51.59N	138-03.27E	25.Nov.2001	11:22	12:07	1008.620	1003.6	29.3	4679	○	
Leg3	105	K5S105	01-51.52N	138-51.55E	25.Nov.2001	14:22	14:40	503.850	500.0	29.3	4686		
Leg3	106	K5S106	01-51.73N	138-03.44E	25.Nov.2001	17:22	17:40	504.441	502.2	29.2	4676		
Leg3	107	K5S107	01-52.03N	138-03.45E	25.Nov.2001	20:19	20:26	504.386	500.3	29.2	4667		
Leg3	108	K5S108	01-51.78N	138-03.32E	25.Nov.2001	23:19	23:38	504.442	502.5	29.3	4674		
Leg3	109	K5S109	01-51.76N	138-03.33E	26.Nov.2001	02:20	02:39	504.593	501.4	29.4	4681		
Leg3	110	K5S110	01-51.66N	138-03.23E	26.Nov.2001	05:20	05:38	504.336	502.7	29.9	4669		
Leg3	111	K5S111	01-51.80N	138-03.32E	26.Nov.2001	08:19	08:36	505.322	501.1	29.6	4673		
Leg3	112	K5S112	01-51.76N	138-03.11E	26.Nov.2001	11:21	12:03	1008.578	1002.9	29.5	4678	○	
Leg3	113	K5S113	01-51.81N	138-03.31E	26.Nov.2001	14:21	14:38	504.887	502.3	29.45	4672		
Leg3	114	K5S114	01-51.79N	138-03.22E	26.Nov.2001	17:21	17:40	503.755	502.5	29.3	4675		
Leg3	115	K5S115	01-51.58N	138-03.32E	26.Nov.2001	20:20	20:38	504.787	501.8	29.3	4677		
Leg3	116	K5S116	01-51.60N	138-03.13E	26.Nov.2001	23:20	23:37	504.790	500.7	29.3	4685		
Leg3	117	K5S117	01-51.60N	138-03.12E	27.Nov.2001	02:20	02:38	505.095	500.3	29.5	4681		
Leg3	118	K5S118	01-51.34N	138-03.22E	27.Nov.2001	05:22	05:38	504.000	502.0	29.6	4687		
Leg3	119	K5S119	01-51.50N	138-03.32E	27.Nov.2001	08:20	08:37	505.162	502.5	29.5	4680		
Leg3	120	K5S120	01-51.52N	138-03.03E	27.Nov.2001	11:20	12:06	1008.959	1003.4	29.4	4679	○	
Leg3	121	K5S121	01-51.02N	138-03.32E	27.Nov.2001	14:26	14:44	504.493	502.0	29.4	4696		
Leg3	122	K5S122	01-51.61N	138-03.15E	27.Nov.2001	17:22	17:40	505.404	501.1	29.3	4682		
Leg3	123	K5S123	01-51.53N	138-03.06E	27.Nov.2001	20:21	20:39	504.509	501.4	29.3	4681		
Leg3	124	K5S124	01-51.77N	138-03.15E	27.Nov.2001	23:19	23:37	504.517	500.5	29.4	4677		
Leg3	125	K5S125	01-51.55N	138-03.05E	28.Nov.2001	02:20	02:37	504.906	499.8	29.4	4685		
Leg3	126	K5S126	01-51.44N	138-03.23E	28.Nov.2001	05:20	05:38	504.207	499.2	29.8	4690		
Leg3	127	K5S127	01-51.52N	138-03.23E	28.Nov.2001	08:18	08:37	504.596	501.6	29.6	4684		
Leg3	128	K5S128	01-51.77N	138-03.10E	28.Nov.2001	11:20	12:06	1008.884	1003.8	29.5	4681	○	
Leg3	129	K5S129	01-51.69N	138-03.10E	28.Nov.2001	14:21	14:39	503.747	500.7	29.5	4676		
Leg3	130	K5S130	01-51.66N	138-02.97E	28.Nov.2001	17:21	17:38	504.461	500.9	29.4	4684		
Leg3	131	K5S131	01-51.67N	138-03.14E	28.Nov.2001	20:20	20:37	504.693	500.3	29.3	4679		
Leg3	132	K5S132	01-51.61N	138-03.23E	28.Nov.2001	23:20	23:38	504.880	500.5	29.4	4679		
Leg3	133	K5S133	01-51.59N	138-03.07E	29.Nov.2001	02:19	02:38	504.938	502.2	29.6	4681		
Leg3	134	K5S134	01-51.52N	138-02.97E	29.Nov.2001	05:19	05:37	504.131	499.2	29.7	4682		
Leg3	135	K5S135	01-51.60N	138-03.36E	29.Nov.2001	08:19	08:37	504.498	502.7	29.5	4675		
Leg3	136	K5S136	01-51.76N	138-03.19E	29.Nov.2001	11:20	12:01	1009.462	1003.8	29.5	4677	○	
Leg3	137	K5S137	01-51.63N	138-03.18E	29.Nov.2001	14:20	14:37	505.720	501.6	29.4	4677		
Leg3	138	K5S138	01-51.68N	138-03.15E	29.Nov.2001	17:20	17:39	504.199	500.3	29.4	4682		
Leg3	139	K5S139	01-51.49N	138-03.18E	29.Nov.2001	20:19	20:38	504.495	500.5	29.4	4701		
Leg3	140	K5S140	01-51.70N	138-03.03E	29.Nov.2001	23:19	23:37	504.234	501.6	29.4	4679		
Leg3	141	K5S141	01-51.77N	138-03.10E	30.Nov.2001	02:18	02:36	504.641	500.0	29.4	4675		

Table 6.9-1 CTD Cast Table (continue)

Line	Cast No.	File Name	Lat. [N]	Long. [E]	Date [UTC]	Start Time	End Time	Max. Press. [db]	Max. Wire Out [m]	SST [deg-C]	Depth [m]	Water Sampling	Note
Leg3	142	K5S142	01-51.71N	138-03.18E	30.Nov.2001	05:18	05:37	505.056	500.0	29.5	4683		
Leg3	143	K5S143	01-51.72N	138-03.36E	30.Nov.2001	08:20	08:37	504.512	501.6	29.3	4684		
Leg3	144	K5S144	01-51.54N	138-03.27E	30.Nov.2001	11:20	12:05	1009.800	1004.5	29.3	4693	○	
Leg3	145	K5S145	01-51.55N	138-03.13E	30.Nov.2001	17:23	17:40	503.952	499.2	29.3	4694		
Leg3	146	K5S146	01-51.46N	138-03.04E	30.Nov.2001	23:20	23:39	504.644	502.2	29.2	4695		
Leg3	147	K5S147	01-50.57N	138-04.48E	01.Dec.2001	05:38	05:57	505.186	502.5	29.4	4676		04:30～05:30 Tethered sonde
Leg3	148	K5S148	01-51.49N	138-03.39E	01.Dec.2001	11:20	12:01	1008.642	1002.7	29.3	4680	○	
Leg3	149	K5S149	01-51.71N	138-03.18E	01.Dec.2001	17:20	17:38	504.118	500.9	29.2	4673		
Leg3	150	K5S150	01-51.61N	138-03.14E	01.Dec.2001	23:20	23:40	504.626	501.1	29.2	4690		
Leg3	151	K5S151	01-51.33N	138-03.06E	02.Dec.2001	05:19	05:37	507.324	508.8	29.3	4693		
Leg3	152	K5S152	01-51.48N	138-03.14E	02.Dec.2001	11:18	12:03	1008.919	1003.4	29.1	4696	○	
Leg3	153	K5S153	01-51.45N	138-03.25	02.Dec.2001	17:20	17:38	504.633	500.7	29.1	4685		
Leg3	154	K5S154	01-51.56N	138-03.22E	02.Dec.2001	23:21	23:56	1007.981	1009.1	29.2	4688	○	
Leg3	155	K5S155	02-01.63N	138-05.52E	03.Dec.2001	05:18	05:36	504.759	502.5	29.3	4277		
Leg3	156	K5S156	01-51.38N	138-03.33E	03.Dec.2001	11:20	12:08	1007.256	1003.1	29.2	4684	○	
Leg3	157	K5S157	01-51.66N	138-03.17E	03.Dec.2001	17:21	17:40	504.552	500.0	29.2	4689		
Leg3	158	K5S158	01-51.46N	138-03.27E	03.Dec.2001	23:20	00:04	1009.471	1007.1	29.1	4688	○	
Leg3	159	K5S159	01-51.55N	138-03.41E	04.Dec.2001	05:17	05:37	506.382	506.0	29.1	4682		
Leg3	160	K5S160	01-51.38N	138-03.14E	04.Dec.2001	11:20	12:00	1009.081	1003.3	29.1	4695	○	
Leg3	161	K5S161	01-51.69N	138-03.07E	04.Dec.2001	17:20	17:38	504.343	500.3	29.1	4680		
Leg3	162	K5S162	01-51.50N	138-03.10E	04.Dec.2001	23:23	00:10	1008.451	1004.0	29.0	4696	○	
Leg3	163	K5S163	01-51.89N	138-03.30E	05.Dec.2001	05:19	05:37	505.299	501.8	28.7	4669		
Leg3	164	K5S164	01-51.60N	138-03.19E	05.Dec.2001	11:26	12:10	1008.996	1005.8	28.9	4691	○	
Leg3	165	K5S165	01-51.77N	138-03.51E	05.Dec.2001	17:28	17:48	504.790	503.8	29.0	4680		
Leg3	166	K5S166	01-51.12N	138-03.07E	05.Dec.2001	23:26	00:07	1008.234	1007.7	29.0	4694	○	
Leg3	167	K5S167	01-51.46N	138-03.57E	06.Dec.2001	05:18	05:37	505.795	502.7	29.1	4679		
Leg3	168	K5S168	01-51.37N	138-03.27E	06.Dec.2001	11:20	12:05	1008.853	1005.5	28.9	4686	○	
Leg3	169	K5S169	01-51.51N	138-03.24E	06.Dec.2001	17:21	17:38	504.580	501.6	28.9	4680		
Leg3	170	K5S170	01-51.30N	138-03.38E	06.Dec.2001	23:20	23:38	502.262	500.3	28.8	4680		
Leg3	171	K5S171	01-51.35N	138-03.55E	07.Dec.2001	05:17	05:36	505.735	501.1	28.8	4687		
Leg3	172	K5S172	01-51.53N	138-03.19E	07.Dec.2001	11:19	12:01	1009.021	1002.2	28.8	4694	○	
Leg3	173	K5S173	01-51.51N	138-03.18E	07.Dec.2001	17:20	17:38	505.370	504.0	28.9	4696		
Leg3	174	K5S174	01-51.34N	138-03.34E	07.Dec.2001	23:20	23:39	505.311	504.0	28.9	4684		
Leg3	175	K5S175	01-51.26N	138-03.26E	08.Dec.2001	05:16	05:35	509.104	523.5	28.8	4684		
Leg3	176	K5S176	01-51.48N	138-03.29E	08.Dec.2001	11:19	12:05	1007.107	1006.0	28.8	4688	○	
Leg3	177	K5S177	01-51.50N	138-03.33E	08.Dec.2001	17:19	17:38	505.537	501.1	28.8	4679		
Leg3	178	K5S178	01-51.46N	138-03.18E	08.Dec.2001	23:19	23.38	504.173	508.2	28.8	4686		
Leg4	01	K54S01	06-56-99N	134-07.87E	13.Dec.2001	06:07	06:56	1175.098	-	-	1241	○	
Leg4	02	K54S02	07-30.09N	134-40.13E	13.Dec.2001	21:59	22:49	1111.101	1104.5	-	1176.0	○	

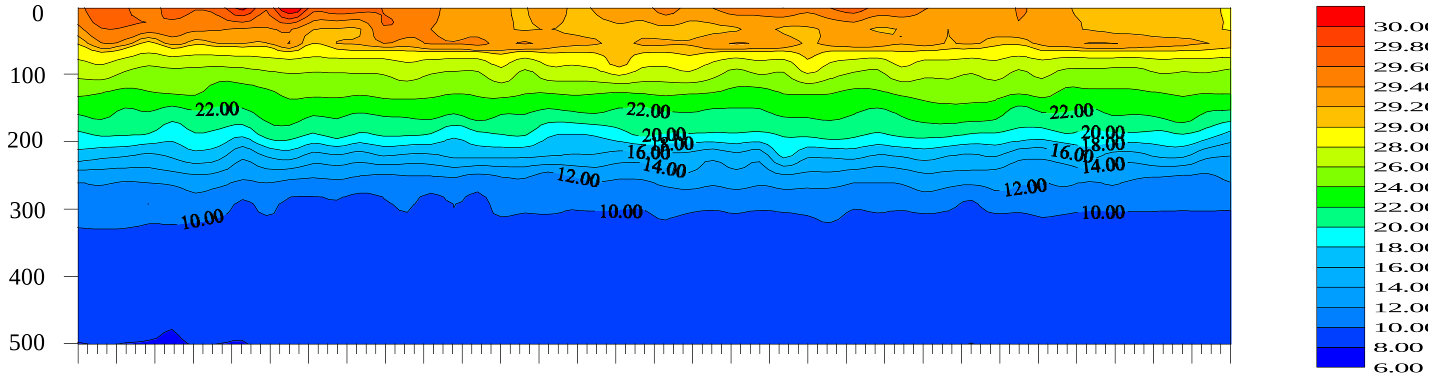

Temperature ITS-90 [deg-C]

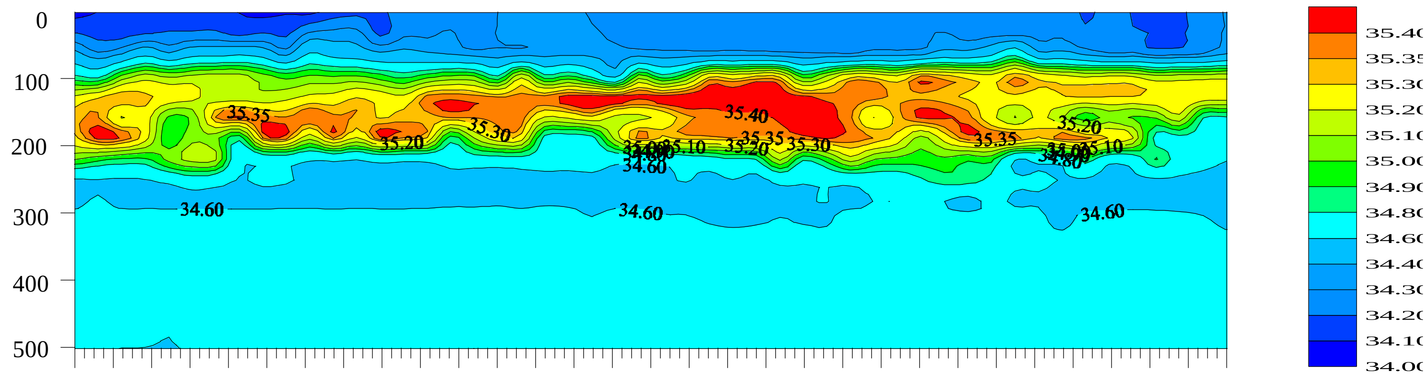

Salinity PSS-78 [PSU]

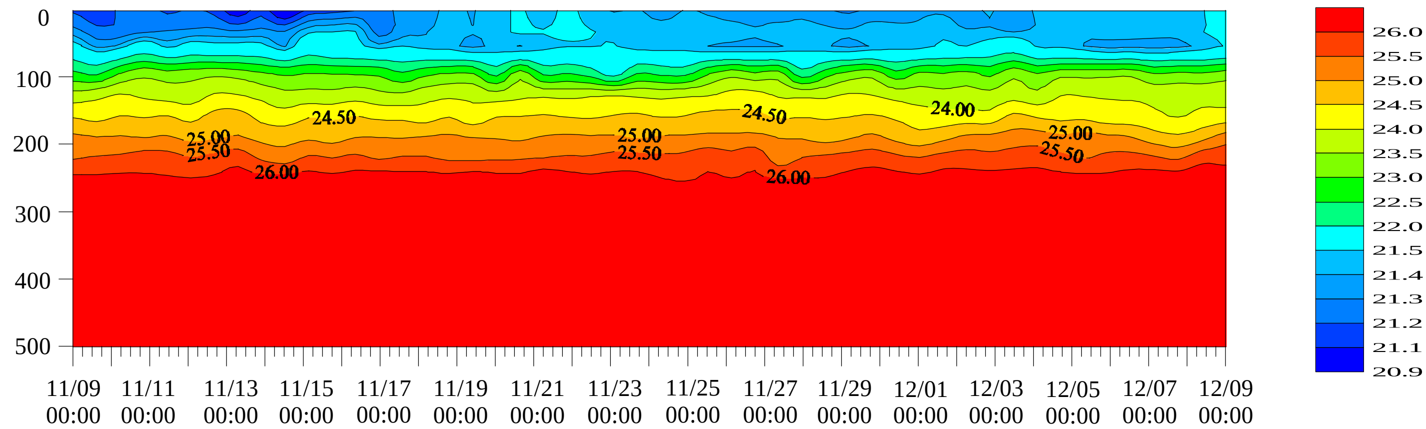

Sigma-theata [kg/m^3]

Fig 6.9.1-1 Temporal variation of the vertical profile

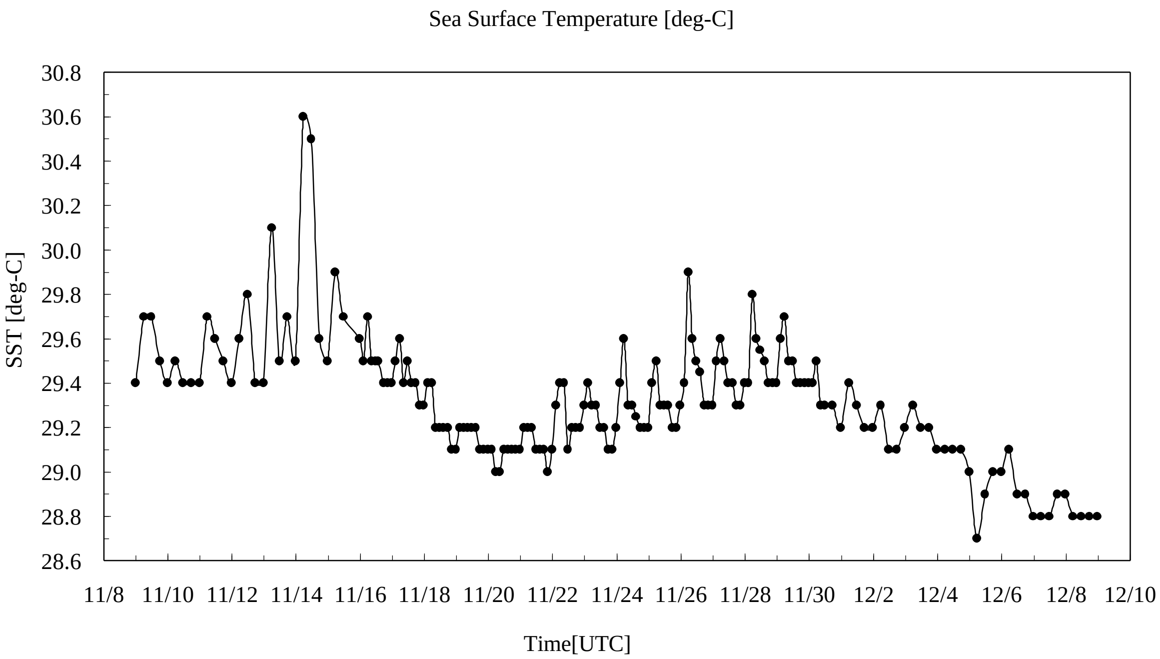

Fig.6.9.1-2 : Temporal variation of the sea surface temperature obtained from bucket water sampling.

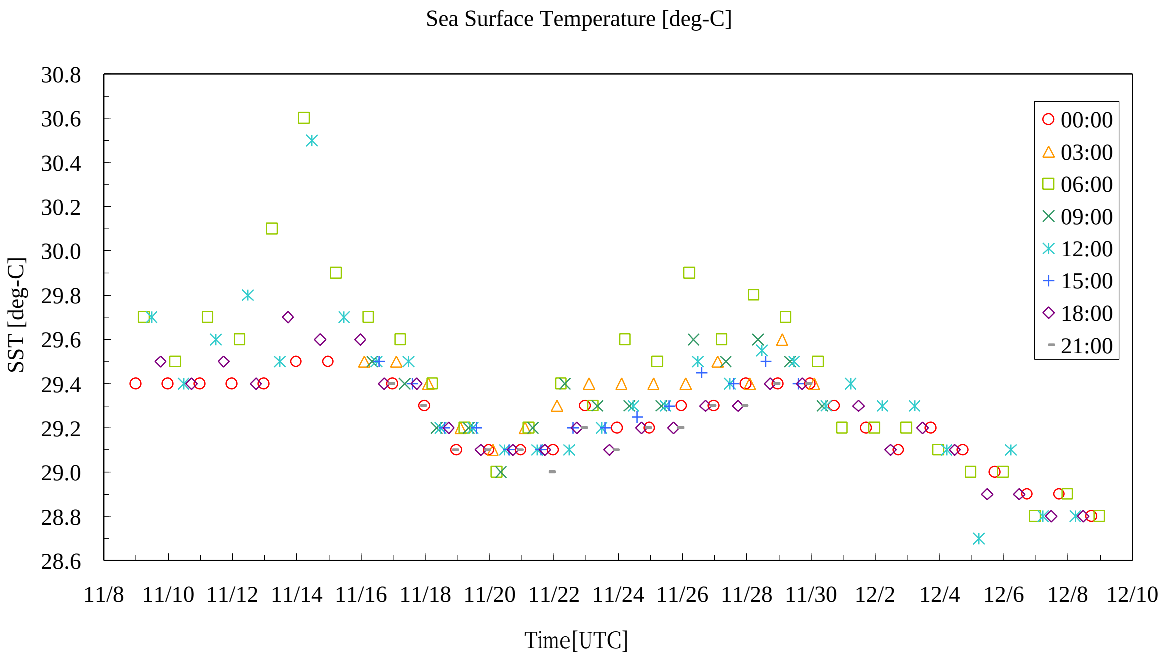

Fig.6.9.1-3 : Same as Fig.6.9.1-2, but for each local time.

6.9.2 Salinity Measurements of Sampled Water

(1) Personnel

Satoshi Ozawa (MWJ): Operation leader
Kentaro Shiraishi (MWJ)
Minoru Kamata (MWJ)
Miki Yoshiike(MWJ)
Naoko Takahashi (MWJ)

(2) Objectives

Investigation of the oceanic structure and its time variation by measuring salinity and calibration of the salinity data obtained by CTD.

(3) Methods

Guildline Autosal salinometer model 8400B, with the sample intake pump of Ocean Science International peristalitic-type, is used to measure the salinity of sampled water. A double conductivity ratio was defined as median of 31 times readings of the salinometer. Data collection started after 5 seconds and it took 10 seconds to collect 31 reading by a personal computer.

In Leg3, water to be measured was sampled at 12 layers on CTD cast of 11:20UTC every day. In Leg4, water sampled at 30m above the bottom.

The salinometer was operated in the air-conditioned ship's laboratory at bath temperature of 24℃. Room temperature varied from approximately 23.5℃ to23.7℃.

1. Salinity Sample Bottles

The bottle in which the salinity samples are collected and stored are 250ml brown glass bottles with screw caps.

2. Salinity Sample Collection and Temperature Equilibration

Each bottle was rinsed three times with sample water and was filled to the shoulder oh the bottle. Its cap was also thoroughly rinsed. Salinity samples were stored more than 24 hours in same laboratory were the salinity measurement was made.

3. Standardization

Autosal model 8400B was standardization before and after sequence of measurements by use of IAPSO Standard Seawater batch P139 (conductivity ratios were 0.99993).

4. Sub-standard Seawater

We also used sub-standard seawater which was deep-sea water filterd by pore size of 0.45 micrometer and stored in a 20 liter cubical made of polyethylence and stirred for at least 24hours before measuring. It was measured every 8 samples in order to check the drift.

(4) Preliminary results

In Leg3, The average of difference of salinity between CTD and sample water at 1000m is 0.0020 (Sample water value is lower than that of CTD) with standard deviation is 0.0016. As a result, it made a revision value -0.0020.

In Leg4, The average of difference of salinity between CTD and sample water at Bottom-30m is 0.0018 (Sample water value is lower than that of CTD) with standard deviation is 0.0003. As a result, it made a revision value -0.0018.

The all of the preliminary results are in Appendix.

(5) Data archive

The data of sample measured and worksheets of calculation of salinity concentration were stored on magnetic optional disks (MO). All data will be submitted to JAMSTEC Data Management Office (DMO) and under its control.

6.9.3 Dissolved Oxygen Measurement of Sampled Water

(1) Personel

Katsunori Sagishima (Marine Works Japan Ltd.)
Minoru Kamata (Marine Works Japan Ltd.)

(2) Objectives

Dissolved oxygen (D.O.) is major parameter for deciding the seawater characteristic on oceanography. In this cruise, the method of dissolved oxygen determination is based on WHP Operations and Methods manual (Culberson, 1991, Dickson, 1994).

(3) Methods

(a) Instruments and Apparatus

Glass bottle:	Glass bottle for D.O. measurements consist of the ordinary BOD flask (ca.180 ml) and glass stopper with long nipple, modified from the nipple presented in Green and Carritt (1966).
Dispenser:	Eppendorf Comforpette 4800 / 1000µl
	OPTIFIX / 2 ml (for $MnCl_2$ & NaOH / NaI aq.)
	Metrohm Model 725 Multi Dosimat / 20 ml (for KIO_3)
Titrator:	Metrohm Model 716 DMS Titrino / 10 ml of titration vessel
	Metrohm Pt Electrode / 6.0403.100 (NC)
Software:	Data acquisition and endpoint evaluation / “The Brinkmann Titrino Workcell”

(b) Methods

Sampling and analytical methods were based on to the WHP Operations and Methods (Culberson, 1991, Dickson, 1996).

(b-1) Sampling

Seawater samples for dissolved oxygen measurement were collected from 12 litter Niskin bottles to calibrated dry glass bottles. During each sampling, 3 bottle volumes of seawater sample were overflowed to minimize contamination with atmospheric oxygen. The seawater temperature at the time of collection was measured for correction of the sample volume. After the sampling, $MnCl_2$ (aq.) 1ml and NaOH / NaI (aq.) 1ml were added into the glass bottle, and then shook the bottle well. After the precipitation has settled, we shook the bottle vigorously to disperse the precipitate.

(b-2) D.O. analysis

The samples were analyzed by Metrohm titrator with 10 ml piston burette and Pt Electrode using whole bottle titration. Titration was determined by the potentiometric methods and the endpoint for titration was evaluated by software of Metrohm, “The Brinkmann Titrino Workcell”.

Concentration of D.O. was calculated by equation (10) and (13) of WHP Operations and Methods (Dickson, 1994). Salinity value of the equation (14) was used from the value of salinity of AutoSal. We prepared and used one batch of 5 liter of 0.05N thiosulfate solutions and 5 liter of 0.0100N standard KIO_3 solutions (JM010908).

(4) Preliminary Result

(4-1) Comparison of our KIO_3 standards to CSK standard solution.

After this cruise, we compared our standards with CSK standard solution (Lot. ELQ9442) which is the commercially available standard solution prepared by Wako Pure Chemical Industries, Ltd. The results are shown in table 3.9.3.-1.

Table 6.9.3-1. Comparison of each standards

Titrator	KIO_3 Lot No.	Nominal Normality	Average Titer (ml)	Standard Deviation	n
	ELQ9442	0.0100	1.976^7	0.0008	10
	JM010908	0.010017	1.979^3	0.0006	10

(4-2) Reproducibility

In this cruise, 458 samples for D.O. samples were collected. 69 pairs (17.7%) of total samples were analyzed as “duplicates” which were collected from same Niskin bottle (fig 6.9.3-1). Average and precision (1 std. dev.) of difference of oxygen concentration obtained for duplicate samples analyses were 0.12 (µmol/kg) and 0.32 (?). Results of each casts show Fig.6.9.3-2 (1) – (4)

(5) References

Culberson, C.H.(1991) Dissolved Oxygen, in WHP Operations and Methods, Woods Hole., ppl-15

Culberson, C.H., G.Knapp, R.T.Williams and F.Zemlyak(1991) A comparison of methods for the determination of dissolved oxygen in seawater. (WHPO 91-2)

Dickson, A.G. (1994) Determination of dissolved oxygen in sea water by Winkler titration, in WHP Operations and Methods, Woods Hole., ppl-14.

Green, E.J. and D.E.Carritt (1996) An Improved Iodine Determination Flask for Whole-bottle Titrations, Analyst, 91, 207-208.

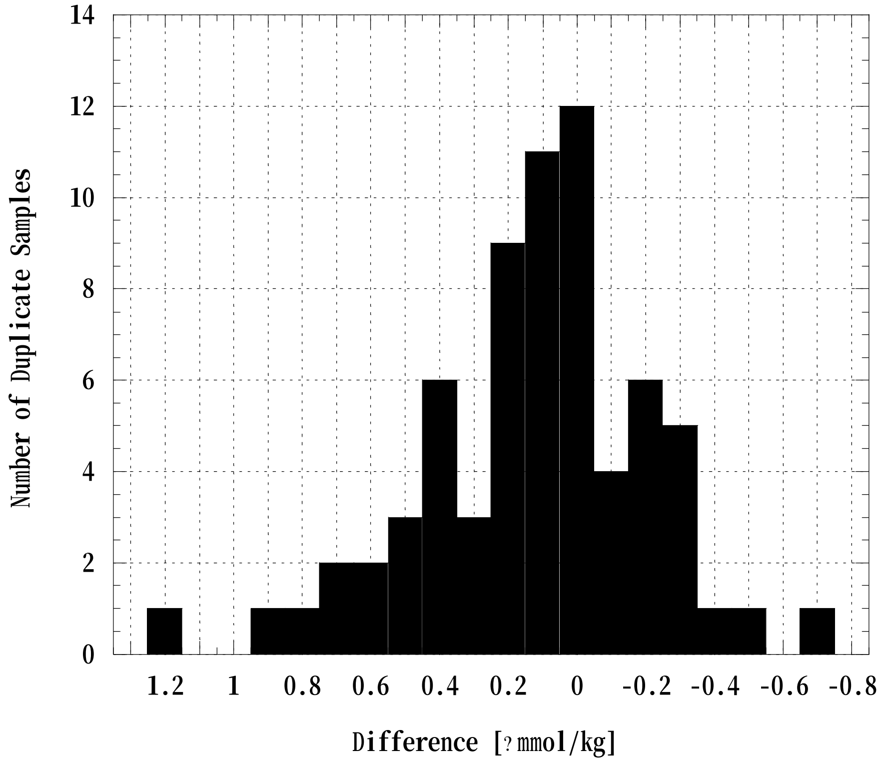

Fig 6.9.3-1: Histogram of difference in oxygen concentration obtained for duplicate sample analyses from leg.3 to leg.4.

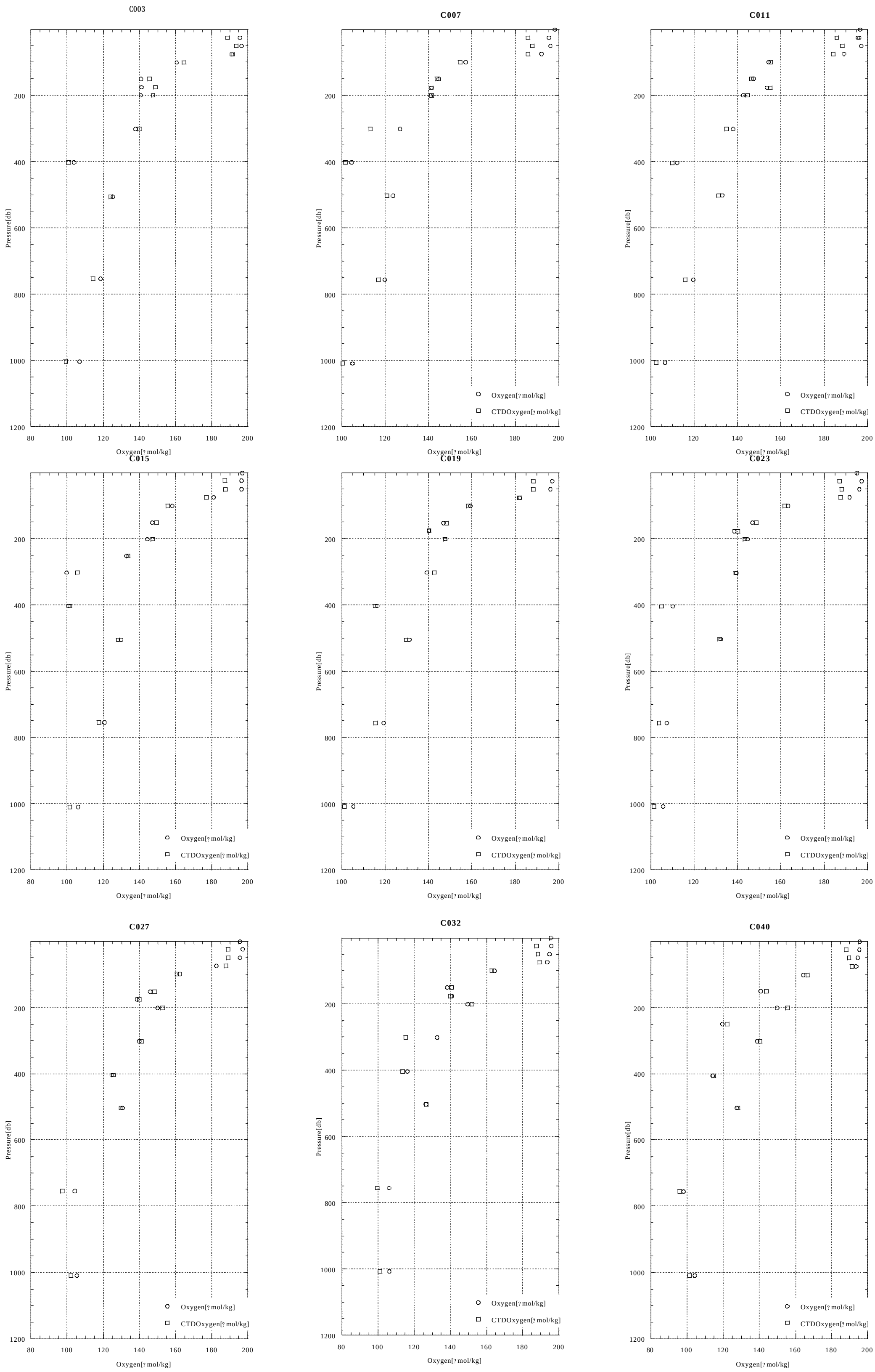

Fig.6.9.3 -2 (1) Vertical profiles at each cast.

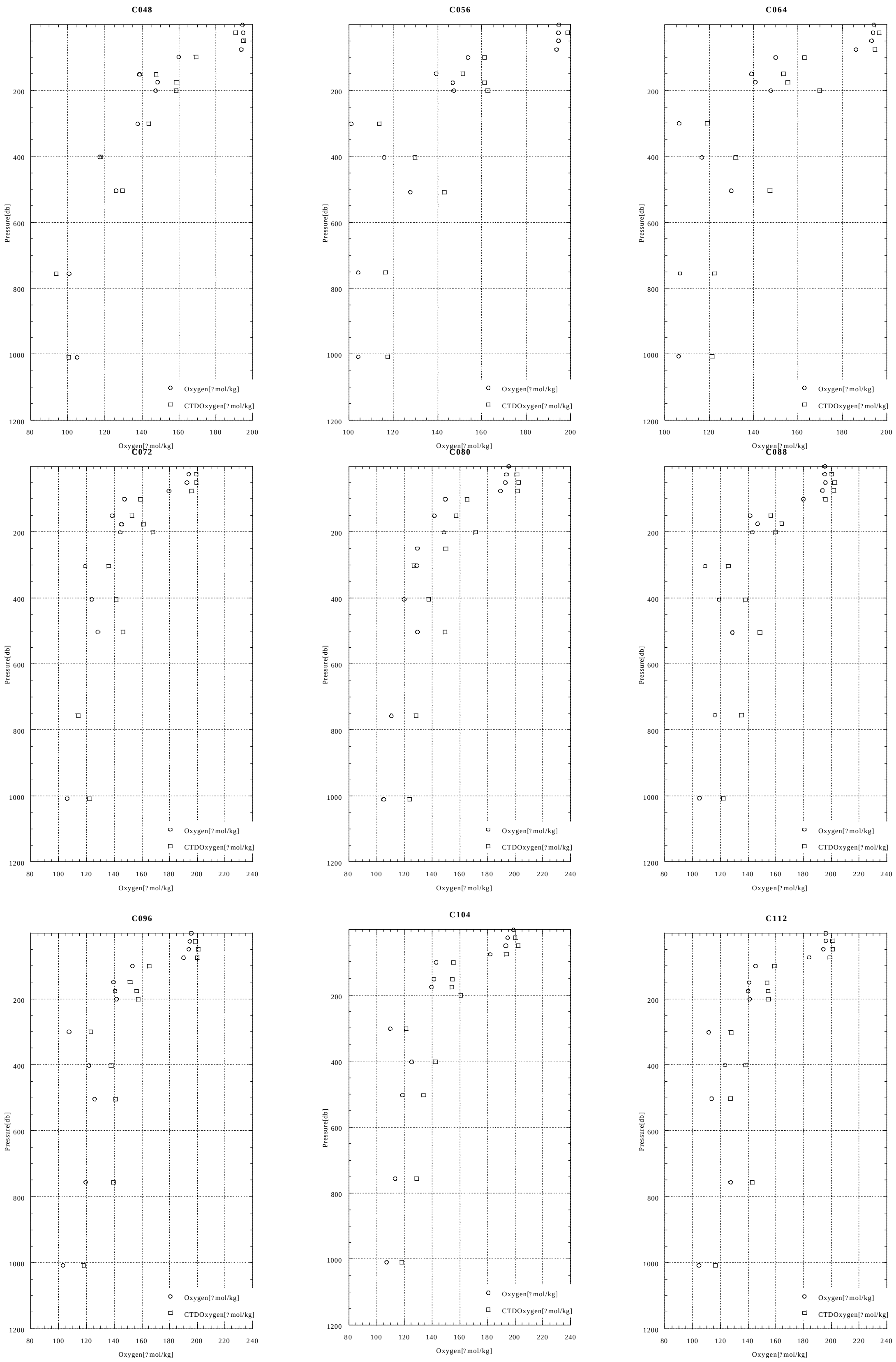

Fig.6.9.3 -2 (2) Vertical profiles at each cast.

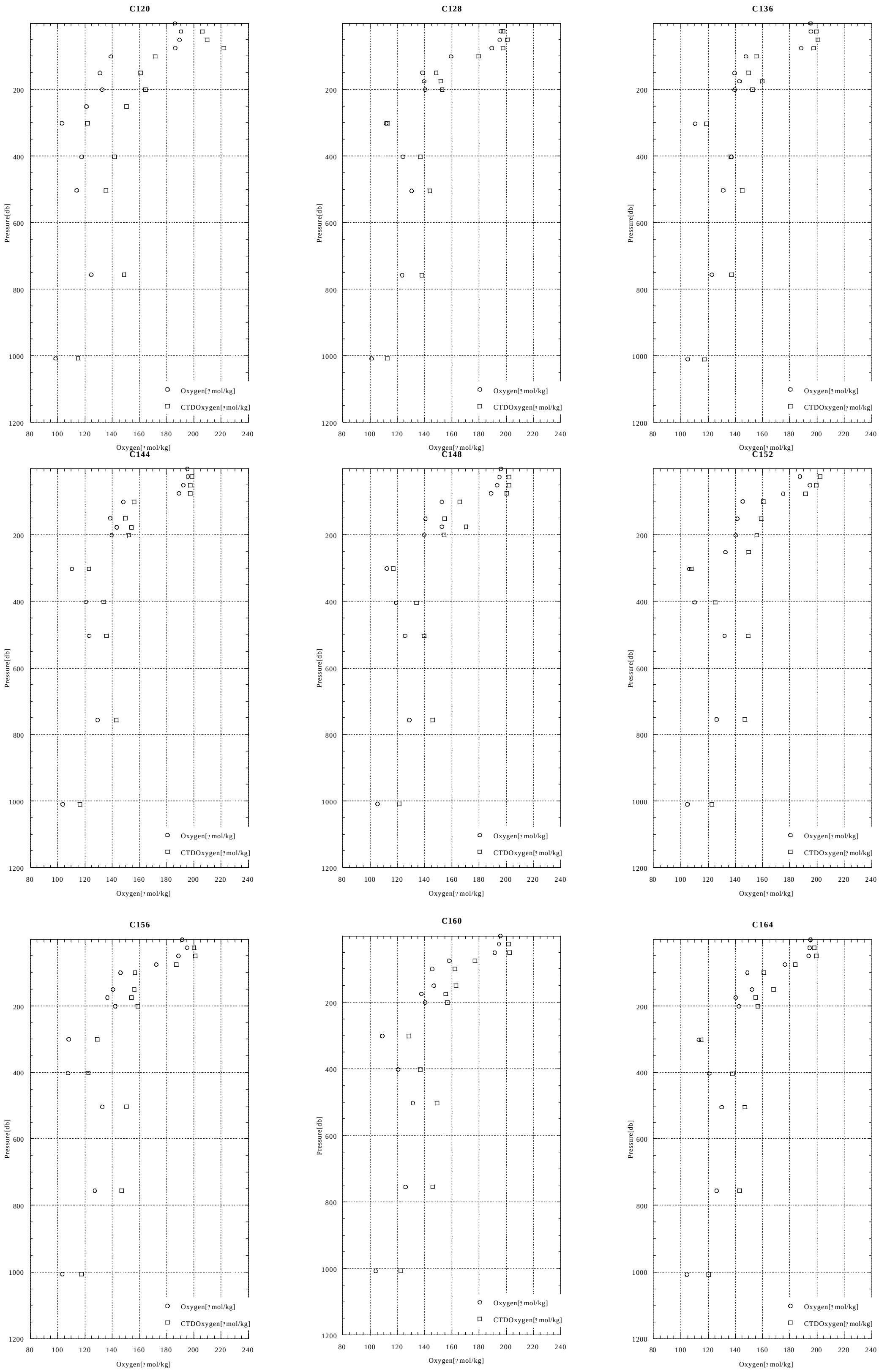

Fig. 6.9.3 -2 (3) Vertical profiles at each cast.

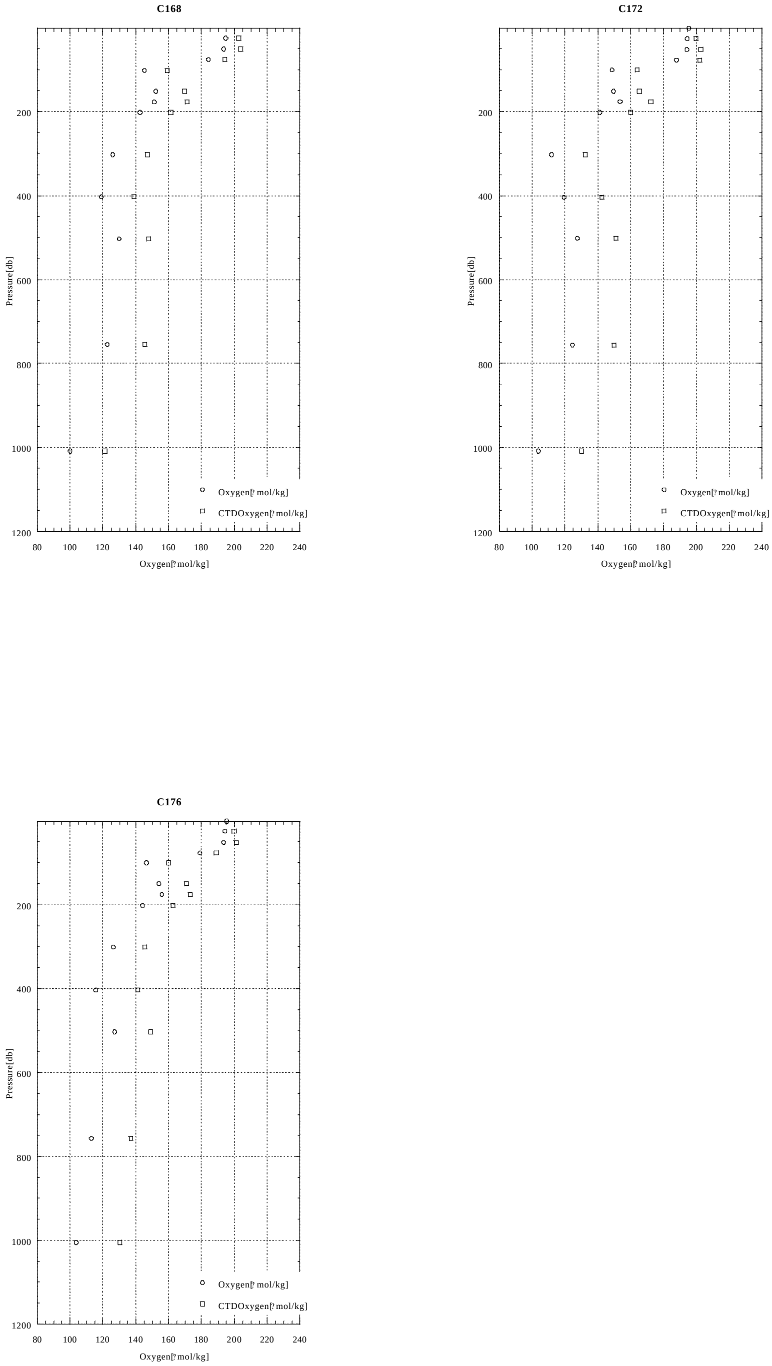

Fig. 6.9.3 -2 (4) Vertical profiles at each cast.

6.9.4 Shallow Water CTD and Chlorophyll Observation

(1) Personnel

Mitsuru Hayashi (Maritime University of Kobe): Principal Investigator
Naoki Nakatani (Osaka Prefecture University)

(2) Objectives

We curried out the shallow water observation to understand the temporal and spatial variations of environment with biological production in the euphotic layer.

(3) Methods

We observed vertical profiles of temperature, conductivity, fluorescence, light intensity, dissolved oxygen and turbidity by the shallow water measurement unit (Chlorothec ACL-220-RS, Alec Electronics Co. Ltd.) from surface to 200 m depth every 0.2 sec. The log data is shown in Table 6.9.4-1. We could not get dissolved oxygen data after cast 8, because sensor was broken. Also, we canceled casting at 03 LMT 28th Nov. and 15 LMT 30th Nov. because of measuring device trouble. Fluorescence was recorded as the raw data (N value: 0 to 65520), and we will calibrate the fluorescence data using the pigment analysis data by MWJ.

Transparency was also observed by the Secchi Disk in day time. We thank Mr. Omote, Mr. Yamamoto and Mr. Horita, seaman of R/V MIRAI for cooperates of transparency observation.

Accuracy of the sensors is as follows;

Depth : ±0.2 m
Temperature :±0.05 ℃
Conductivity : ±0.05 mS/cm
Fluorescence : ±0.1%FS
Light intensity : ±0.4%
Dissolved oxygen : ±0.2mg/l
Turbidity : ±0.2%

(4) Results

Fig. 6.9.4 shows Depth-Time cross sections of (a) temperature, (b) salinity, (c) fluorescence, (d) light intensity and (e) turbidity at 2N, 138E. The depth of the mixing layer is about 80 m in depth, and the fluorescence maximum layer exists just below the mixing layer until 18 Nov. As it was overcast form 18 Nov. to 22 Nov., light intensity decreased and fluorescence maximum layer almost disappeared. After 23 Nov., fluorescence increased in mixing layer as light intensity became strong.

(5) Data Archives

The raw data will be submitted to the DMO of JAMSTEC. And the data will have a quality check in Maritime University of Kobe and Osaka Prefecture University, and will be distributed to the public later.

Table 6.9.4-1 The shallow water observation table.

CAST	LMT=UTC+9h			File name	Transparency
No.	mm	dd	hh	*.raw	m
1	11	9	9	11090935	27
2	11	9	15	11091445	32
3	11	9	21	11092112	N/A
4	11	10	3	11100248	N/A
5	11	10	9	11100909	N/A
6	11	10	15	11101512	35
7	11	10	21	11102137	N/A
8	11	11	3	11110306	N/A
9	11	11	9	11110909	38
10	11	11	15	11111506	35
11	11	11	21	11112135	N/A
12	11	12	3	11120307	N/A
13	11	12	9	11120905	36
14	11	12	15	11121505	38
15	11	12	21	11122134	N/A
16	11	13	3	11130306	N/A
17	11	13	9	11130904	44
18	11	13	15	11131503	43
19	11	13	21	11132129	N/A
20	11	14	3	11140306	N/A
21	11	14	9	11140903	43
22	11	14	15	11141502	46
23	11	14	21	11142132	N/A
24	11	15	3	11150303	N/A
25	11	15	9	11150902	39
26	11	15	15	11151504	48
27	11	15	21	11152131	N/A
28	11	16	9	11160903	25
29	11	16	12	11161201	30
30	11	16	15	11161505	28
31	11	16	18	11161803	N/A
32	11	16	21	11162135	N/A
33	11	17	0	11170012	N/A
34	11	17	3	11170308	N/A
35	11	17	6	11170607	N/A
36	11	17	9	11170904	25
37	11	17	12	11171202	32
38	11	17	15	11171505	25
39	11	17	18	11171801	N/A
40	11	17	21	11172127	N/A
41	11	18	0	11180003	N/A
42	11	18	3	11180307	N/A
43	11	18	6	11180606	N/A
44	11	18	9	11180901	30
45	11	18	12	11181201	25
46	11	18	15	11181508	28
47	11	18	18	11181759	N/A
48	11	18	21	11182135	N/A
49	11	19	0	11190006	N/A
50	11	19	3	11190304	N/A
51	11	19	6	11190601	N/A
52	11	19	9	11190903	29
53	11	19	12	11191201	28
54	11	19	15	11191503	21
55	11	19	18	11191801	N/A
56	11	19	21	11192127	N/A
57	11	20	0	11200001	N/A
58	11	20	3	11200304	N/A
59	11	20	6	11200610	N/A
60	11	20	9	11200904	26
61	11	20	12	11201205	21
62	11	20	15	11201504	20
63	11	20	18	11201804	N/A
64	11	20	21	11202127	N/A
65	11	21	0	11210002	N/A
66	11	21	3	11210306	N/A
67	11	21	6	11210603	N/A
68	11	21	9	11210902	30
69	11	21	12	11211201	30
70	11	21	15	11211500	29
71	11	21	18	11211800	N/A
72	11	21	21	11212133	N/A
73	11	22	0	11220012	N/A
74	11	22	3	11220304	N/A
75	11	22	6	11220602	N/A
76	11	22	9	11220859	33
77	11	22	12	11221158	32
78	11	22	15	11221503	30
79	11	22	18	11221802	N/A
80	11	22	21	11222130	N/A
81	11	23	0	11230006	N/A
82	11	23	3	11230302	N/A
83	11	23	6	11230559	N/A
84	11	23	9	11230919	32
85	11	23	12	11231205	N/A
86	11	23	15	11231503	28
87	11	23	18	11231759	N/A
88	11	23	21	11232135	N/A
89	11	24	0	11232359	N/A
90	11	24	3	11240311	N/A
91	11	24	6	11240600	N/A
92	11	24	9	11240901	29
93	11	24	12	11241158	29
94	11	24	15	11241459	30
95	11	24	18	11241755	N/A
96	11	24	21	11242130	N/A
97	11	25	0	11250002	N/A
98	11	25	3	11250303	N/A
99	11	25	6	11250558	N/A
100	11	25	9	11250858	28
101	11	25	12	11251158	29
102	11	25	15	11251459	26
103	11	25	18	11251759	N/A
104	11	25	21	11252126	N/A
105	11	26	0	11260000	N/A
106	11	26	3	11260300	N/A
107	11	26	6	11260556	N/A
108	11	26	9	11260858	26
109	11	26	12	11261159	32
110	11	26	15	11261458	32
111	11	26	18	11261756	N/A
112	11	26	21	11262122	N/A
113	11	27	0	11262357	N/A
114	11	27	3	11270301	N/A
115	11	27	6	11270559	N/A
116	11	27	9	11270856	29
117	11	27	12	11271157	32
118	11	27	15	11271457	34
119	11	27	18	11271756	N/A
120	11	27	21	11272125	N/A
121	11	28	0	11280003	N/A
	11	28	3	N/A	N/A
122	11	28	6	11280559	N/A
123	11	28	9	11280856	33
124	11	28	12	11281156	35
125	11	28	15	11281456	27
126	11	28	18	11281756	N/A
127	11	28	21	11282126	N/A
128	11	29	0	11282358	N/A
129	11	29	3	11290257	N/A
130	11	29	6	11290556	N/A
131	11	29	9	11290858	33
132	11	29	12	11291157	25
133	11	29	15	11291455	29
134	11	29	18	11291757	N/A
135	11	29	21	11292121	N/A
136	11	30	0	11292356	N/A
137	11	30	3	11300300	N/A
138	11	30	6	11300557	N/A
139	11	30	9	11300857	30
140	11	30	12	11301155	27
	11	30	15	N/A	25
141	11	30	18	11301756	N/A
142	11	30	21	11302125	N/A
	12	1	9		36
	12	1	15		32
	12	2	9		30
	12	2	15		27
	12	3	9		36
143	12	4	9	12040923	27
144	12	4	15	12041457	29
145	12	4	21	12042120	N/A
146	12	5	3	12050257	N/A
147	12	5	9	12050936	32
148	12	5	15	12051510	N/A
149	12	5	21	12052129	N/A
150	12	6	3	12060307	N/A
151	12	6	9	12060928	28

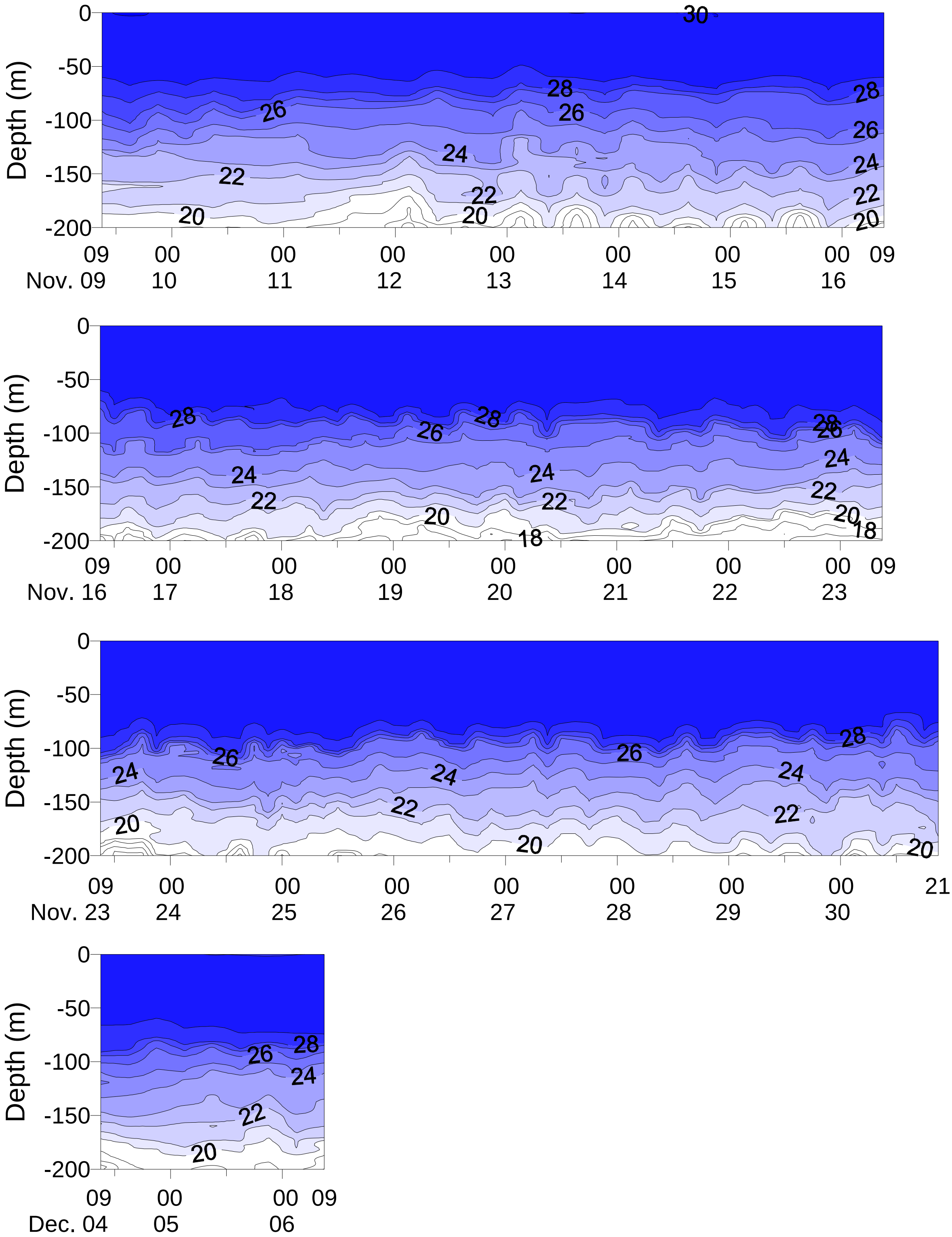

Fig.6.9.4.(a) Depth-Time cross sections of temperature(deg-C).

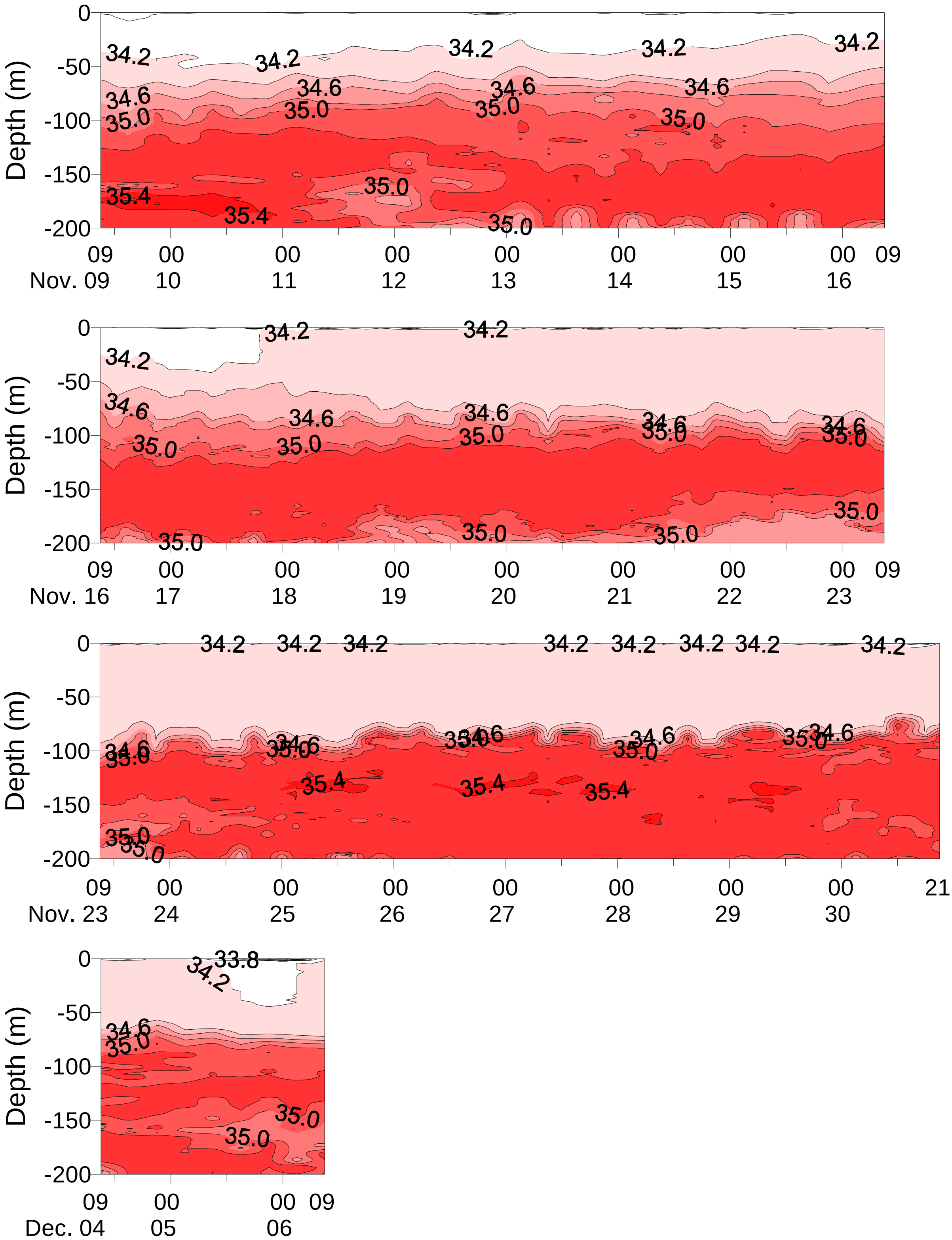

Fig.6.9.4.(b) Depth-Time cross sections of salinity(PSU).

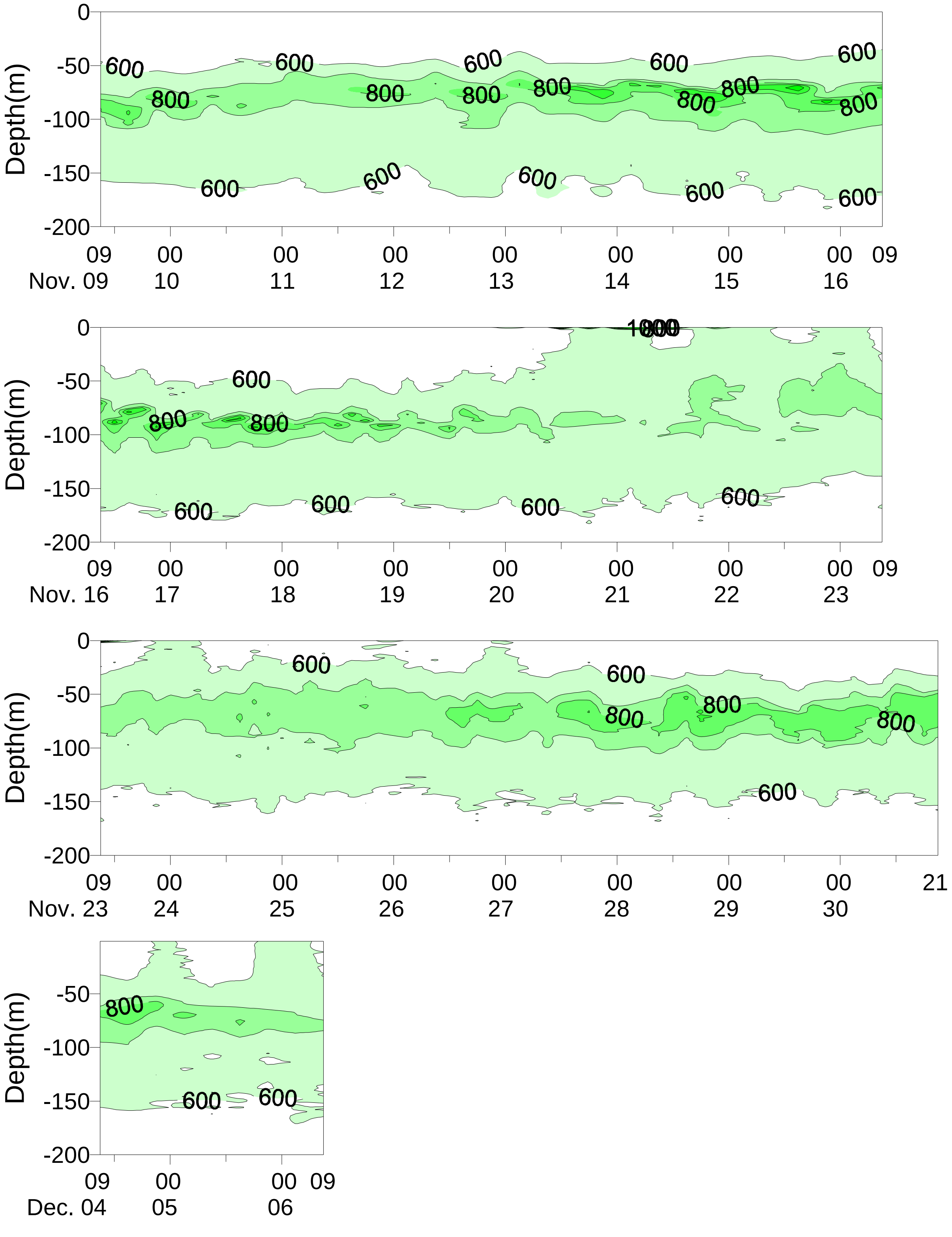

Fig.6.9.4.(c) Depth-Time cross sections of fluorescence.

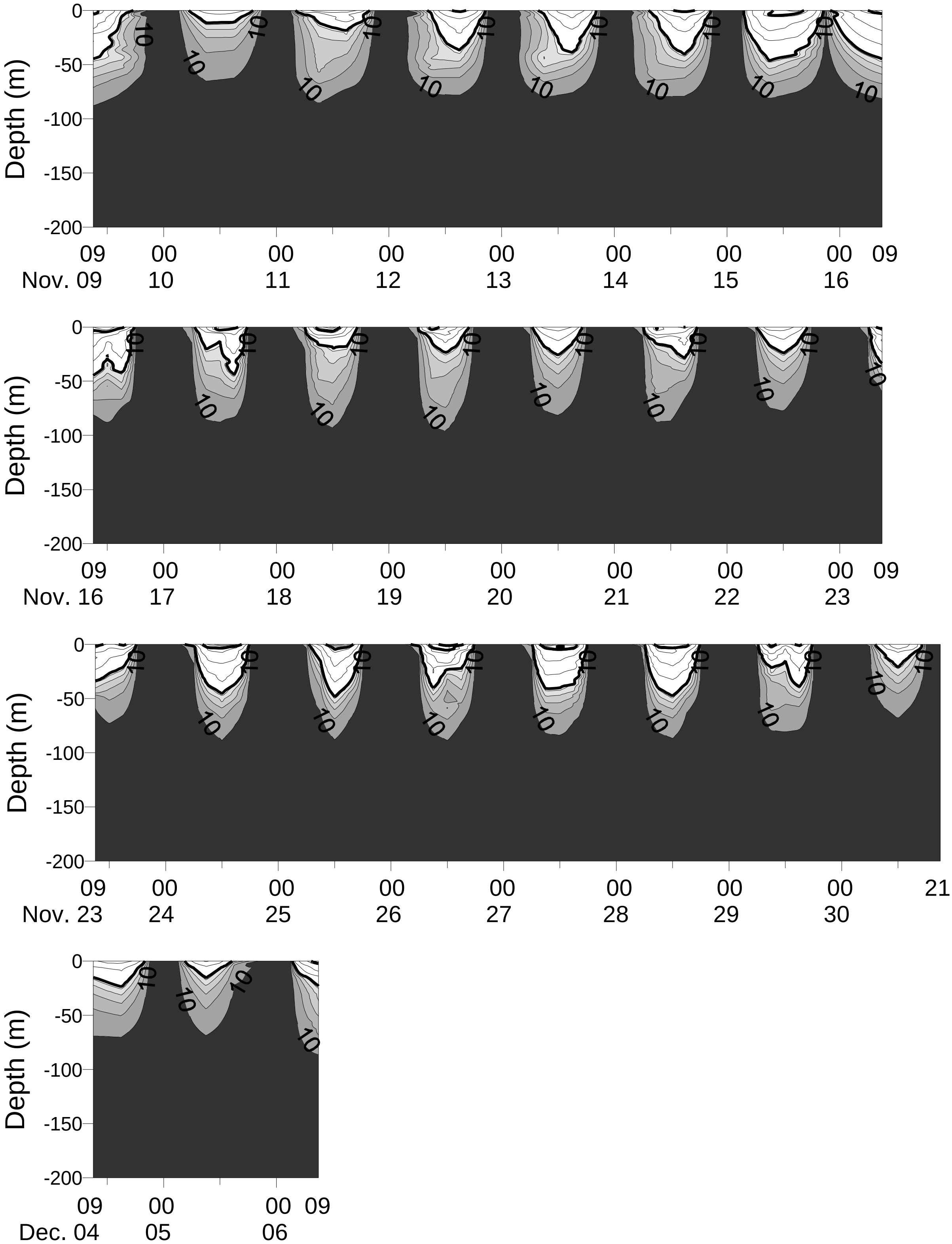

Fig.6.9.4.(d) Depth-Time cross sections of ligth intensity.

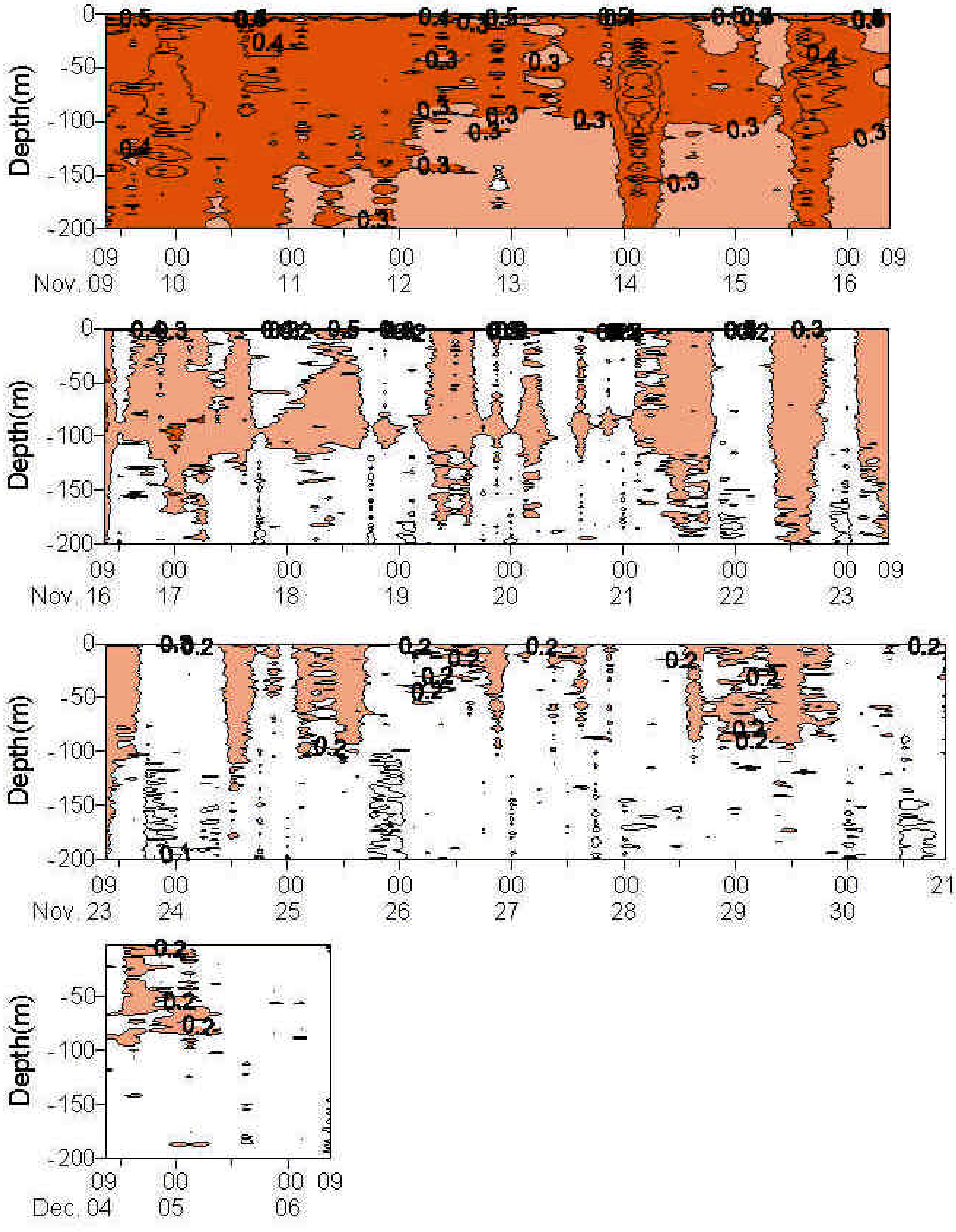

Fig.6.9.4.(e) Depth-Time cross sections of turbidity.

6.10 Shipboard ADCP observation

(1) Personnel name and affiliation

Masaki Hanyu (GODI): Operation Leader
Souichiro Sueyoshi (GODI)
Kohei Sakamoto (GODI)

(2) Objectives

The ocean current profiles are measured for the use of large fields of oceanography, as the basic dataset.

(3) Methods

We measured current profiles by VM-75 (RD Instruments Inc., U.S.A.) shipboard ADCP (Acoustic Doppler Current Profiler) from 7 November 2001 to 19 December 2001. The N-S (North-South) and E-W (East-West) velocity components of each depth cell [cm/s], and echo intensity of each depth cell [dB] are measured.

Major parameters for the measurement configuration are as follows:

Frequency:	75kHz
Average:	every 300 sec
Depth cell length:	1600cm
Number of depth cells:	40
First depth cell position:	30.9m
Last depth cell position:	654.9m
Ping per ADCP raw data:	32

(4) Preliminary Results

Figures 6.10-1 and 2 shows time series of current velocity component profile during the IOP. Figure 6.10-3 shows time series of current velocity vector profile during the IOP.

(5) Data Archive

ADCP data obtained in this cruise will be submitted to the DMO (Data Management Office), JAMSTEC and will be under their control.

(6) Remarks

We used Navigation-track data to convert from RAW data to RDI-ASCII data.

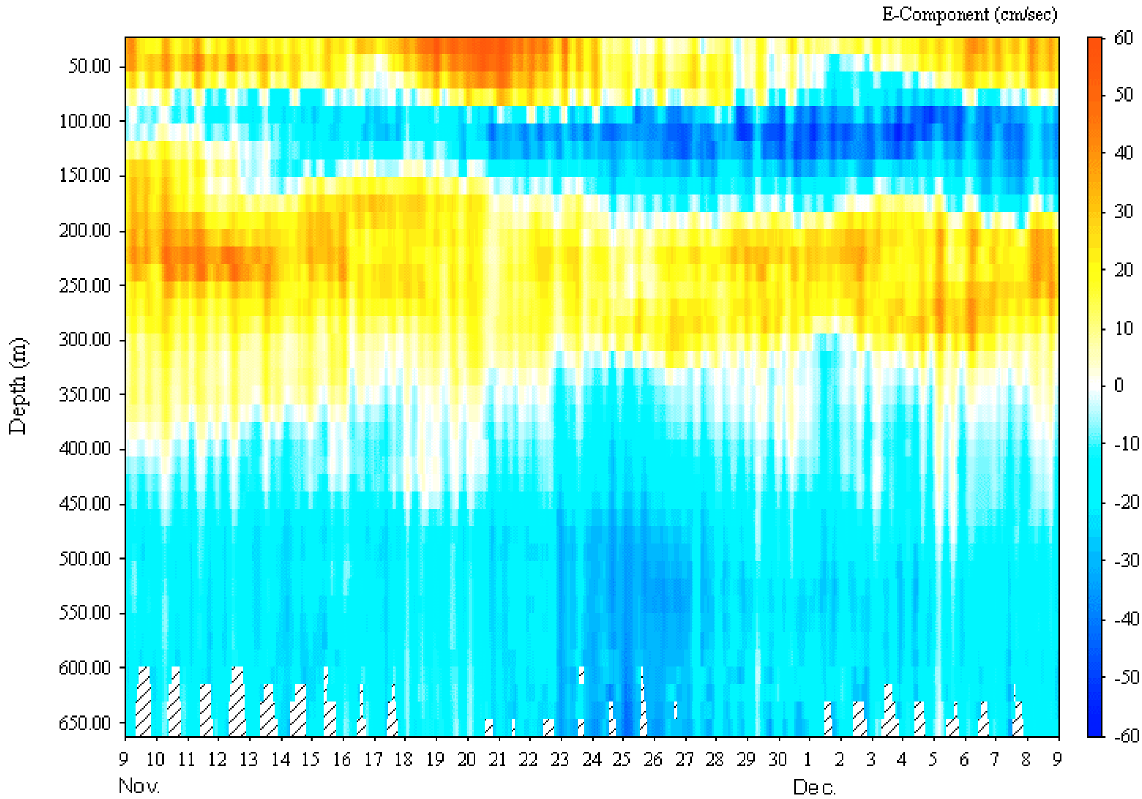

Fig. 6.10-1 Time-depth current velocity component (E-W) during the IOP

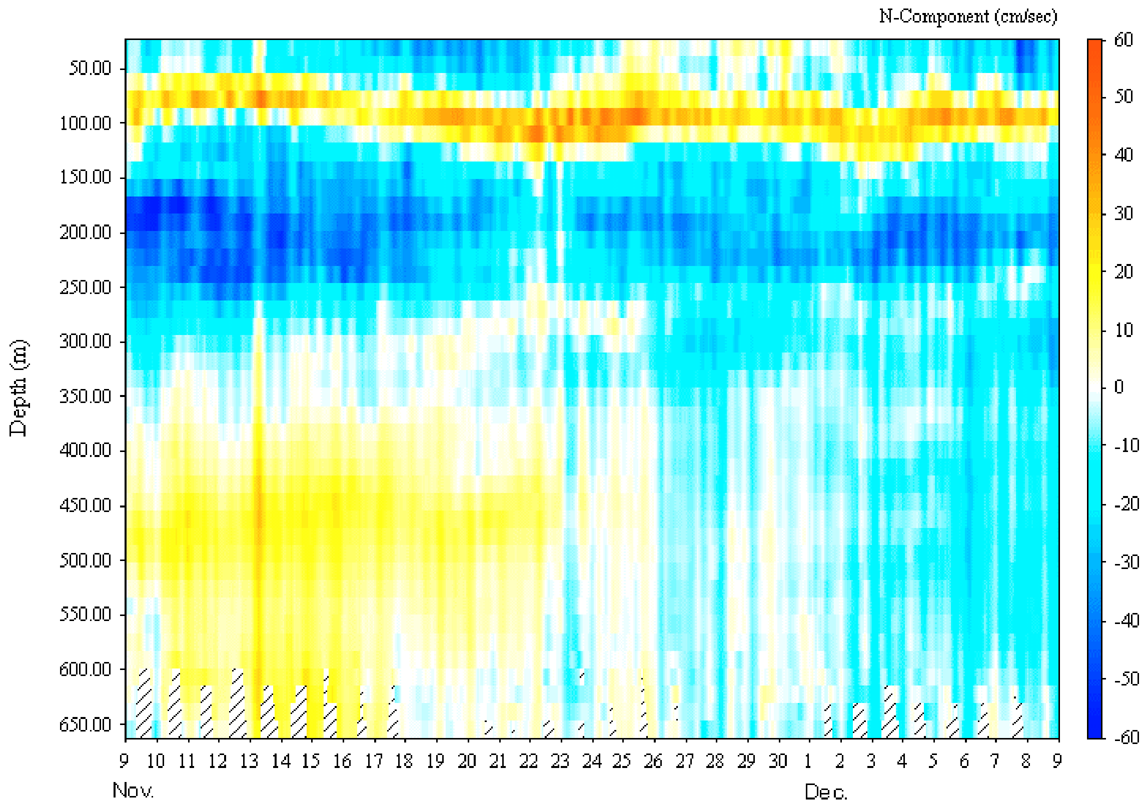

Fig.6.10-2 Time-depth current velocity component (N-S) during the IOP

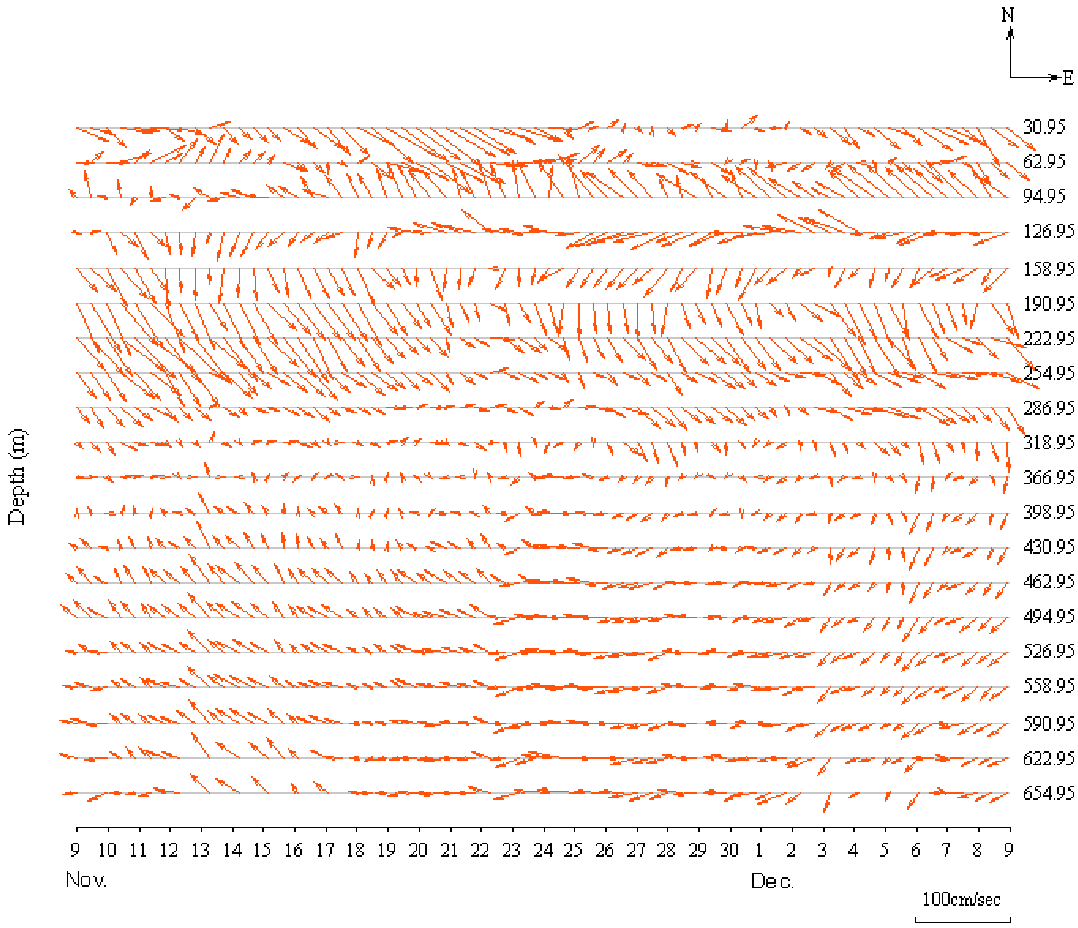

Fig.6.10-3 Time-depth current velocity vectors during the IOP

6.11 Sea Surface Water Monitoring

(1) Personnel

Nobuharu Komai	(Marine Works Japan Ltd.): Operation leader
Katsunori Sagishima	(Marine Works Japan Ltd.)
Minoru Kamata	(Marine Works Japan Ltd.)

(2) Objectives

Measurements of Temperature, salinity, dissolved oxygen, fluorescence, particle size of plankton in the near-surface water.

(3) Methods

The *Sea Surface Water Monitoring System* (Nippon Kaiyo Co., Ltd.) is located in the "*sea surface monitoring laboratory*" on R/V Mirai. It can automatically measure temperature, salinity, dissolved oxygen, fluorescence and particle size of plankton in the near-surface water every 1-minute. Sea surface temperature is measured by the ship bottom oceanographic thermometer situated on the suction side of the uncontaminated seawater supply in the forward hold. Measured data are saved every one-minute together with time and the position of ship, and displayed in the data management PC machine. This system is connected to shipboard LAN-system and provides the acquired data for p-CO_2 measurement system, etc. WGS 84 used geodetic reference system for the positioning at this cruise.

Near-surface water was continuously pumped up at the rate of about 200 l/min from the intake at the depth of 4.5 m below the sea surface to the laboratory. Then the water was distributed among the *Sea Surface Water Monitoring System* and p-CO_2 measurement system etc. The flow rate of surface water for this system was 12 l/min, which controlled by some valves and passed through some sensors except with fluorometer (about 0.3 l/min) through vinyl-chloride pipes.

The measured duration at leg 3 and leg 4 were from November 7 to December 9 2001 and December 13 to December 19 2001, respectively.

Specification and calibration date of the each sensor in this system were listed below.

a-1) Temperature and salinity sensors

SEACAT THERMOSALINOGRAPH

Model:	SBE-21, SEA-BIRD ELECTRONICS, INC.
Serial number:	2126391-3126
Measurement range:	Temperature -5 to +35 deg-C, Salinity 0 to 6.5 S/m
Accuracy:	Temperature 0.01 deg-C/6month, Salinity 0.001 S/m/month
Resolution:	Temperature 0.001 deg-C, Salinity 0.0001 S/m
Calibration date:	05-Jun-01 (mounted on 17-Sep.-01 in this system)

a-2) Ship bottom oceanographic thermometer (mounted at the back of the pump for surface water)

Model:	SBE 3S, SEA-BIRD ELECTRONICS, INC.
Serial number:	032175
Measurement range:	-5 to +35 deg-C
Initial Accuracy:	0.001 deg-C per year typical
Stability:	0.002 deg-C per year typical
Calibration date:	15-Jun.-01 (mounted on 17-Sep.-01 in this system)

b) Dissolved oxygen sensor

Model:	2127, Oubisufair Laboratories Japan INC.
Serial number:	31757

Measurement range:	0 to 14 ppm
Accuracy:	±1% at 5 deg-C of correction range
Stability:	1% per month
Calibration date:	5-Nov.-01 (at Palau)

c) Fluorometer

Model:	10-AU-005, TURNER DESIGNS
Serial number:	5562 FRXX
Detection limit:	5 ppt or less for chlorophyll *a*
Stability:	0.5% per month of full scale

d) Particle size sensor

Model:	P-05, Nippon Kaiyo Co. Ltd.
Serial number:	P5024
Accuracy:	±10% of range
Measurement range:	0.02681mm to 6.666mm
Reproducibility:	±5%
Stability:	5% per week
Calibration date:	17-Apr.-00

e) Flow meter

Model:	EMARG2W, Aichi Watch Electronics Ltd.
Serial number:	8672
Measurement range:	0 to 30 L/min
Accuracy:	±1%
Stability:	±1% per day

(4) Preliminary Result

(4-1) Salinity sensor

We sampled each day for salinity validation and in situ salinity calibration during this cruise. We collected two times each day during this cruise. The water was taken midway of flow line from the intake to the system. All samples were analyzed on the Guildline 8400B (see section 6.9.2).

The results were shown in table 6.11-1 and Figure 6.11-1. It seemed that salinity of the sensor tended to be higher than the sample during this cruise. It may be caused that the temperature and the conductivity sensor of SBE21 were drifting.

The precision of the sensor at each leg 3 was summarized in table 6.11-2.

Table 6.11-1 Comparison of salinity between salinity sensor of Sea Surface Monitoring System and samples analyzed by Autosal salinometer.

Sampling Date	Sampling Time	Sampling Position		Tctd	Salinity		Difference	Remarks
	(UTC)	latitude	longitude	(IPTS-90)	Sctd	Ssal	Sctd-Ssal	
2001/11/8	01:21	03-10.680N	137-07.554E	29.7057	33.8946	33.8898	0.0048	
2001/11/8	14:16	02-02.430N	138-04.296E	29.6455	34.0374	34.0349	0.0025	
2001/11/9	01:16	01-58.487N	138-03.796E	29.6756	33.9939	33.9858	0.0081	
2001/11/9	13:27	01-57.292N	138-04.623E	29.9919	34.1583	34.1475	0.0108	
2001/11/10	01:56	02-03.528N	138-03.164E	29.5178	34.0946	34.0901	0.0045	
2001/11/10	13:10	01-54.282N	138-02.565E	29.5323	34.1334	34.1296	0.0038	
2001/11/11	02:24	01-50.905N	138-03.430E	29.8672	34.1512	34.1475	0.0037	
2001/11/11	13:00	01-50.949N	138-00.872E	29.7345	34.1547	34.1502	0.0045	
2001/11/12	02:05	01-51.139N	138-01.952E	29.8954	34.1435	34.1406	0.0029	
2001/11/12	13:17	01-50.820N	137-59.159E	29.7339	34.1150	34.1083	0.0067	
2001/11/13	12:54	01-51.483N	138-00.913E	30.1810	34.1044	34.0980	0.0064	
2001/11/14	02:02	01-51.543N	138-02.449E	29.7766	34.0676	34.0604	0.0072	
2001/11/14	12:56	01-53.221N	138-01.725E	30.0548	34.1040	34.0960	0.0080	
2001/11/15	01:42	01-52.433N	138-01.235E	29.8924	34.0991	34.0918	0.0073	
2001/11/15	12:49	01-53.641N	138-03.068E	29.8540	34.1412	34.1365	0.0047	
2001/11/16	03:41	01-52.503N	137-58.903E	29.7910	34.1858	34.1779	0.0079	
2001/11/16	12:47	01-52.077N	138-02.744E	29.6551	34.1772	34.1686	0.0086	
2001/11/17	01:29	01-50.752N	138-00.208E	29.6365	34.1739	34.1662	0.0077	
2001/11/17	13:02	01-52.494N	138-00.960E	29.5666	34.2962	34.2909	0.0053	
2001/11/18	03:26	01-51.718N	138-01.551E	29.5178	34.2913	34.2849	0.0064	
2001/11/18	12:51	01-51.722N	138-02.551E	29.3972	34.2749	34.2666	0.0083	
2001/11/19	03:43	01-48.236N	138-01.027E	29.4014	34.2755	34.2677	0.0078	
2001/11/19	12:43	01-51.051N	138-02.544E	29.3199	34.2716	34.2636	0.0080	
2001/11/20	02:46	01-51.375N	138-03.604E	29.3096	34.3100	34.3017	0.0083	
2001/11/20	12:42	01-50.688N	138-02.721E	29.2249	34.3482	34.3410	0.0072	
2001/11/20	23:25	01-51.349N	138-03.414E	29.2890	34.3392	34.3314	0.0078	
2001/11/21	12:44	01-50.416N	138-02.553E	29.2679	34.3602	34.3520	0.0082	
2001/11/22	01:04	01-47.254N	137-59.056E	29.3259	34.3642	34.3573	0.0069	
2001/11/22	13:07	01-47.185N	138-04.320E	29.4973	34.3146	34.3140	0.0006	
2001/11/22	23:12	01-51.612N	138-03.187E	29.3053	34.2769	34.2702	0.0067	
2001/11/23	12:48	01-50.333N	138-05.211E	29.3923	34.2827	34.2757	0.0070	
2001/11/24	02:40	01-51.623N	138-03.541E	29.4183	34.2642	34.2566	0.0076	
2001/11/24	12:43	01-50.932N	138-04.451E	29.4038	34.2695	34.2630	0.0065	
2001/11/25	04:40	01-50.579N	138-04.661E	29.6551	34.2764	34.2676	0.0088	
2001/11/25	12:42	01-51.101N	138-04.069E	29.4461	34.2783	34.2709	0.0074	
2001/11/26	02:45	01-51.777N	138-03.316E	29.4919	34.2810	34.2734	0.0076	
2001/11/26	12:44	01-53.555N	138-03.336E	29.5811	34.2823	34.2736	0.0087	
2001/11/27	04:58	01-52.870N	138-01.980E	29.9464	34.2798	34.2709	0.0089	
2001/11/27	13:05	01-52.892N	137-59.525E	29.5618	34.2737	34.2656	0.0081	
2001/11/28	02:26	01-51.535N	138-03.037E	29.6389	34.2887	34.2728	0.0159	
2001/11/28	12:44	01-50.726N	138-01.797E	29.7141	34.2834	34.2742	0.0092	
2001/11/29	05:07	01-50.956N	138-02.846E	29.8096	34.2830	34.2746	0.0084	
2001/11/29	12:38	01-52.419N	138-02.227E	29.6539	34.2772	34.2689	0.0083	
2001/11/30	05:09	01-51.557N	138-03.236E	29.6660	34.2859	34.2777	0.0082	
2001/11/30	12:38	01-50.630N	138-02.372E	29.5546	34.2868	34.2779	0.0089	
2001/12/1	05:26	01-50.647N	138-04.401E	29.7520	34.2881	34.2794	0.0087	
2001/12/1	12:32	01-51.156N	138-01.376E	29.4268	34.2661	34.2575	0.0086	
2001/12/2	05:41	01-51.150N	138-03.221E	29.4274	34.2498	34.2415	0.0083	
2001/12/2	13:00	01-50.196N	137-58.558E	29.3495	34.2533	34.2437	0.0096	
2001/12/3	04:21	02-03.685N	138-03.271E	29.5950	34.2976	34.2882	0.0094	
2001/12/3	12:47	01-53.014N	138-01.702E	29.3972	34.2612	34.2526	0.0086	
2001/12/4	03:32	01-49.974N	137-58.502E	29.3247	34.2905	34.2833	0.0072	
2001/12/4	12:38	01-50.736N	138-01.883E	29.3047	34.3106	34.2995	0.0111	
2001/12/5	04:16	01-48.833N	137-56.368E	29.2558	34.2870	34.2766	0.0104	
2001/12/5	12:49	01-50.948N	138-01.652E	29.1819	34.2282	34.2189	0.0093	
2001/12/6	03:58	01-51.158N	137-58.735E	29.2182	34.2798	34.2726	0.0072	
2001/12/6	12:44	01-52.833N	138-01.581E	29.0413	34.1392	34.1282	0.0110	
2001/12/7	04:50	01-53.919N	138-03.045E	29.2527	34.2247	34.2157	0.0090	
2001/12/7	12:56	01-53.284N	138-00.395E	29.0825	34.2034	34.1928	0.0106	
2001/12/8	03:55	01-46.710N	137-59.520E	29.0874	34.2363	34.2266	0.0097	
2001/12/8	12:43	01-52.423N	138-01.584E	29.0528	34.2894	34.2793	0.0101	
2001/12/9	03:47	02-37.685N	137-54.164E	29.1032	34.2054	34.1898	0.0156	
						Average	0.0078	
						Std. Dev.	0.0025	

Table 6.11-2 Precision of Salinity at leg 3.

	Difference of salinity (Sctd-Ssal)
Average	0.0078
Standard Deviation	0.0025
Average of absolute difference	0.0078
Standard Deviation of absolute difference	0.0025
R.M.S.	0.0058
Min	0.0006
Max	0.0159
n	62

We calculated the Root Mean Squares (R.M.S.) of difference of salinity for 62 samples at leg 3. R.M.S. of salinity (one sigma) was 0.0058. There were two samples which difference of salinity was higher than three times of standard deviation in this cruise. We suspected that the sampling might cause these differences. The final results omitted the two sample were shown in table 6.11-3 and figure 6.11-2.

Table 6.11-3 Precision of Salinity omitted two samples at leg 3.

	Difference of salinity (Sctd-Ssal)
Average	0.0076
Standard Deviation	0.0021
Average of absolute difference	0.0076
Standard Deviation of absolute difference	0.0021
R.M.S.	0.0056
Min	0.0006
Max	0.0111
n	60

These results showed that the validation of salinity was within 0.01.

(4-2) Dissolved Oxygen (D.O.) sensor

D.O. sensor of this system was calibrated at Palau just before this cruise. To estimate of accuracy of the sensor, we collected the samples from the course of the system and analyzed by the Winkler method each day at leg 3 (see section 6.9.3).

The results of leg 3 were shown in table 6.11-4 and Figure 6.11-3. It seemed that D.O. of the sensor tended to be higher than the sample. The average and standard deviation (one sigma) of differences (D.O. sensor - Winkler) in this cruise was summarized in table6.11-5.

Table 6.11-5 Precision of the D. O. sensor at leg 3.

	Difference (mg/l)
Average	1.185
Standard Deviation	0.058
n	30

(4-3) Fluorometer

In order to calibrate the data of fluorescence from this system, we collected surface seawater samples from the course of the system four times each day.

We determined the concentrations of chlorophyll *a* and phaeopigments board. The method of measurement was indicated below. Sea surface water samples (0.5 liter) were filtered through a Nucrepore filters (pore size: 0.4 µm; diameter: 47 mm) in the dark room. The filters were stored at -20 deg-C in the dark until the analysis and then, the samples were extracted in 6 ml of N,N'-dimethylformamide (DMF) before the analysis.

Fluorescence of extracts was measured by Turner fluorometer (10-AU-005, TURNER DESIGNS). After the each sample measurement, the extracts were acidified with 2 drops of 1N HCl and the second measurement was done. The concentration of chlorophyll *a* and phaeopigments were calculated from the following equation:

chlorophyll *a* (µg/L) = $(Fm/Fm\text{-}1)\times(F_0\text{-}Fa)\times Kx\times(vol_{ex}/ vol_{filt})$

Phaeopigments (µg/L) = $(Fm/Fm\text{-}1) \times[Fm\cdot Fa] – F_0]Kx\times(vol_{ex}/ vol_{filt})$

Fm	=	acidification coefficient (F_0/Fa) for pure Chl *a* (1.89)
F_0	=	fluorescence of seawater sample before acidification
Fa	=	fluorescence of seawater sample after acidification
Kx	=	door factor from calibration calculations (0.91)
vol_{ex}	=	extraction volume (6ml)
vol_{filt}	=	filter volume (500ml)

(5) Preliminary Results

Preliminary data every 10 minutes from 8 November to 8 December, 2001 were shown in figure 6.11-4. They showed the respective trend of temperature, salinity, D.O., and fluorescence variations.

(6) Data archive

All the files of raw data, Microsoft excel files of raw data were stored on a magneto-optical disk. All the data will be submitted to the Data Management Office at JAMSTEC.

(7) Reference

Culberson, C. H. (1991) Dissolved Oxygen, in WHP Operations Methods, Woods Hole, pp.1-15.

SEACAT THERMOSALINOGRAPH SBE21 OPERATING MANUAL, APPLICATION NOTE No. 2D, Revised January 1998

T. J. Muller and H. -W. Schenk (1991) Near-Surface Temperature, salinity, and Bathymetry Measurements, in WHP Operations Methods, Woods Hole, pp.1-4.

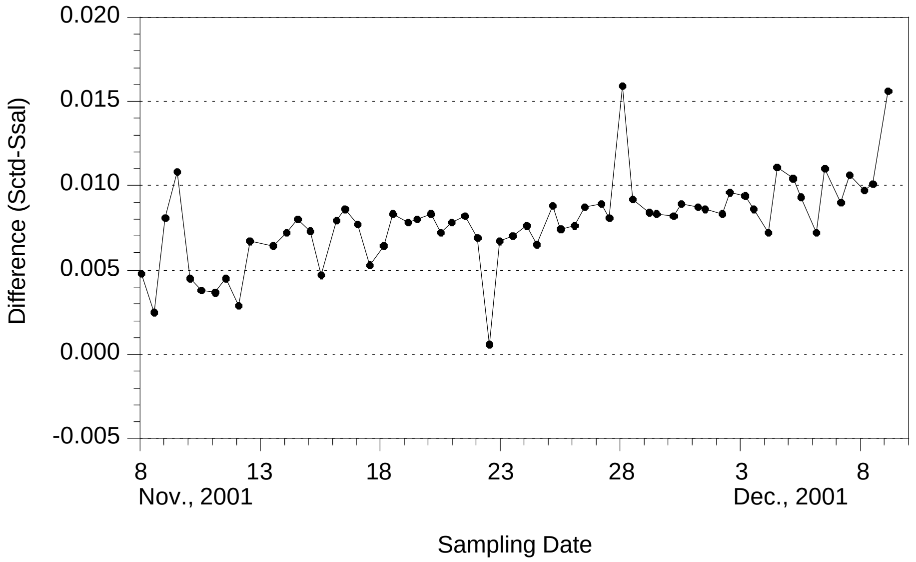

Fig. 6.11-1: Difference between the salinities measured by conductivity and temperature sensor (Sctd) of Sea Surface Monitoring System and the Autosal salinometer (Ssal).

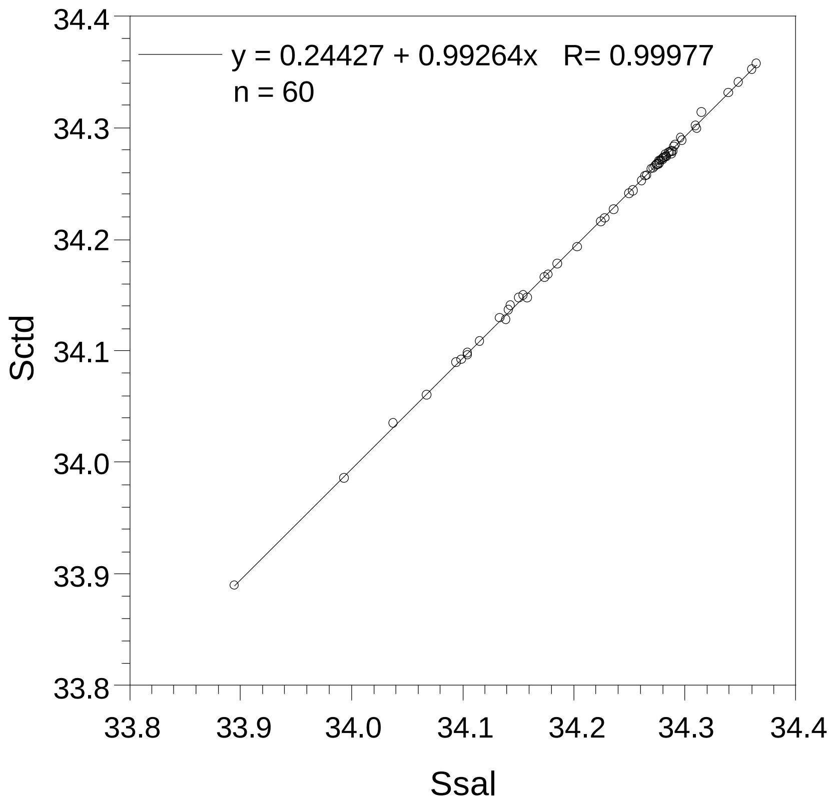

Fig. 6.11-2: Comparison between the salinity values measured by SBE21 of Sea Surface Monitoring System and by the Autosal salinometer.

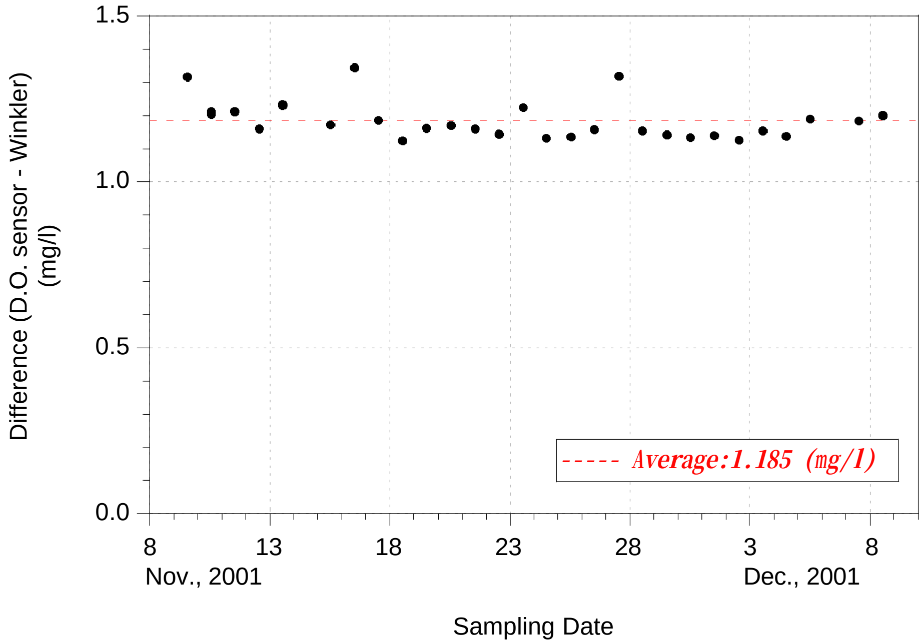

Fig. 6.11-3: Difference between the D.O. values measured by the D.O. sensor of Sea Surface Monitoring System and by the Winkler method.

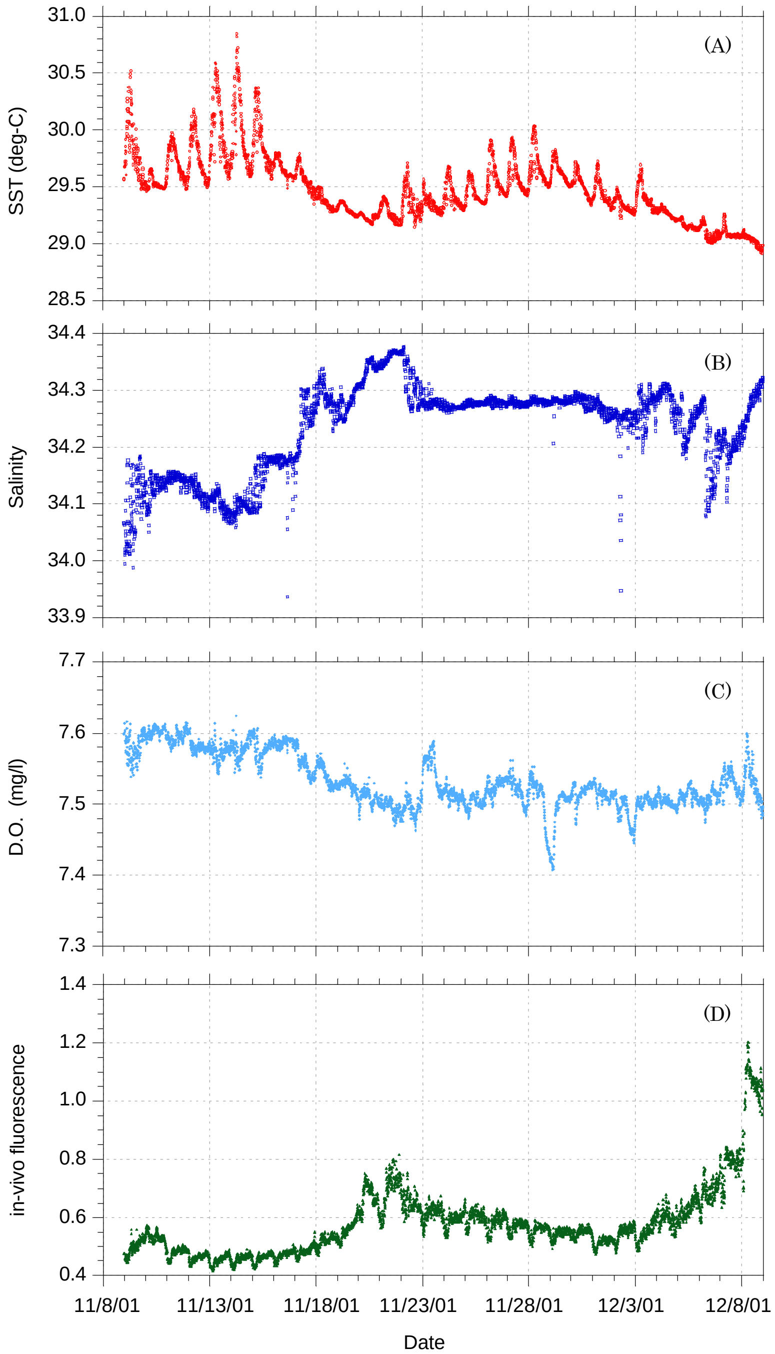

Fig. 6.11-4: Temporal variation in temperature (A), salinity (B), D.O. (C), in-vivo fluorescence (D) of surface water during from 8 November to 8 December 2001.

Table 6.11-4 Comparison of D.O. value between a D.O. sensor of Sea Surface Monitoring System and water samples using Winkler method

Sampling Date	Sampling Time (UTC)	Sampling Position latitude	longitude	Sctd	T_{SBE21} (ITS-90)	D.O. sensor (mg/l)	Winkler (mg/l)	Difference (mg/l)	Remarks
11/9/01	13:22	01-56.649N	138-04.586E	34.1437	30.0279	7.567	analysis failed	-	
11/9/01	13:25	01-57.035N	138-04.609E	34.1540	30.0183	7.561	6.245	1.316	
11/10/01	13:16	01-54.863N	138-02.306E	34.1358	29.5359	7.605	6.393	1.211	
11/10/01	13:19	01-55.151N	138-02.172E	34.1360	29.5377	7.605	6.401	1.204	
11/11/01	13:00	01-50.949N	138-00.872E	34.1547	29.7345	7.597	6.385	1.213	
11/12/01	13:20	01-50.807N	137-58.834E	34.1122	29.7327	7.577	6.419	1.158	
11/13/01	12:57	01-51.475N	138-00.599E	34.1035	30.1690	7.567	6.334	1.234	
11/13/01	12:59	01-51.470N	138-00.391E	34.1027	30.1601	7.569	6.340	1.229	
11/14/01	12:55	01-53.150N	138-01.803E	34.1041	30.0578	7.571	analysis failed	-	
11/15/01	12:48	01-53.515N	138-03.104E	34.1413	29.8498	7.573	6.401	1.172	
11/16/01	12:45	01-51.954N	138-02.835E	34.1785	29.6564	7.589	6.245	1.344	
11/17/01	13:05	01-52.619N	138-00.728E	34.2960	29.5751	7.554	6.369	1.185	
11/18/01	12:50	01-51.680N	138-02.616E	34.2756	29.3972	7.534	6.411	1.122	
11/19/01	12:40	01-51.028N	138-02.816E	34.2720	29.3193	7.527	6.366	1.161	
11/20/01	12:43	01-50.685N	138-02.624E	34.3488	29.2231	7.507	6.338	1.168	
11/21/01	12:42	01-50.455N	138-02.726E	34.3593	29.2691	7.508	6.348	1.160	
11/22/01	13:05	01-47.381N	138-04.278E	34.2988	29.4841	7.500	6.357	1.143	
11/23/01	12:47	01-50.421N	138-05.151E	34.2817	29.3917	7.586	6.362	1.224	
11/24/01	12:42	01-50.971N	138-04.354E	34.2697	29.4014	7.505	6.375	1.131	
11/25/01	12:46	01-50.915N	138-04.392E	34.2792	29.4479	7.505	6.369	1.137	
11/26/01	12:42	01-53.376N	138-03.287E	34.2817	29.5799	7.531	6.374	1.156	
11/27/01	13:04	01-52.848N	137-59.611E	34.2739	29.5636	7.522	6.205	1.317	
11/28/01	12:42	01-50.826N	138-01.949E	34.2838	29.7135	7.524	6.370	1.154	
11/29/01	12:40	01-52.528N	138-02.093E	34.2773	29.6570	7.514	6.373	1.141	
11/30/01	12:38	01-50.630N	138-02.372E	34.2868	29.5546	7.520	6.387	1.133	
12/1/01	12:31	01-51.161N	138-01.456E	34.2662	29.4286	7.518	6.380	1.139	
12/2/01	12:56	01-50.279N	137-58.904E	34.2553	29.3477	7.494	6.368	1.126	
12/3/01	12:45	01-52.891N	138-01.794E	34.2585	29.4020	7.512	6.358	1.154	
12/4/01	12:38	01-50.736N	138-01.883E	34.3106	29.3047	7.502	6.364	1.138	
12/5/01	12:32	01-51.112N	138-02.995E	34.2261	29.1777	7.528	6.339	1.190	
12/6/01	12:43	01-52.782N	138-01.638E	34.1418	29.0407	7.505	analysis failed	-	
12/7/01	12:53	01-53.141N	138-00.570E	34.2020	29.0856	7.544	6.360	1.184	
12/8/01	12:44	01-52.466N	138-01.517E	34.2888	29.0516	7.535	6.335	1.199	
							Average	1.185	
							Std. Dev.	0.058	

6.12 Greenhouse Effect Gasses Measurement

(1) Personnel

Mitsuru Hayashi (Maritime University of Kobe) : Principle Investigator
Masaya Shimanoue (Maritime University of Kobe)
Masakuzu Egawa (Maritime University of Kobe)
Naoki Nakatani (Osaka Prefecture University)

(2) Objectives

N_2O (Nitrous oxide) and CO_2 (Carbon dioxide) gasses play important roles and function of the global warming. It is required to get more accurate information of those gasses exchanges between the sea and atmosphere in order to understand the mechanism of the global warming process. So we carried out measurements of N_2O and CO_2 concentrations in the atmosphere and sea water, and NOx and SOx concentrations in the atmosphere as background.

(3) Method

The measurements of N_2O and CO_2 concentrations in the atmosphere and sea water were made in the Equatorial Western Pacific, 01N and 138E, for 18 days from 14 Nov. to 6 Dec. 2001. The observational period or dates are listed in Table 6.12-1. The sample air was intaken at the foremast about 11m height above the sea level, and surface sea water was intaken at about 5m depth. Sea water for the vertical distribution measurement was sampled by the niskin sampler. N_2O and CO_2 concentrations in the atmosphere were measurement using each analyzer. N_2O and CO_2 concentrations in sea water were obtained by the babbling method.

NOx and SOx concentrations in the air were measured from 1 Dec. to 8 Dec. also. A sampling interval is 50 sec, and data was collected to PC.

Specification of analyzer is as follows;

N_2O analyzer	MODEL:46C (Thermo Environmental Instruments Inc.)
	Accuracy : 10 % of full scale < 50 ppm (using 1ppm scale)
CO_2 analyzer	MODEL:VIA-510 (HORIBA Ltd.)
	Accuracy: 0.5 % of full scale
NOx analyzer	MODEL:42C-TL (Thermo Environmental Instruments Inc.)
	Accuracy : 0.05 ppb (using 50 ppb range)
N_2O analyzer	MODEL:43C (Thermo Environmental Instruments Inc.)
	Accuracy : 1 % of measuring value or 1 ppb

Table 6.12.1 Observational period and date

Period or date	Maesurement (Atmosphere and Surface sea watar /Vertical distribution)
14-15 Nov	6 hourly measurement of N2O and CO2 in surface sea watar
16-21 Nov	3 hourly measurement of N2O and CO2 in surface sea watar
19-28 Nov	Continuously measurement of N2O and CO2 in atmosphere
21-28 Nov	6 hourly measurement of N2O and CO2 in surface sea watar
4-Dec	Measurement of vertical distrbution of N2O (0,25,75,125,150,175,200,250,300,325,375,500,1000m)
5-Dec	Measurement of vertical distrbution of N2O (0,25,75,125,200,250,300,325,375,450,500,700,1000m)
6-Dec	Measurement of vertical distrbution of N2O (0,75,125,175,300,400,450,600,700,850,1000m)

(4) Preliminary Result

6 hourly time series and 3 hourly time series of N_2O and CO_2 concentrations in the atmosphere and sea water from 14 to 21 Nov. are shown in Fig.6.12-1 and Fig.6.12-2, respectively. 6 hourly time series of N_2O and CO_2 concentrations in the atmosphere and sea water from 21 to 28 Nov. are shown in Fig.6.12-3 and Fig.6.12-4, respectively. CO_2 concentrations in the atmosphere are higher than those in surface sea water during observation period. N_2O concentrations in the atmosphere are higher than those in surface sea water from 14 to 19 Nov., and are about equal or lower than those in surface sea water from 19 to 28 Nov.. It is considered that N_2O concentrations in surface sea water were near that in the atmosphere with increased rain was brought westerly burst. N_2O and CO_2 concentrations in the atmosphere and sea water shifted at 24 Nov., because we exchanged the bottle of background gas new one.

The vertical distributions of the N_2O concentrations in sea water from 0 to 1,000m in depth are shown in Fig.6.12-5. The concentrations increase from surface to 450m and tend to be variable in deep sea water from 500 to 1000m depth. The peak of N_2O concentration may exist around 450m in depth.

All observational data will be analyzed in detail later.

(5) Data archives

The data are archived in MO disks and will have a quality check in Maritime University of Kobe, and will be distributed to public later. The raw data is submitted to JAMSTEC DMO.

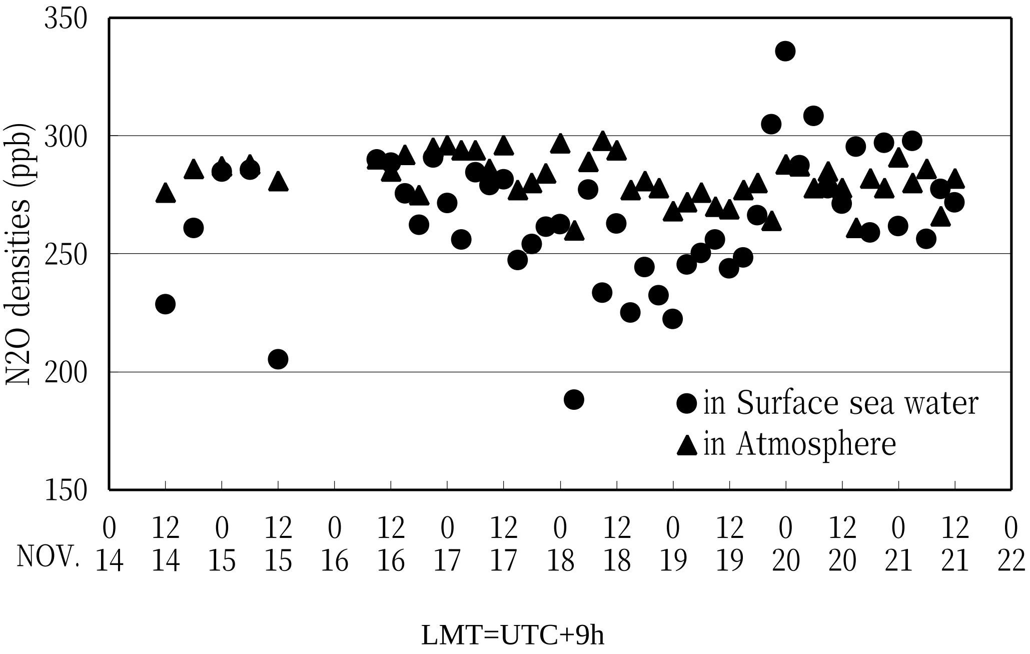

Fig.6.12-1: Temporal variation of N2O densities in atmosphere and surface sea water from 14 to 21 Nov.

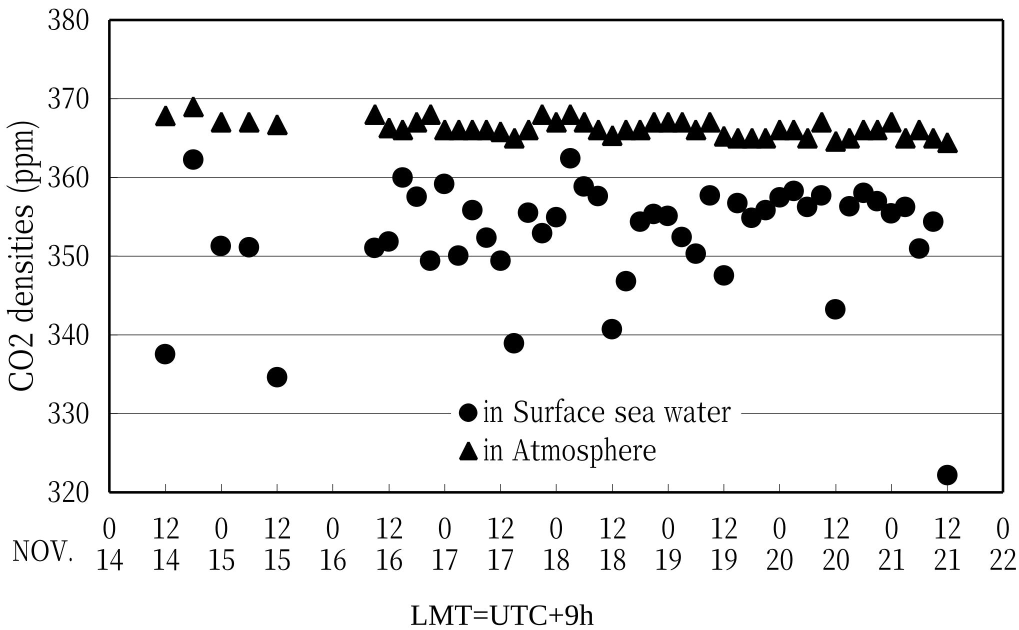

Fig.6.12-2: Temporal variation of CO2 densities in atmosphere and surface sea water from 14 to 21 Nov.

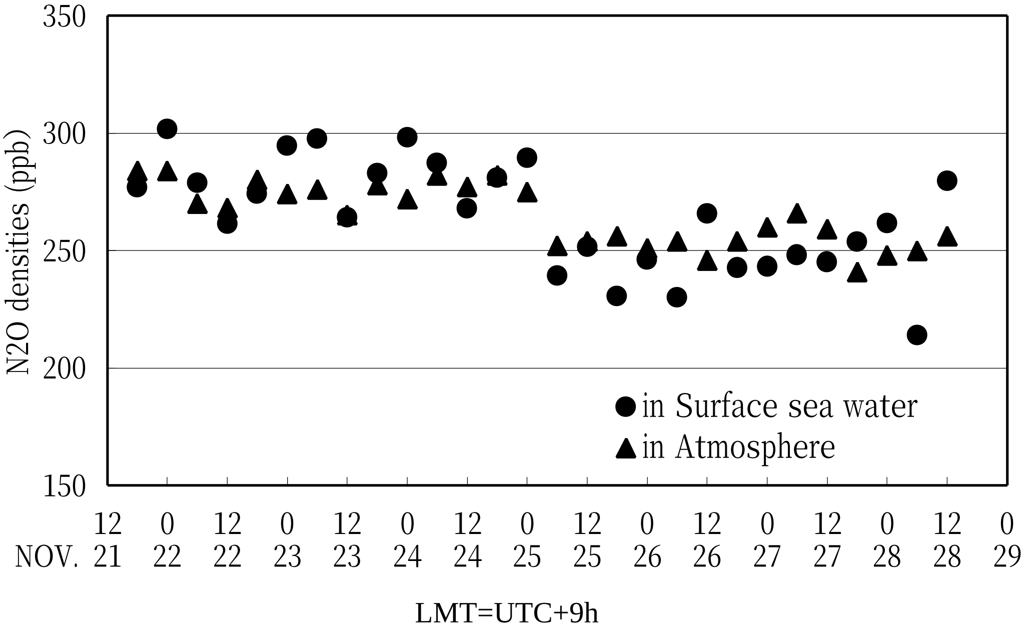

Fig.6.12-3: Temporal variation of N2O densities in atmosphere and surface sea water from 21 to 28 Nov.

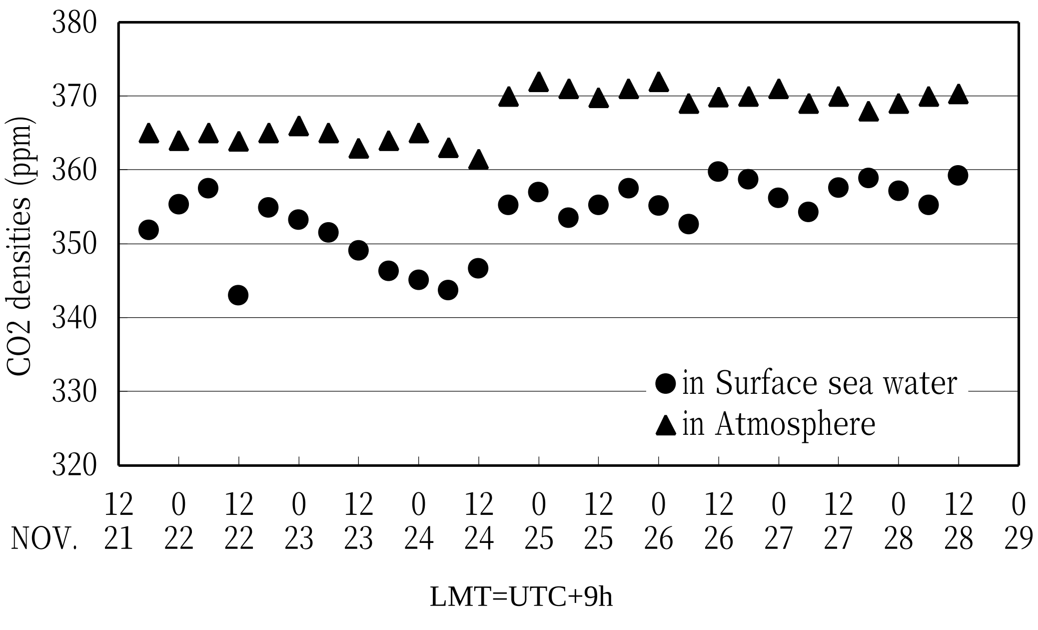

Fig.6.12-4: Temporal variation of CO2 densities in atmosphere and surface sea water from 21 to 28 Nov

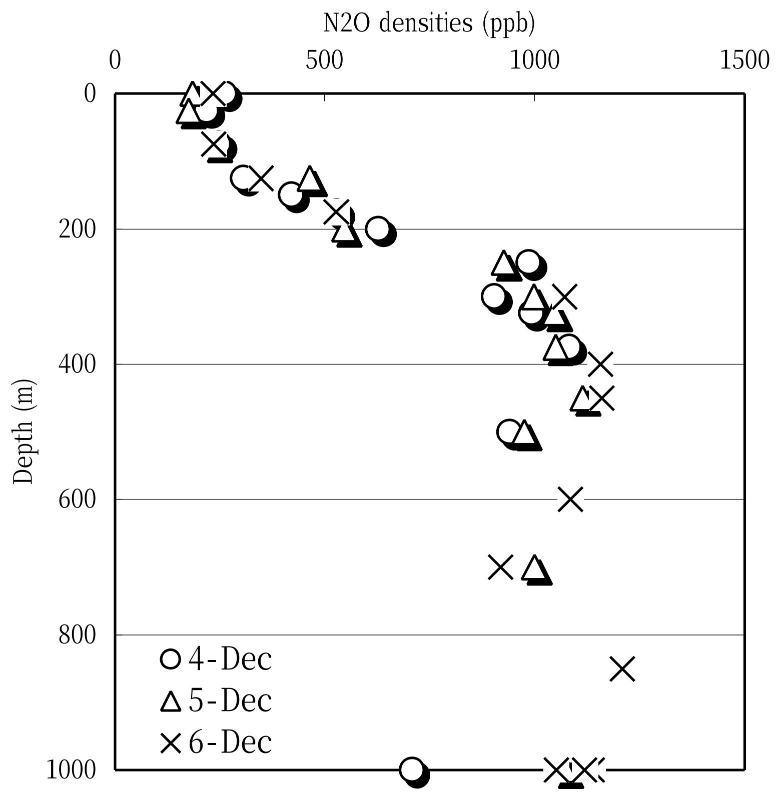

Fig.6.12-5: Vertical distributions of N2O densities in sea water from 0 to 1,000m in depth.

6.13 CO2 Measurement

6.13.1 pCO_2/PCO_2 Measurment

(1) Personnel

Hirohisa IDEHARA(Okayama University of Science)
Kaori MORITO(Okayama University)
Eiji YAMASITA(Okayama University of Science):Observation leader

(2) Objective

The objective of this cruise is to measure following temporal and spatial variations at the equatorial Station(2^{o}N,138^{o}E).

・Time variation of pCO_2 in the ocean and PCO_2 in the atmosphere
・Vertical profile of pCO2 in the ocean

(3) Method

Carbon dioxide in seawater and carbon dioxide in the atmosphere were measured using the measurement system which is produced by S-ONE INC.

The present CO_2 instrument only requires small amount of seawater sample to measure pCO_2. 500ml of seawater is enough to determine pCO_2.

The system is located in the sea surface laboratory on the ship.

Surface seawater was pumped up to the laboratory and deep seawater was obtained by CTD-RMS seawater sampling system. Sample air was introduced from foremast.

We had measured from Nov. 7 to Dec. 6,2001. The system had been checked everyday.

Specification of the carbon dioxide measurement system was listed below.

Unit 1: CO_2 analyzer
Model:LI-6252 LI-COR,INC.
Serial number: IR-62-286
Measurement rang: 0-5V

Unit 2: Gas mixing unit
Model: SO96NL-T,S-ONE,INC.

Unit 3: Equilibrumeter
Model: SO96NL-T,S-ONE,INC.

Unit 4: Data processing equipment (personal computer)

(4) Results

Fig.6.13.1 shows mean value of pCO_2 in a day during November 7 to December 5. The mean value of pCO_2 in a day was in the range between 355.4 and 366.1 ppmv. The minimum value of PCO_2 was 366.1 ppmv. And pCO_2 was in the range between 342.9 and 379.5 ppmv.

The PCO_2 concentrations were higher than concentrations of pCO_2 on this station. This result supports that during this cruise, this area is a CO_2 sink. But sometimes, pCO_2 is higher than PCO_2. This kind of phenomenon can be seen on the condition that the ser-surface temperature is more than 30.0 degrees C.

Fig.6.13.2 shows time variation of pCO_2 in November 12,17,22 and 27,2001,respectivery The raw pCO_2 concentrations show that low value in nighttime and high value in daylight hours.

Fig.6.13.3 shows the vertical profile of carbon dioxide in the seawater (pCO_2) at the Station (2°N,138°E) in November 12, 17, 22 and 27, 2001, respectively. As a whole, pCO_2 increased with increasing the depth. The raw pCO_2 values of 1000m depth were above 1700ppmv. The raw pCO_2 concentrations of 75 – 250 m depth increased suddenly and become from 350 ppmv to 1200ppmv. It can be considered that the phenomenon of pCO_2 increase with depth is caused by the biological activity.

(6) Data archive

The raw data were stored on a magnetic optical disk which will be kept on Ocean Research Department, JAMSTEC. The raw data will be corrected and published.

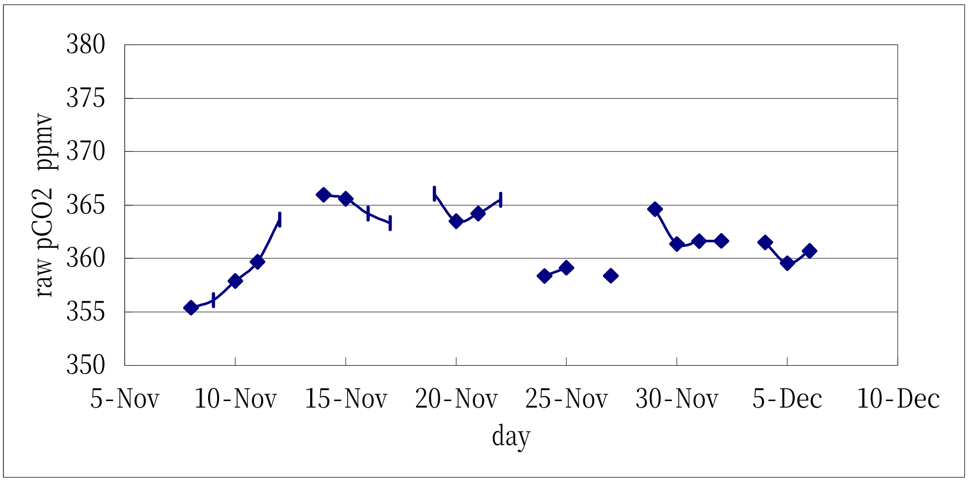

Fig.6.13.1 Mean value of pCO_2 at the Station(2° N,138° E) in a day during November 7 to December 5, 2001.

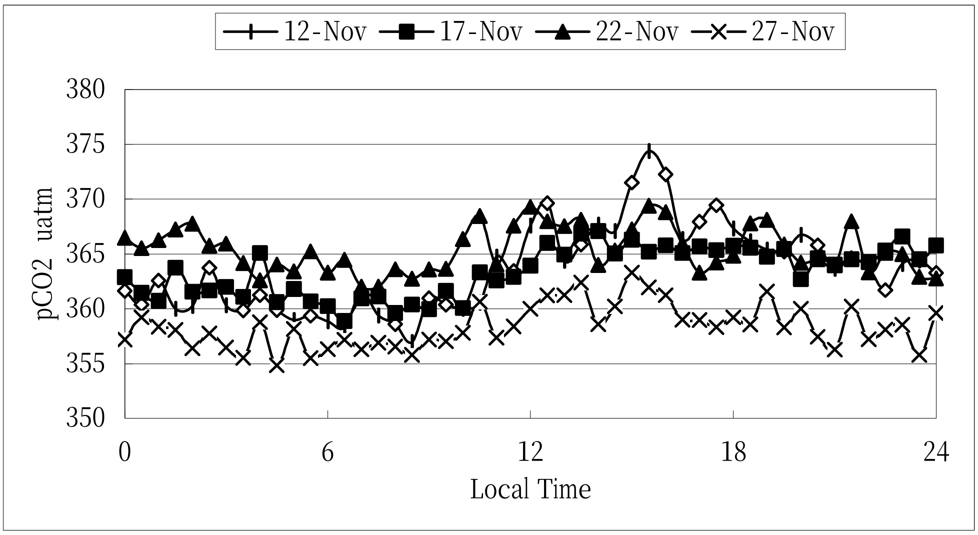

Fig.6.13.2: Time variation of pCO_2 at the Station (2°N,138°E) in November 12,17,22 and 27,2001.

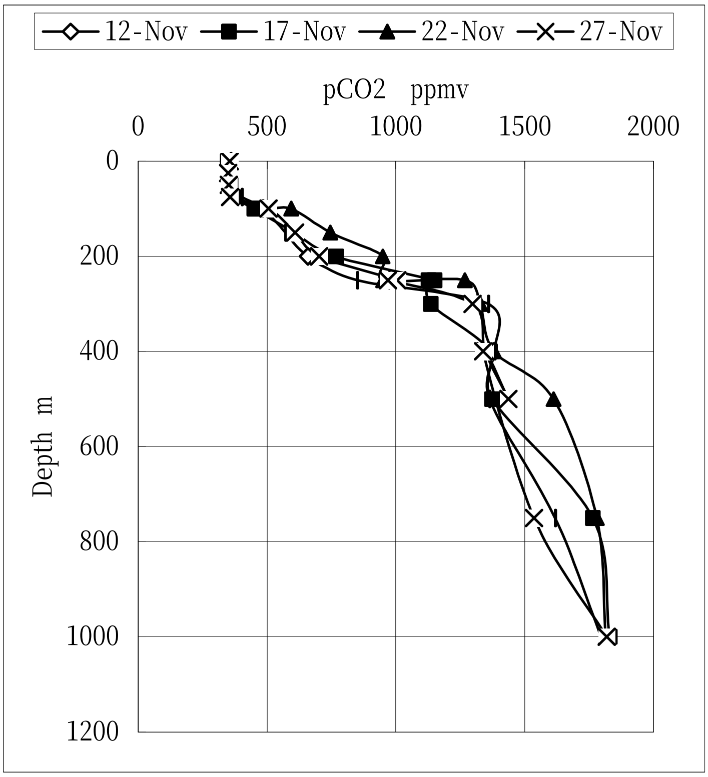

Fig.6.13.3: Vertical profile of pCO_2 at the Station ($2^oN,138^oE$) in November 12,17,22 and 27,2001.

6.13.2 Total Dissolved Inorganic Carbon (TDIC) Measurement

(1) Personnel

Minoru KAMATA (MWJ)

(2) Objective

Global warming caused by green house gasses such as carbon dioxide has become much attention all over the world. In order to verify carbon dioxide parameters in the Central Pacific, TDIC was measured with analytical instruments installed on R/V MIRAI in this cruise.

(3) Methods

(i) Seawater sampling

Surface seawater samples were drawn every 2 hours from a jacket of Okayama University of Science pCO_2 measurement system (S-ONE INC.) into 250ml glass bottles with sampling tube. The jacket was filled up surface seawater collected by a pumping system from a depth of 4.5m.

Seawater samples were collected layer-by-layer at the five stations (C015, C040, C080, C120 and C152). The samples were drawn from 12L Niskin bottles to 250ml glass bottles with sampling tubes. All bottles were not rinsed and filled from the bottom, overflowing a volume while taking care not to entrain any bubbles. After the sampling, 3ml seawater (1% of the bottle volume) was removed from glass bottle by a plastic pipette, and bottles were sealed using Apiezon M grease and stopper, and stored in the refrigerator.

(ii) TDIC measurement

Concentration of TDIC was measured by a coulometer (Carbon Dioxide Coulometer Model 5012, UIC Inc.). The method of TDIC measurement was as follows. Approx. 24ml of seawater was taken into a receptacle and $2cm^3$ of 10% (v/v) phosphoric acid was added. The CO_2 gas evolved was purged by nitrogen gas (CO_2 free) for 12 minutes at the flow rate of $130cm^3$ min^{-1} and absorbed into an electrolyte solution. Acids formed by reacting with the absorbed CO_2 in the solution were titrated with hydrogen ions using the coulometer. Calibration of the coulometer was carried out using sodium carbonate solutions (0-2.5mM). All the data were referenced to the Certified Reference Material (CRM). The precision of TDIC measurements in this cruise was less than 1.0 μmol kg^{-1}.

(4) Preliminary results

Preliminary data of TDIC were shown in Fig 6.13.2-1 and 6.13.2-2.

(5) Data Archives

The datasets, which stored on floppy disks will be submitted to JAMSTEC Data Management Office (DMO).

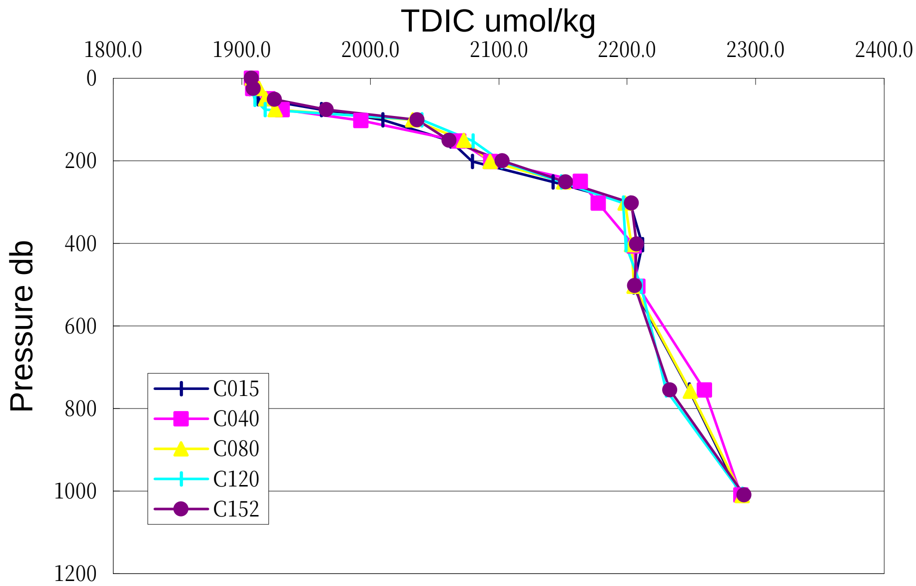

Fig. 6.13.2-1: Results of Vertical distribution of TDIC

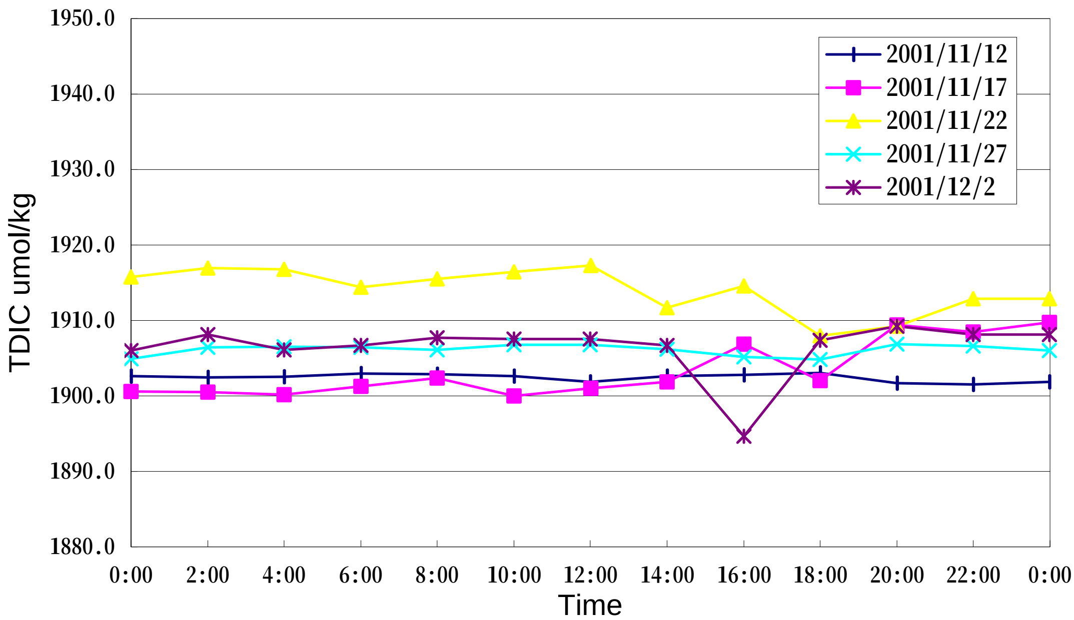

Fig. 6.13.2-2: Results of surface measurements of TDIC

6.13.3 Total alkalinity measurement

(1) Personnel name and affiliation

Kaori Morito (Okayama University)
Minoru Kamata (Marine Works Japan Ltd.)
Eiji Yamashita (Okayama University of Science)

(2) Objectives

Global warming caused by green house gas such as carbon dioxide has become much to be paid attention all over the world. In the flux study of the equator area, it is important to understand its volume of transportation. In order to verify carbon cycle at the equator area, we measured total alkalinity (TA), which is one of carbon dioxide parameters, with analytical instruments installed on R/V MIRAI during this cruise. In this study, we measured its time variation (surface seawater) and vertical distribution at the fixed point (2^{o}N, 138^{o}E) at the same day.

(3) Instruments and Methods

<Time variation>

pCO_2 measurement system was made by S-ONE INC., located in the sea surface laboratory on this ship. Surface seawater samples were drawn from the jacket of pCO_2 measurement system into 250ml Nalgene polyethylene bottles with sampling tubes every 2 hours. Bottles were rinsed twice and filled from the bottom while taking care not to entrain any bubbles. The bottles were then sealed by a screw cap with an inner cap and stored in refrigerator for maximum of 36 hours prior to analysis.

<Vertical distribution>

Seawater samples were drawn from 12L Niskin™ bottles into 250ml Nalgene polyethylene bottles with sampling tubes at 21:00LST. Bottles were rinsed twice and filled from the bottom while taking care not to entrain any bubbles. The bottles were then sealed by screw cap with an inner cap and stored in refrigerator for maximum of 12 hours prior to analysis.

The method of total alkalinity measurement was titration of 0.1M hydrochlolic acid made from 0.7M sodium chloride. The titration system consists of a titration manager (Radiometer, TIM900), an auto-burette (Radiometer, ABU901), a pH glass electrode (Radiometer, pHG201-7), an installed reference operating software (Lab Soft, Tim Talk9) and the another software for calculation.

Before titration, the temperature of the bottles was brought to 25 degree C in the water bath, and water sample was taken by a Knudsen pipette (100ml) into a tall beaker (200ml). The titration carried out adding HCl (0.1N) to seawater past the carbonic acid point with a set of electrodes used to measure electromotive force at 25 degree C. After titration, data of titrated HCl volume and electromotive force and temperature then were used to calculate to total alkalinity. All the values reported were corrected with the Dickson's CRM, sea temperature, and salinity.

(5) Results

We measured time variation and vertical distribution of total alkalinity in Nov.12, 17, 22, 27, and Dec.2, 2001. Time variation of total alkalinity is shown in Figure 6.13.3-1. Vertical distribution of total alkalinity is represented in Figure 6.13.3-2. The absolute differences of duplicate measurements (dTA) were plotted sequentially to evaluate the precision of the measurement process (Figure 6.13.3-3). The average and standard deviation from the differences of sets of duplicate measurement was 0.905

umol/kg and 0.764 umol/kg, respectively.

(6) Data archive

The raw data were stored on a magnetic optical disk which will be kept on Ocean Research Department, JAMSTEC. The raw data will be corrected and published.

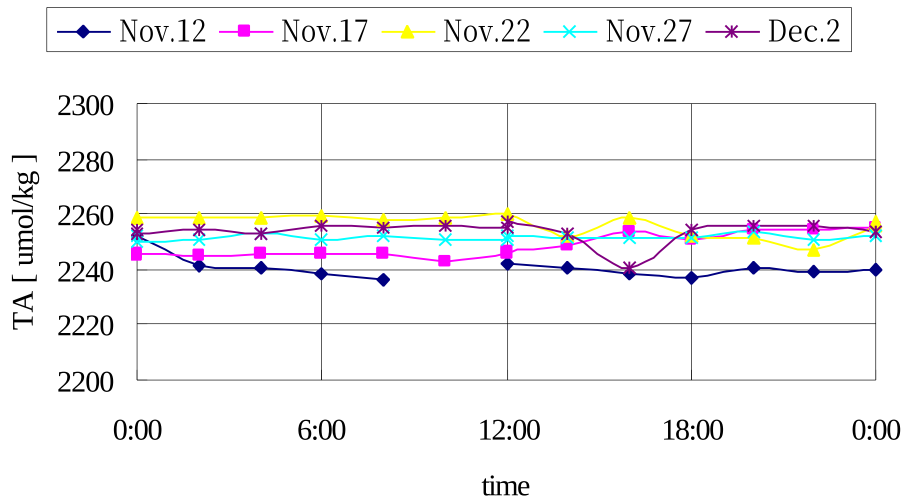

Figure 6.13.3-1: Time variation of total alkalinity

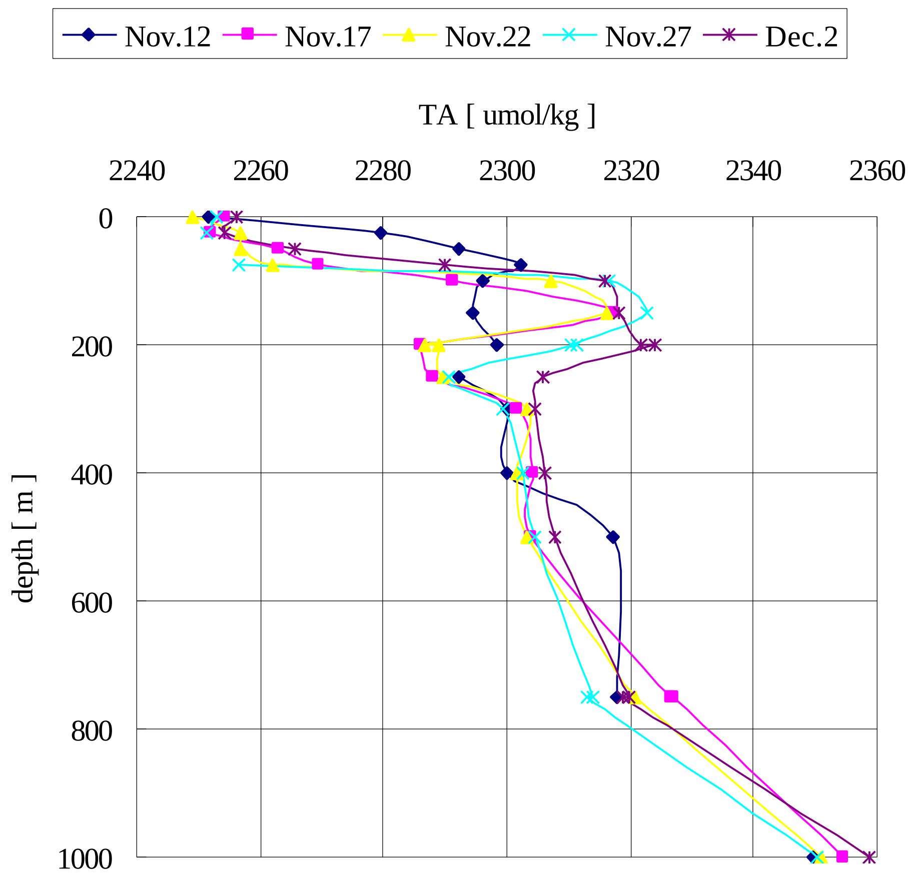

Figure 6.13.3-2 Vertical distribution of total alkalinity

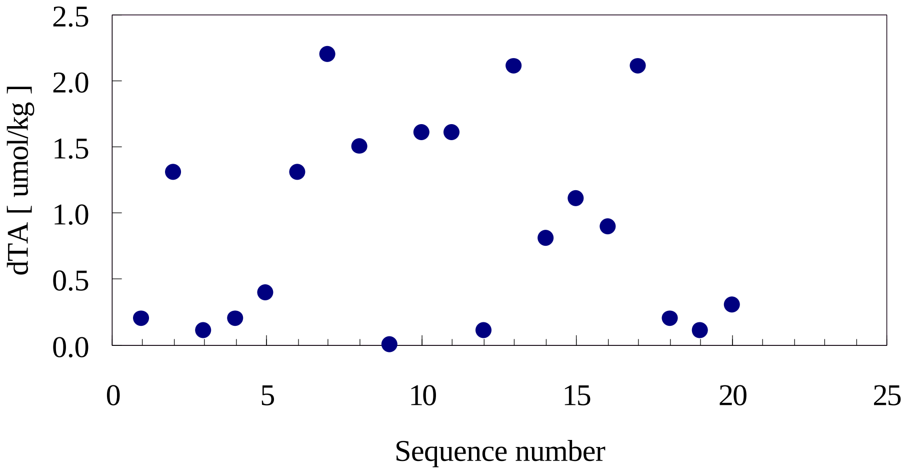

Figure 6.3.13-3 Difference of duplicates

6.13.4 Atmospheric and surface seawater pCO_2

(1) Personnel

Akihiko Murata (JAMSTEC): Principle Investigator
Minoru Kamata (MWJ): Operation Leader

(2) Objectives

To clarify distributions of atmospheric and surface seawater partial pressure of CO_2 (pCO_2) over the western North Pacific Ocean.

(3) Methods

We used the CO_2 measuring system installed onboard the Mirai. The main part of the CO_2 measuring system consists of:

Non-dispersive infrared gas analyzer	BINOS® model 4.1, Fisher-Rosemount
Equilibrator	Shower-head type
Standard gases	Traceable to SIO scale

Concentrations (mole fraction) of CO_2 in dry air (xCO_2a) and in dry air equilibrated with seawater (xCO_2s) were measured continuously with the non-dispersive infrared gas analyzer. The air was sampled from the inlet (approx. 30 m height from the sea surface) situated at the bow of the ship. The equilibrated air was sampled from a showerhead type equilibrator, and seawater for equilibration was taken from a depth of 4.5 m. The rise in seawater temperature between the intake and the equilibrator was 0.5°C at maximum, which was corrected based on the Gordon and Jones's (1973) formula. Calibration was made at a maximum interval of 1.5 hours by measuring four standard gases, with nominal concentrations of 250, 310, 334 and 370 ppmv in synthetic air The standard gases were calibrated against the primary standard gases calibrated by Dr. C.D. Keeling of Scripps Institution of Oceanography (SIO).

(4) Results

Atmospheric CO_2 was about 370 ppmv in low latitudes about 10°N, but increased gradually northward. Surface seawater pCO_2 was almost equilibrated with atmospheric CO_2 in the low latitudes. However, surface seawater pCO_2 decreased gradually northward in parallel with decrease in water temperature. Overall, in this season, the western North Pacific Ocean acted as a sink for atmospheric CO_2, except for the low latitudes.

(5) Data Archives

The inventory information and dataset will be submitted to the DMO (Data Management Office) of JAMSTEC.

6.14 Sampling of the stable isotopes in precipitation

(1) Personnel

Jingyang Chen (Frontier Observation Research System for Global Change)
Suginori Iwasaki (Frontier Observation Research System for Global Change)
Kimpei Ichiyanagi (Frontier Observation Research System for Global Change)
Naoyuki Kurita (Frontier Observation Research System for Global Change)

(2) Objectives

The samples of precipitation are collected to obtain temporal variation of stable isotopes in Tropical rainfall and special distributions of stable isotopes in precipitation all over the Asia.

(3) Methods

The samples of precipitation are collected by the 6 ml glass bottle with plastic cap (see Fig. 1). Stable isotopic composition for hydrogen and oxygen in water is determined by the isotope ratio mass spectrometry (IRMS). The IRMS used in this study is Finnigan MAT 252 (Thermo Quest K. K.) with CO_2 & H_2 equilibration device

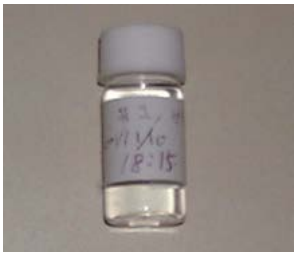

Fig. 1: The sample of precipitation at 18:15 (LT), 10 November, 2001.

(4) Results

We collect the samples of precipitation from 10 November, 2001 to 8 December (Table 1). Because it is impossible to analyze them in the Mirai vessel, we show the results of observed stable isotopic composition for hydrogen (δD) and oxygen ($\delta^{18}O$) in precipitation, from 17 June to 2 July, 2000 (see Table 2). The stable isotopic compositions are -100 to 0 for δD and -1 to -14 for $\delta^{18}O$, respectively. The d-excess values ($\delta D \quad 8\times \quad \delta^{18}O$) are 1 to 13, most of them are near to the global mean value (10). The equation obtained by the least squares method is $\delta D = 7.9 \times \delta^{18}O + 8.4$, and the correlation coefficient is 0.99. This slope (7.9) is very near to the Meteoric Water Line (8.0) that is global mean value. In generally, monthly mean values of stable isotopic composition in Tropical rainfall is usually higher than -5 for $\delta^{18}O$. Some data that were sampled for every rainfall show the very low values (-9.58, -13.78 for $\delta^{18}O$). The further analyses are in future work.

(5) Data Archives

The original samples will be preserved at Frontier Observation Research System for Global Change. The inventory information will be submitted to JAMSTEC DMO. The analyzed dataset will be submitted to JAMSTEC DMO.

Table 1: List of samples of rain in MR01K05.

Date (LT)	01/11/10 18:15	01/11/17 7:05	01/11/20 2:33, 7:17	01/11/24 4:45	01/11/29 20:30	01/12/1 2:20	01/12/2 12:45,20:30
Sample No.	#1	#2	#3, #4	#5	#6	#7	#8, #9

(continued)

Date (LT)	01/12/3 7:15,1430,17:30	01/12/4 4:30, 5:35, 6:40	01/12/5 7:50, 14:30, 20:40	01/12/7 14:20,20:30	01/12/8 12:40
Sample No.	#10, #11, #12	#13, #14, #15	#16, #17, #18	#19, #20	#21

Table 2: Sample of the stable isotopic compositions in precipitation: in case of MR00-K04.

Date	δD	δ^{18}O	d-excess
2000/6/17	-0.70	-1.17	8.68
2000/6/21	-13.63	-2.42	5.70
2000/6/21	-13.34	-2.41	5.93
2000/6/21	-22.90	-4.40	12.30
2000/6/22	-33.30	-4.36	1.61
2000/6/22	-31.96	-4.40	3.23
2000/6/22	-28.10	-4.88	10.96
2000/6/25	-10.36	-2.25	7.66
2000/6/25	-10.92	-2.53	9.33
2000/6/26	-4.34	-1.91	10.92
2000/6/26	-6.56	-2.13	10.45
2000/6/27	-6.01	-2.30	12.37
2000/6/27	-8.02	-2.43	11.43
2000/6/29	-41.63	-6.42	9.76
2000/6/29	-41.57	-5.94	5.97
2000/6/30	-67.19	-9.58	9.42
2000/7/01	-99.35	-13.78	10.87
2000/7/02	-7.78	-2.21	9.89

6.15 Observation of underway geophysics

(1) Personnel

Masaki Hanyu (GODI): Operation Leader
Souichiro Sueyoshi (GODI)
Kohei Sakamoto (GODI)

(2) Objectives

The spatial and temporal variations of the parameters at/below sea bottom – gravity, magnetic force and sea bottom depth – are basic data for the many fields of geophysics. However, the chance to measure these parameters is rare. The observation in this cruise is carried out to accumulate these data to fill the basic dataset of the geophysics.

(3) Methods

Bathymetry data was obtained by using SeaBeam2112.004 (SeaBeam, Inc., U.S.A.) 12kHz multi narrow beam echo sounding system. The sea surface gravity was obtained by S-116 (LaCoste & Romberg, U.S.A.) onboard gravity meter. The sea surface magnetic force was obtained by three-axis fluxgate magnetometer (Tierra Tecnica, Japan) at 8Hz sampling rate.

All of these observations were carried out from 7 November 2001 to 19 December 2001, in the open seas, Palau and Japanese EEZ and Japanese territorial seas.

(4) Preliminary results

The results will be public after the analyses in future.

(5) Data archives

The dataset obtained in this cruise will be submitted to the DMO (Data Management Office), JAMSTEC and will be archived there.

6.16 Ocean Profiling for OTEC application

(1) Personnel

Nobuo Noda (Saga University): On-board Principle Investigator
Kazuya Urata (Saga University)
Kenji Fukumiya (Saga University)

(2) Objectives

Ocean Thermal Energy Conversion (OTEC) is the power plant system which utilized temperature difference between warm surface sea water and cold deep sea water. In this observation, the natural oceanic profiles are obtained to investigate how to apply the system to the natural environment.

(3) Methods

The oceanic profile of the water temperature and density profile is observed by Mirai CTD system (see section 6.9 for detail) to the depth over 1000 m near the coast. The water sample is also obtained at every 100 m between 100 m and 1000 m depth.

The profiles were obtained at:

【SITE１】**Anguar Island**
134゜8’00”E、6゜55’50”N
2001/Dec/13

【SITE２】**Melekeok State**
134゜39’00”E、7゜29’50”N
2001/Dec/14

(4) Preliminary Results

We obtained the temperature and density profiles as shown in Figs.6.16-1 and 6.16-2. The detailed analyses of these profiles and the analyses of the sampled water will be carried out in our laboratory.

(5) Data Archive

The oceanic profiles are provided by JAMSTEC and submitted to JAMSTEC DMO. The sampled water is archived to analyze in Saga University. The result of the analyses will be submitted to JAMSTEC DMO.

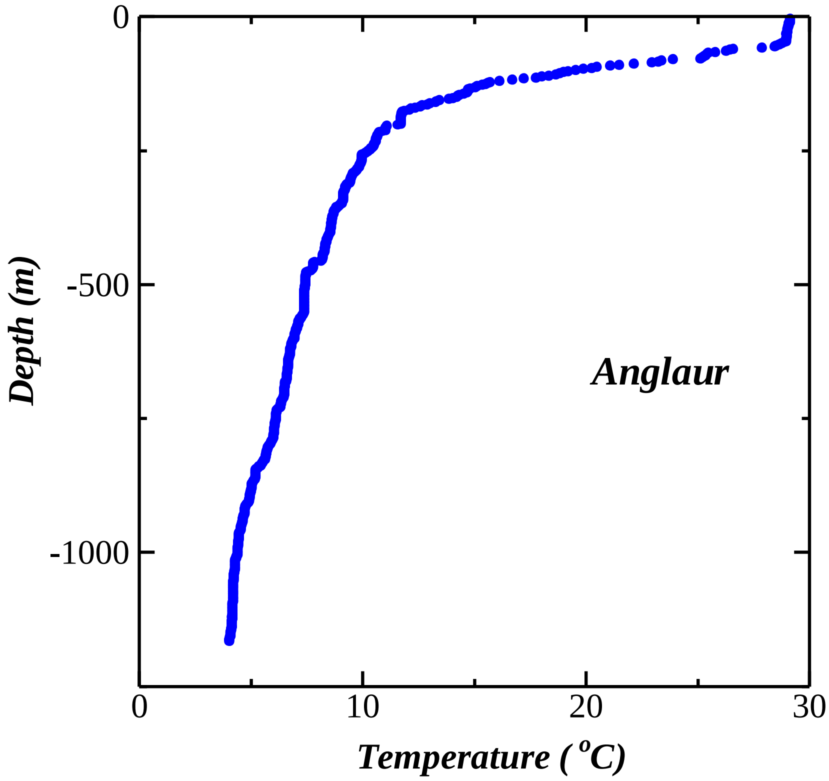

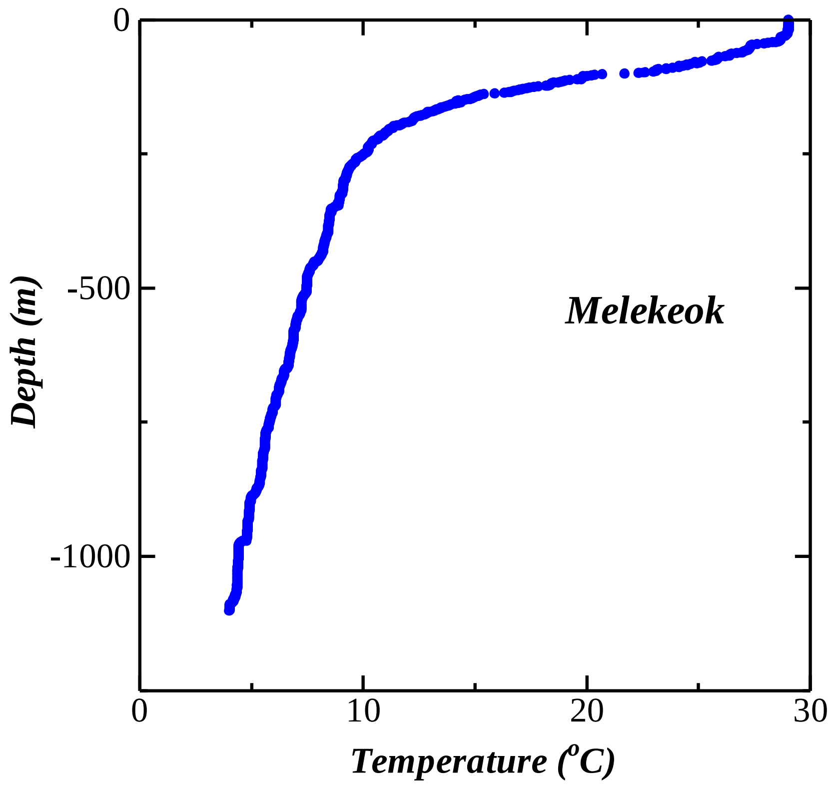

Fig.6.16-1: Observed temperature profiles at Sites 1 (Anglaur) and 2 (Melekeok).

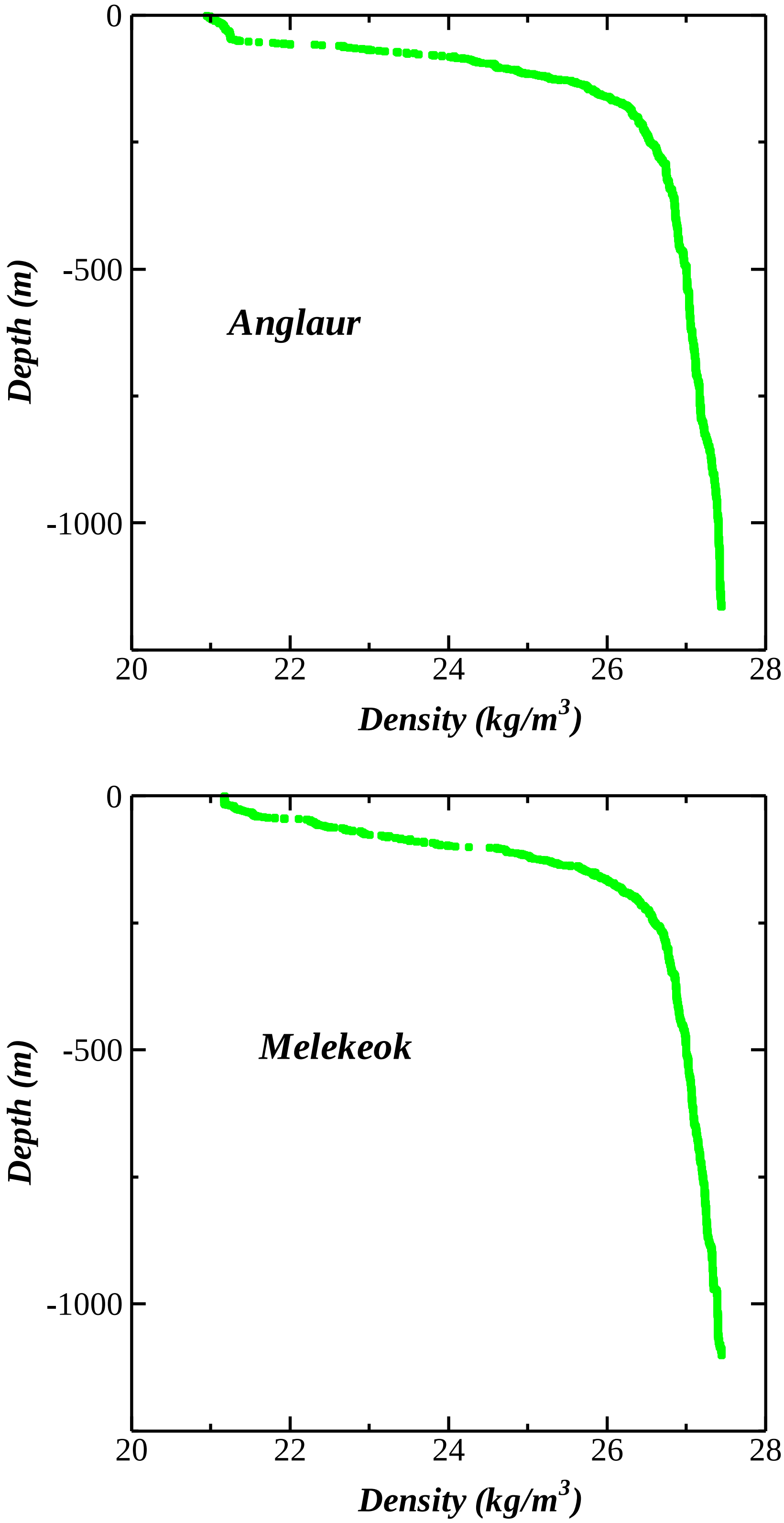

Fig.6.16-2: Observed density profiles at Sites 1 (Anglaur) and 2 (Melekeok).